AVRADCOM-TR-81-D-11

AD A100182

LEVEL II

:RIMENTAL VERIFICATION OF FORCE DETERMINATION GROUND FLYING ON A FULL-SCALE HELICOPTER

nes, W. G. Flannelly, E. J. Nagy, J. A. Fabunmi
KAMAN AEROSPACE CORPORATION
Old Windsor Road
Windsor, Conn. 06002

May 1981

DTIC ELECTE JUN 1 5 1981 E

Final Report for Period May 1977 - December 1980

Approved for public release; distribution unlimited.

Prepared for

APPLIED TECHNOLOGY LABORATORY
U. S. ARMY RESEARCH AND TECHNOLOGY LABORATORIES (AVRADCOM)
Fort Eustis, Va 23604

DTIC FILE COPY

81 6 12 099

404 360

APPLIED TECHNOLOGY LABORATORY POSITION STATEMENT

Force Determination is a method for determining the magnitudes and phasings of vibratory forces and moments on a helicopter through in-flight accelerometer measurements and mobility measurements obtained from shake testing at frequencies corresponding to the vibratory loads.

The subject method was first verified on a 5-foot laboratory model representing a helicopter. The work was reported in USAAMRDL Technical Report 76-38, *Laboratory Verification of Force Determination, A Potential Tool for Reliability Testing.*

The purpose of this program was to determine the feasibility of applying the Force Determination method on a full-scale helicopter. The test vehicle used was a AH-1G. The work involved gathering 2/rev in-flight acceleration readings for 37 degrees of freedom, developing the calibration matrix (mobility matrix) of the aircraft through shake testing, calculating the vibratory loads, and determining seven equivalent loads and applying these loads to the aircraft to duplicate the in-flight recorded accelerations.

The program was conducted under the technical cognizance of Joseph H. McGarvey and Nicholas J. Calapodas, Structures Technical Area, Aeronautical Technology Division.

UNCLASSIFIED

SECURITY CLASSIFICATION OF THIS PAGE (*When Data Entered*)

REPORT DOCUMENTATION PAGE

READ INSTRUCTIONS BEFORE COMPLETING FORM

1. REPORT NUMBER: USAAVRADCOM TR-81-D-11	2. GOVT ACCESSION NO.: AD-A100 182	3. RECIPIENT'S CATALOG NUMBER
4. TITLE (*and Subtitle*): EXPERIMENTAL VERIFICATION OF FORCE DETERMINATION AND GROUND FLYING ON A FULL-SCALE HELICOPTER		5. TYPE OF REPORT & PERIOD COVERED: Final Report, May 1977 — December 1980
		6. PERFORMING ORG. REPORT NUMBER: R-1625
7. AUTHOR(s): R. Jones, W. G. Flannelly, E. J. Nagy, J. A. Fabunmi		8. CONTRACT OR GRANT NUMBER(s): DAAJ02-77-C-0027
9. PERFORMING ORGANIZATION NAME AND ADDRESS: Kaman Aerospace Corporation, Old Windsor Road, Windsor, Connecticut 06002		10. PROGRAM ELEMENT, PROJECT, TASK AREA & WORK UNIT NUMBERS: 62209A 1L262209AH76 00 193 EK
11. CONTROLLING OFFICE NAME AND ADDRESS: Applied Technology Laboratory, U.S. Army Research & Technology Laboratories (AVRADCOM) Fort Eustis, Virginia 23604		12. REPORT DATE: May 1981
		13. NUMBER OF PAGES: 164
14. MONITORING AGENCY NAME & ADDRESS (*if different from Controlling Office*)		15. SECURITY CLASS. (*of this report*): Unclassified
		15a. DECLASSIFICATION/DOWNGRADING SCHEDULE

16. DISTRIBUTION STATEMENT (*of this Report*)

Approved for public release; distribution unlimited.

17. DISTRIBUTION STATEMENT (*of the abstract entered in Block 20, if different from Report*)

18. SUPPLEMENTARY NOTES

19. KEY WORDS (*Continue on reverse side if necessary and identify by block number*)

Force Determination, Ground Flying, Modal Testing, Rotor Forces, Modal Parameters, Shake Testing

20. ABSTRACT (*Continue on reverse side if necessary and identify by block number*)

Force determination is a method of obtaining dynamic loads acting on a vehicle in flight. These loads were determined from measured fuselage responses obtained in flight and calibration matrices obtained in a shake test. These forces obtained were verified by ground flying in a hangar and duplicated the responses obtained in flight.

DD FORM 1 JAN 73 1473 EDITION OF 1 NOV 65 IS OBSOLETE

UNCLASSIFIED

SECURITY CLASSIFICATION OF THIS PAGE (*When Data Entered*)

PREFACE

This program for the Verification of Advanced Vibration Test Concept Utilizing Simulated Hub Forces was performed by Kaman Aerospace Corporation, Division of Kaman Corporation, Bloomfield, Connecticut, under Contract DAAJ02-77-C-0027 for the Applied Technology Laboratory, U.S. Army Research and Technology Laboratories (AVRADCOM), Fort Eustis, Virginia.

This program was originally conducted under the technical direction of Mr. J. McGarvey, and later under the technical direction of Mr. N. J. Calapodas, Aeronautical Technology Division of ATL. At Kaman, Mr. R. Jones was Program Manager, with Messrs. W. G. Flannelly, E. J. Nagy, and Dr. J. A. Fabunmi assisting. The flight testing and instrumentation was done under the supervision of Mr. A. D. Rita, Chief Flight Test Engineer.

TABLE OF CONTENTS

LIST OF ILLUSTRATIONS

LIST OF ILLUSTRATIONS (CONTINUED)

LIST OF ILLUSTRATIONS (CONCLUDED)

LIST OF TABLES

INTRODUCTION

The Army has a continuing goal of improving the reliability of its aircraft and particularly its helicopters. Although in recent years availability rates of helicopters have approached and sometimes exceeded those of fixed-wing aircraft, it has only been at a very high cost in maintenance man-hours, spares bought and stocked, and excessive depot overhaul of aircraft and components.

A fundamental cause of high maintenance man-hours, frequent component replacement, and generally low helicopter reliability is the high vibratory loads the machine experiences. In general, the highest vibratory loads are generated by the rotor and occur at blade passage frequencies, although there are significant loads at other frequencies. All major helicopter manufacturers have published technical reports and papers outlining their efforts to reduce these vibrations and hence increase reliability. One study, (reference 1) performed by Sikorsky under contract to the Applied Technology Laboratory, compared USAF CH-3 helicopters with and without a bifilar pendulum in-plane absorber. The conclusions of this study are that a 54% reduction in vibration levels in the absorber-equipped helicopters resulted in a nearly 49% improvement in reliability and nearly 39% reduction in maintenance.

There are three major technical thrusts in the industry for increasing the reliability of helicopters by reducing the vibratory forces and moments transmitted to the fuselage from the rotor. These are (1) improved rotor design, (2) rotating system dynamic absorbers (hub absorbers, blade absorbers), and (3) rotor isolation (antiresonant, conventional and active). Excellent progress has been made in these areas in recent years in spite of technical problems. However, greater progress could be made through force

---

1 Veca, "Vibration Effects On Helicopter Reliability And Maintainability." Sikorsky Aircraft; USAAMRDL Technical Report 73-11, U. S. Army Air Mobility Research & Development Laboratory, Fort Eustis, Virginia, April 1973, AD 766307.

determination to assist in determining the effectiveness of these three areas of improvement. Force determination is defined as a method for determining the magnitudes and phasings of vibratory forces and moments (and other forces and moments) on a helicopter in flight through accelerometer measurements on the fuselage. Force determination has been developed theoretically and verified in the laboratory on a model by dynamicists at Kaman Aerospace Corporation under contract to the Applied Technology Laboratory. The purpose of this program is to determine the feasibility of applying force determination to a full-scale aircraft and applying those forces to the vehicle such that flight vibration levels will be reproduced in the test stand.

This procedure, known as ground flying, makes possible through force determination accelerated reliability testing by subjecting the aircraft to the loads it actually experiences through a flight spectrum while the aircraft is on the ground.

FLIGHT TEST

TEST VEHICLE

The aircraft used in this program is the Army AH-1G helicopter, serial number 67-15683. The AH-1G helicopter shown schematically in Figure 1 is an armed vehicle with a maximum gross weight of 9500 pounds, powered by a single Lycoming T53-L-13 free gas turbine engine rated at 1400 shaft horsepower (SHP) at sea level, standard day, uninstalled conditions. The engine is derated to 1100 shaft horsepower, due to the maximum torque limit of the main transmission. The AH-1G is configured with two-bladed, teetering main and tail rotors of 44 feet and 8 1/2 feet diameters respectively. Landing gear is of the fixed energy-absorbing skid type. Standard armament is the XM23E1 armament subsystem with the M134 machine gun and XM 129 grenade launcher mounted in the weapon turret. Two store mounting points are located on each side of the helicopter on stub wings. Additional armaments will consist of Launcher Rocket Aircraft 2.75 in., M200L (Army PN 8035608, FJN 1055-168-6164) each capable of carrying a maximum of 19 rockets. Each simulated rocket weighs approximately 22 pounds.

TEST CONDITIONS

The test vehicle configurations and loading conditions which were investigated during the flight test phase of the program are identified in Table 1. These flight test conditions are within the current approved handbook flight envelope of the AH-1G aircraft. No structural modifications were required for the force determination flight test program. The only changes to the normal AH-1G configuration were the addition of an instrumentation package in the ammunition compartment and straingage type accelerometers mounted throughout the helicopter. Consequently, the configurations and loadings specified in Table 1 were easily accommodated within the present AH-1G flight envelope.

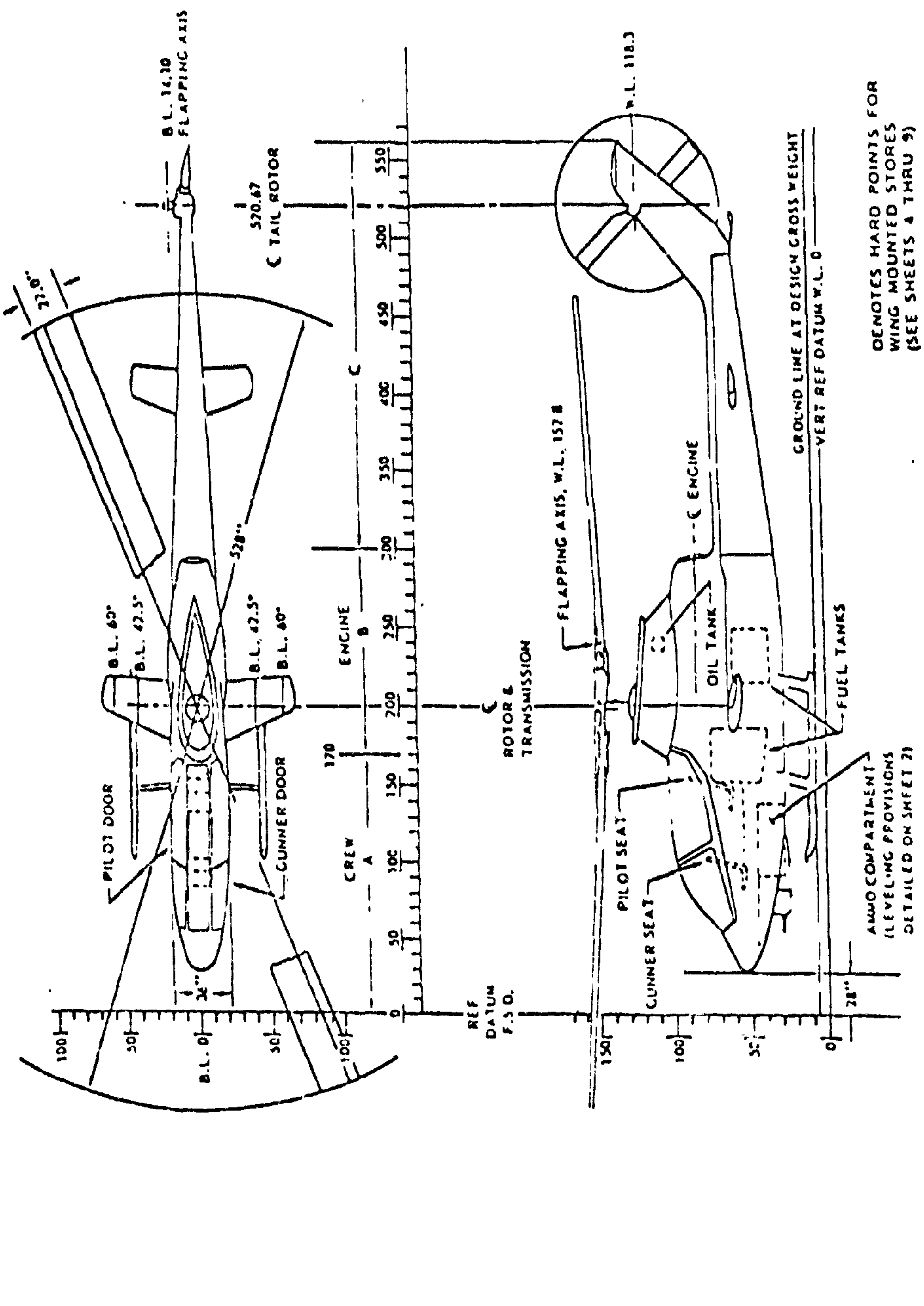

Figure 1. AH-1G plan and side views.

TABLE 1. AH-1G GROSS WEIGHT/CONFIGURATION

Gross Weight (lb)	CG	Configuration
8000	Forward	Clean
9000	Forward	2 rocket/launchers 19 rocket/launchers
9500	Aft	4 rocket/launchers
9500	Forward	19 rocket/launchers

The flight test program consisted of approximately 10 flight hours. One of the requirements of the force determination is to determine the broadest range in magnitude and frequency content of hub vibratory forces and moments through a flight test program and to apply those same loads sustained in flight to the helicopter in a ground-based condition. Therefore, flight conditions were selected to provide the widest range of rotor loads from a magnitude and frequency control viewpoint. These flight conditions given in Table 2 include nap-of-the-earth maneuvers and are representative of the overall requirements for both the AH-1G/R and AH-1Q/S model aircraft.

TABLE 2. FLIGHT CONDITIONS

CONDITION
Ground Conditions
Normal start
Shutdown
IGE maneuvers
Takeoff
Normal
Hovering
* IGE to OGE - pop-up maneuver
* OGE to IGE - rapid descent

TABLE 2. CONTINUED

CONDITION	
IGE maneuvers	
Deceleration	
* Rapid deceleration from 50 kts	
Level flight to hover	
Approach and landing	
Forward level flight	
Airspeed	Rpm
0.50 V_H	324
0.60 V_H	324
0.70 V_H	324
0.80 V_H	324
0.90 V_H	324
V_H	324
Nonfiring maneuvers	
Full power climb	
Normal	
Sideward flight	
*1. Accelerate to 35 kts right and reverse to same airspeed.	
*2. Accelerate to 35 kts left and reverse to same airspeed.	
Normal turns	
To the right	
0.7 V_H	
To the left	
0.7 V_H	

TABLE 2. CONCLUDED

CONDITION
Gunnery maneuvers
Gunnery runs
PT target dives
To 0.9 V_L
Spray fire dives to indicated speed, followed by rolling pullouts to the right and left
To 0.9 V_L
Right rolling pullout - 1.0 V_L
Left rolling pullout - 1.0 V_L
Gunnery turns
To the right - 0.7 V_H
To the left - 0.7 V_H
Autorotation
Stabilized flight - 0.6 V_H
Auto turns
To the right - 0.6 V_H
To the left - 0.6 V_H
* 90^0 turn to right from OGE hover followed by maximum acceleration to 60 kts.
* 90^0 turn to left from OGE hover followed by maximum acceleration to 60 kts.
* TOW missile mission maneuvers pertinent to AH-1Q/S type aircraft.

INSTRUMENTATION

Transducers

The principal vibratory excitations expected on the AH-1G helicopter were vertical, lateral and longitudinal forces and torque at the hub, and possibly a vertical force at the horizontal stabilizer. To successfully measure aircraft responses necessary to the force determination methodology, 37 Statham Model A69TC strain-gage accelerometers were attached to the helicopter structure at selected points. The accelerometers are designed for flight and general purpose use with a measurement range of ± 5 g and an approximate natural frequency of 375 Hz. Strain-gage accelerometers can be readily flip calibrated for a 2g reading on site and have a measurement capability down to 0 Hz.

All accelerometers were calibrated for frequency response (amplitude and phase) over range of 0 to 100 Hz through filtered circuitry to minimize frequencies above 10/rev of main rotor (54 Hz).

Curves of the frequency response characteristic of the total system were derived for use in the harmonic analysis of flight data.

The accelerometers were placed to minimize coupling in planes other than the primary forcing plane. Twenty accelerometers measured vertical response, and their locations are shown in Figure 2. Ten accelerometers were placed to measure response in the lateral direction, as shown in Figure 3, and were spaced from nose to tail to minimize the effects of coupling between hub lateral force and hub torque. Longitudinal accelerations were measured by seven accelerometers dispersed as shown in Figure 4. Because the butt line 0 plane is essentially a plane of symmetry, accelerometers in the vicinity of the center of gravity were laterally displaced to the extreme butt line (wing stores stations) to aid in separating response due to hub torque and hub longitudinal force. Accelerometers were placed with direction of the main axis of sensitivity oriented for measurement along either the butt line, water line, or fuselage station

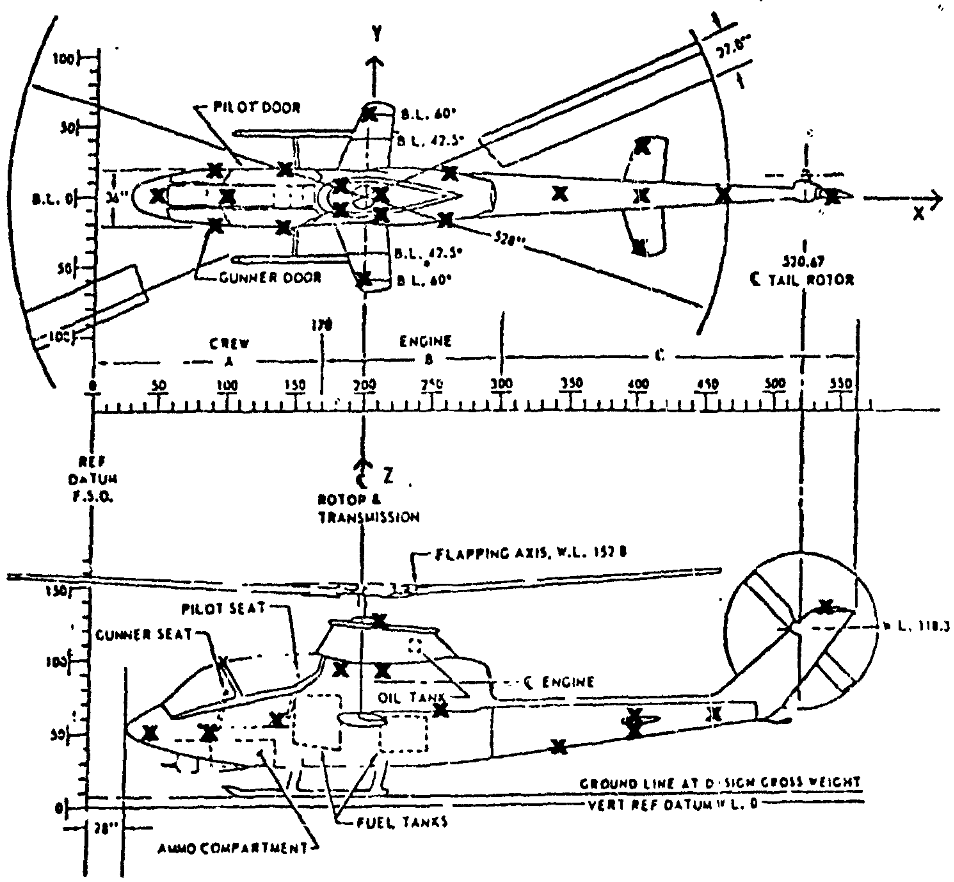

Figure 2. Placement of accelerometers for vertical response measurements.

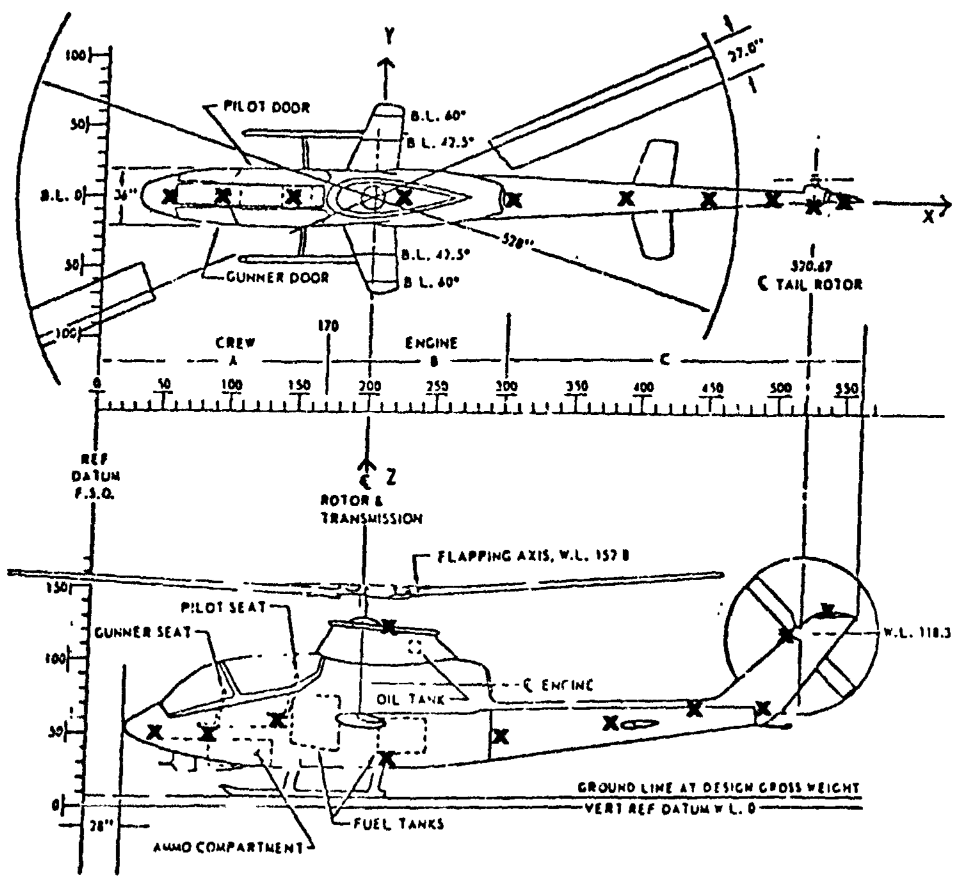

Figure 3. Placement of accelerometers for lateral response measurements.

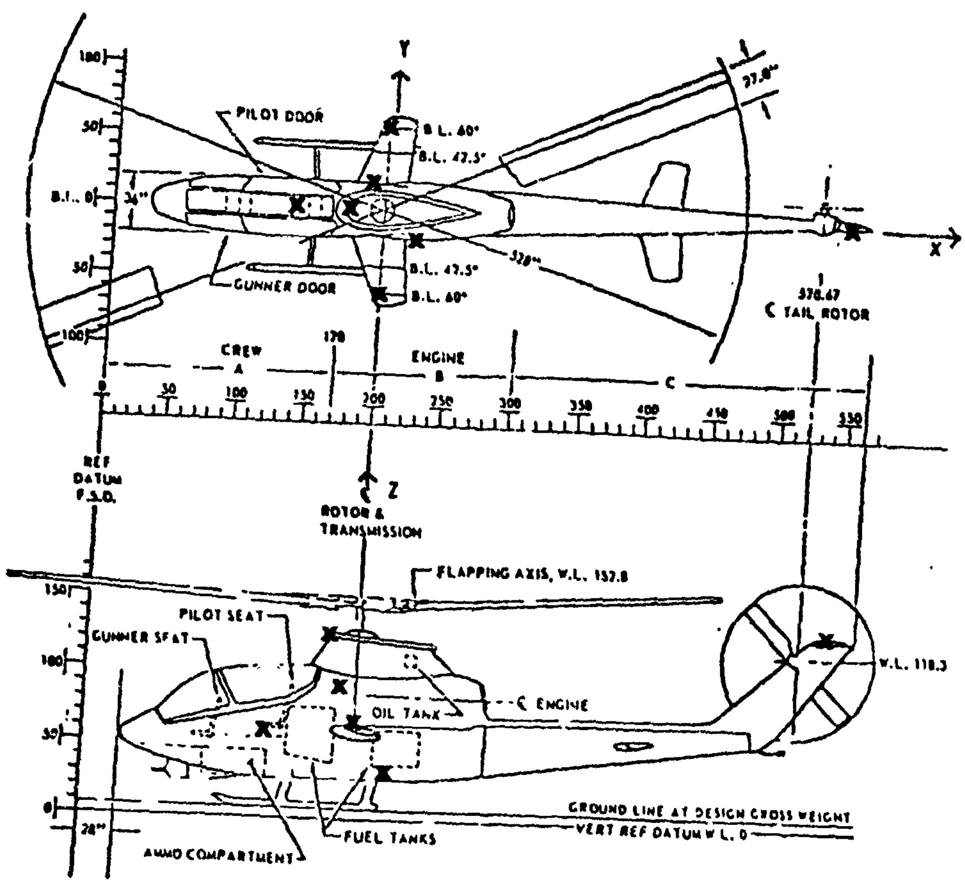

Figure 4. Placement of accelerometers for longitudinal response measurements.

axis, with positive accelerations directed up, to the right, and forward. Locations are further detailed in Table 3, with abbreviated notation to be used in data processing.

All accelerometers were placed internally, where possible, to minimize degradation of helicopter performance. Furthermore, the accelerometers were rigidly attached to structure, via mounting blocks using existing bolt or connector holes or with appropriate bonding agents, to minimize extraneous localized response effects. Impacts of each local area were recorded on an oscillograph to check for undesirable bracket or local structural response.

Three vertical accelerometers were placed on the vehicle at the fuselage locations of the collective longitudinal, and lateral control actuators. The purpose of these accelerometers was to determine the magnitude of the control loads via the flight test data and calibration matrix.

In addition to the accelerometers, data was also recorded for airspeed and load factor. Parameters such as altitude, airspeed, engine and rotor speed, attitude, heading, vertical speed, torque pressure and outside air temperature were continually monitored by the pilot during flight.

DATA ACQUISITION AND REDUCTION

All of the accelerometers given in Table 3 were wired to B&F Instrument Model 24-200 balance boxes and bridge power supplies. The balance boxes, utilized as signal conditioning units, have their outputs wired to a PCM (Pulse Code Modulation) encoder. This encoder sampled each accelerometer 500 times a second. The PCM data signal was transmitted from the aircraft to the ground station via an L-band telemetry link. This instrumentation package was located in the ammunition bay of the AH-1G helicopter.

TABLE 3. ACCELEROMETER LOCATION AND DESIGNATION

General Location	Fuse Sta.	Butt Line	Water Line	Instrumentation Designation
Vertical Axis:				
Nose	50	0	52	Z 50
Gunner area, right side	90	20R	52	Z 90R
Gunner area, left side	90	20L	52	Z 90L
Gunner area, top	100	0	100	Z100T
Pilot area, right side	140	20R	58	Z140R
Pilot area, left side	140	20L	58	Z140L
Wing tip, right	200	60R	65	Z200R
Wing tip, left	200	60L	65	Z200L
Transmission cowling, top	210	0	125	Z210T
Aft body fairing, right	260	18R	55	Z260R
Aft body fairing, left	260	18L	55	Z260L
Tail boom	340	0	42	Z340
Tail boom at elevator	400	0	48	Z400
Elevator tip, right	400	40R	60	Z400R
Elevator tip, left	400	40L	60	Z400L
Tail boom, aft	460	0	60	Z460
Vertical fin, top	540	0	135	Z540
Longitudinal control hydraulic actuator	196	12R	59	ZLONG
Lateral control hydraulic actuator	196	12L	59	ZLATR
Collective control hydraulic actuator	207	12L	57	ZCOLL

TABLE 3. CONCLUDED

General Location	Fuse Sta.	Butt Line	Water Line	Instrumentation Designation
Lateral Axis:				
Nose	50	0	52	Y 50
Gunner seat	90	0	52	Y 90
Pilot seat	140	0	58	Y140
Aft fuel tank, bottom	220	0	35	Y220B
Transmission cowling, top	220	0	125	Y220T
Tail boom at fuselage attachment	300	0	50	Y300
Tail boom	380	0	60	Y380
Tail boom	440	0	60	Y440
Tail boom at vertical fin	490	0	70	Y490
Vertical fin, top	517	0	135	Y517
Longitudinal Axis:				
Pilot seat	140	0	58	X140
Transmission cowling, top fwd.	180	0	125	X180T
Transmission, lower right	190	20R	90	X190R
Wign tip, right	200	60R	65	X200R
Wing tip, left	200	60L	65	X200L
Aft fuel tank, bottom left	220	20L	35	X220L
Vertical fin, top	540	135	135	X540

At the receiving station, all channels were suitably formatted and put on digital magnetic tape for analysis. The magnetic tape containing the PCM data was processed on the IBM 360 computer in two stages:

(1) The first computer run used Kaman program DARTRAM. It evaluates for each test point specified, the average vibratory and steady magnitudes (vibratory being one-half the peak-to-peak excursion in each rotor cycle, with no recognition of frequency content nor adjustment for frequency response; and steady being the simple midpoint of peaks, rather than a time-sample average). It also lists the average maximum and minimum peaks, the single greatest maximum and minimum peaks, and the highest vibratory rotor cycle with its accompanying steady and its location in the record. This printed output was scanned for length of record available and for integrity of telemetered signal. For non-steady-state conditions, the time of highest vibration for each accelerometer can be pinpointed. (This highest vibration point includes all accelerometer output, and therefore its usefulness for rotor-induced frequencies will be dependent on the accelerometer filter characteristics).

(2) The second computer run used Kaman program HARMFDET. It extracts the first 10 harmonics of each accelerometer and record specified, with frequency response corrections. These values result from processing one rotor cycle or an average of a number of cycles (max. of 5), or a longer period combining many cycles. The program summarizes in printed tabular form for each accelerometer the real and imaginary components of the fundamental and even harmonics. This same summary data can be saved on magnetic tape for subsequent computer analysis.

The flight test program, as planned, consisted of a limited and relatively small number of flight hours. The intent was to obtain flight accelerations at the 37 accelerometer locations over a wide range of the aircraft flight envelope. Since these flight accelerations were measured essentially

instantaneously, the flight loads calculated from these accelerations can be considered to be valid for the purpose of this program. The reader must be cautioned, however, that the measured flight accelerations and the subsequent calculated flight loads were not necessarily the average values to be expected for the AH-1G helicopter. One can more fully appreciate this fact if one understands that certain of the high performance maneuvers can be flown by the same pilot on the same aircraft at very similar conditions and the accelerations measured will be different and will occur at different times in the maneuver.

Pilot technique, gusts, varying atmospheric conditions, varying amounts of fuel burn-off, variations in airspeed and load factor, etc., manually are averaged out in normal flight test programs by performing replications and obtaining averages from these replicated maneuvers. However, this was not necessary for this program.

The first computer run used was program DARTRAN. This program lists for each of the 37 accelerometers the rotor cycle in which the highest vibration occurred. For all non-steady-state flight conditions, frequency of occurrence plots similar to Figures 5 and 6 were made. These plots showed for each selected flight record which rotor cycles contained the highest vibratory accelerations. These plots included up to 280 rotor cycles in some cases and were used to determine which rotor cycles and how many of them were to be specified for harmonic processing. Frequency of occurrence plots were not needed for the stabilized flight records, and only five rotor cycles were specified for harmonic processing.

The rotor cycles for harmonic analysis for the non-steady flight condition were selected by the number of accelerometers having peak values. For example, record #3 of flight #7 had two regions wherein various accelerometers reached their highest vibratory accelerations in rotor cycles 13 through 16 and seventeen accelerometers had their highest vibratory accelerations in rotor cycles 25 through 29. Therefore, the five rotor cycles 25 through

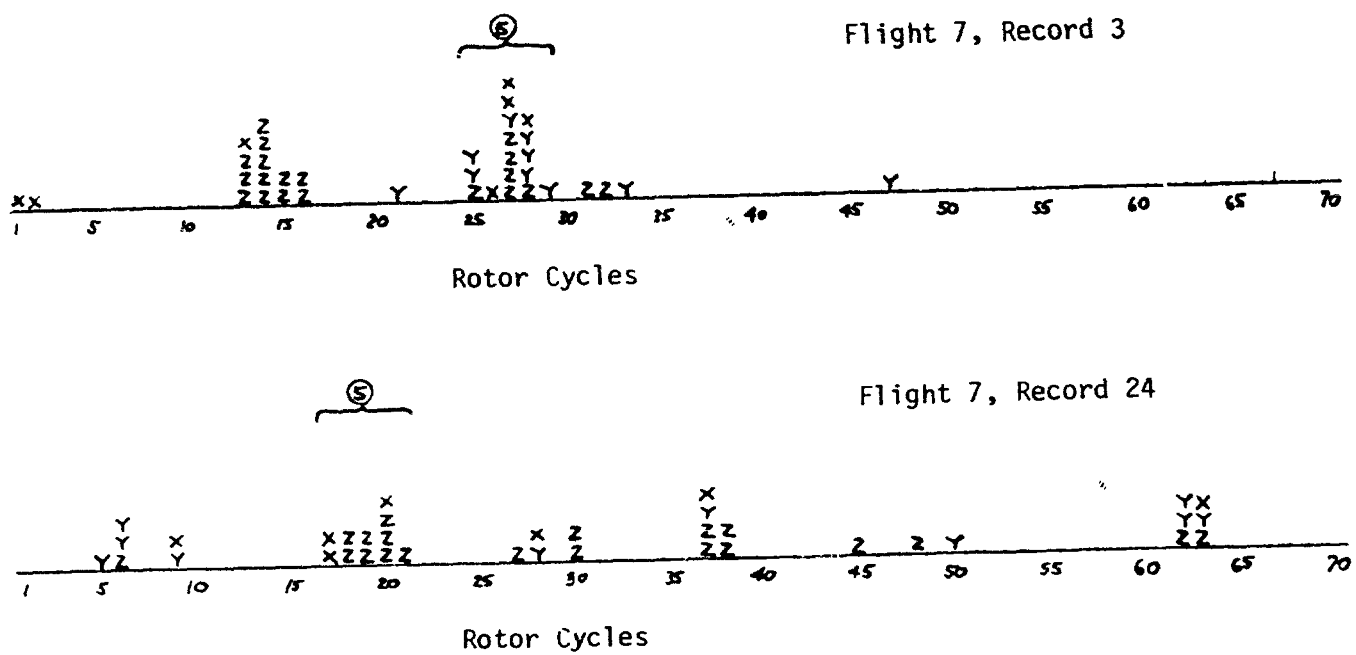

Figure 5. Frequency of occurrence of high vibration level; flight conditions 3 and 24.

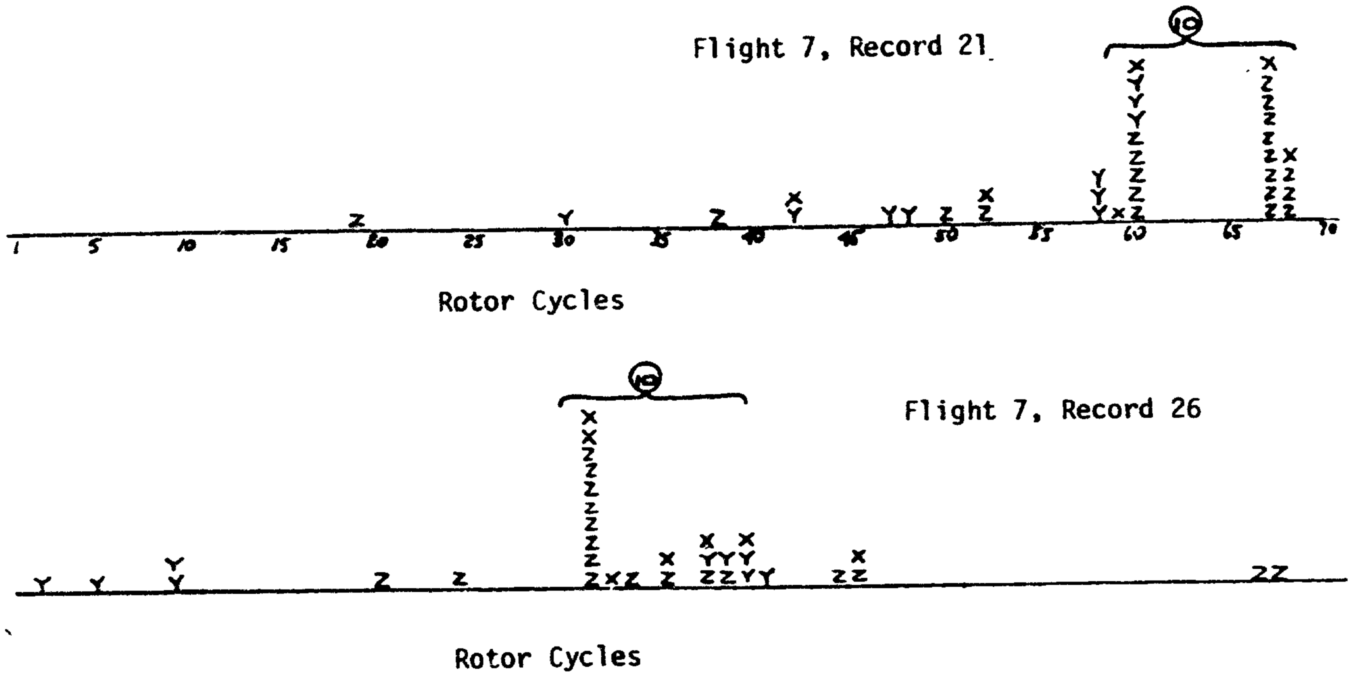

Figure 6. Frequency of occurrence of high vibration level; flight conditions 10 and 26.

29 were chosen for harmonic processing by the program HARMFDET. It is important to note that rotor cycles 13 through 16 may have exhibited higher vibratory accelerations than the five cycles chosen, but this did not enter into the decision. Record #24 of flight #7 shown in Figure 5 is a good example of this type of result. Eleven accelerometers reached their peak vibratory accelerations during rotor cycles 17 through 21 with another six accelerometers exhibiting peak vibratory accelerations in rotor cycles 37 and 38 and also six additional accelerometers peaking in rotor cycles 62 and 63. The average vibratory acceleration for the eleven accelerometers was only $\pm$ .60 g compared to $\pm$ 2.71 g for the six accelerometers at rotor cycles 37 and 38 and $\pm$ 0.80 g for the six at rotor cycles 62 and 63.

Referring to record #3, flight #7, Figure 5, no consideration was given to the location of the accelerometers. Thus, the thirteen accelerometers from rotor cycles 13 through 16 may have been located all in the tail boom area, whereas the seventeen accelerometers chosen may have been located in the center fuselage area.

Figure 6 shows records #21 and 26 from flight #7. These two plots show a contrast between actual rotor cycles selected. Both records had ten rotor cycles selected for analysis, but record #21 had six rotor cycles with no accelerometers peaking whereas record #26 had only two rotor cycles with no accelerometers peaking. The program HARMFDET actually averaged 10 rotor cycles for both records, but no consideration was given to how much the average for any particular accelerometer could have been reduced if six of the 10 rotor cycles actually had low accelerations.

FLIGHT TEST RESULTS

Table 4 shows the two-per-rev results obtained in the flight test for all of the steady state and maneuver conditions. Selected conditions from these results were used to calculate forces acting on the test vehicle and also to compare flight test and ground flying of the vehicle.

TABLE 4. TWO-PER-REV FLIGHT TEST RESULTS (g's)

8465 Pound Vehicle								Fwd. c.g.						
REC	Z50		Z100T		Z210T		Z340		Z400		Z460		Z540	
	REAL	IMAG	REAL	IMAG	REAL	IMAG	REAL	IMAG	REAL	IMAG	REAL	IMAG	REAL	IMAG
1	-0.052	0.000	-0.010	0.016	0.009	-0.024	0.312	0.069	0.204	0.069	-0.049	0.016	-0.627	-0.140
2	-0.075	-0.002	-0.005	-0.012	-0.016	-0.009	0.297	0.039	0.191	0.056	-0.028	0.029	-0.566	-0.105
3	-0.122	-0.025	-0.042	-0.046	-0.035	-0.042	0.255	-0.132	0.175	-0.065	-0.053	-0.008	-0.053	0.116
4	-0.131	-0.021	-0.052	-0.061	-0.048	-0.049	0.328	-0.256	0.249	-0.145	-0.065	0.025	-0.757	0.379
5	-0.175	-0.009	-0.083	-0.057	-0.080	-0.039	0.348	-0.303	0.249	-0.179	-0.034	0.071	-0.703	0.540
6	-0.210	-0.046	-0.117	-0.079	-0.130	-0.011	0.333	-0.395	0.248	-0.239	-0.001	0.053	-0.508	0.577
7	-0.097	-0.035	-0.029	-0.022	-0.058	-0.081	0.153	0.059	0.078	0.082	-0.052	0.030	-0.363	-0.069
8	-0.115	-0.037	-0.037	-0.067	-0.035	-0.066	0.324	-0.189	0.234	-0.114	-0.060	-0.020	-0.733	0.181
9	-0.132	-0.035	-0.053	-0.069	-0.047	-0.080	0.310	-0.173	-0.008	-0.237	-0.052	-0.005	-0.666	0.158
10	-0.124	-0.018	-0.042	-0.047	-0.050	-0.050	0.283	-0.114	-0.115	0.141	-0.054	0.006	-0.584	0.085
11	-0.084	-0.059	-0.011	-0.075	-0.050	-0.099	0.011	-0.397	0.257	-0.034	-0.033	-0.002	-0.703	0.040
12	-0.019	0.018	0.040	-0.036	0.061	-0.069	0.242	-0.117	-0.011	-0.165	-0.054	0.010	-0.466	0.150
[illegible]	-0.029	-0.000	-0.004	-0.057	0.009	-0.090	0.195	-0.207	0.141	-0.115	-0.052	0.029	-0.472	0.337
[illegible]	0.014	-0.043	0.056	-0.044	0.059	-0.108	0.276	-0.031	0.157	0.001	-0.067	-0.003	-0.520	-0.027
5	0.068	0.024	0.056	0.007	0.086	-0.015	0.079	0.020	0.047	0.031	--*	--*	-0.145	0.008
6	0.088	0.036	0.071	0.014	0.175	-0.057	0.119	-0.005	0.071	0.007	-0.013	0.030	-0.197	0.047
17	0.087	0.030	0.037	0.043	0.052	0.016	-0.067	0.146	-0.046	0.101	0.003	0.015	0.054	-0.144
18	-0.110	-0.034	-0.030	-0.037	-0.060	-0.073	0.186	0.037	0.120	0.051	-0.020	0.033	-0.357	-0.064
19	-0.071	-0.059	-0.000	-0.045	-0.025	-0.105	0.187	0.075	0.131	0.077	-0.010	0.029	-0.342	-0.092
20	-0.035	-0.052	0.020	-0.061	-0.026	-0.064	0.297	-0.043	0.190	-0.014	-0.050	-0.009	-0.582	-0.004
21	-0.093	-0.050	-0.104	-0.080	-0.111	-0.030	-0.282	-0.277	-0.165	-0.186	0.005	0.006	0.326	0.432
22	0.011	-0.030	0.014	0.023	0.002	-0.051	-0.013	0.328	-0.015	0.233	0.020	0.004	0.006	-0.496
23	0.034	-0.089	0.089	-0.038	0.066	-0.091	0.345	0.148	0.248	0.110	--*	--*	-0.684	-0.315
24	-0.109	0.014	-0.025	0.002	-0.062	-0.017	0.264	0.066	0.169	0.077	-0.053	0.015	-0.550	-0.151
25	-0.488	-0.214	-0.281	-0.301	-0.409	-0.033	0.511	-0.982	0.399	-0.714	0.021	-0.170	-0.963	1.090
26	-0.337	-0.299	-0.173	-0.338	-0.258	-0.264	0.412	-0.962	0.336	-0.692	0.013	-0.101	-0.828	1.203
27	-0.306	-0.121	-0.219	-0.216	-0.101	-0.133	0.125	-1.032	0.108	-0.785	-0.047	-0.054	-0.323	1.425
28	-0.317	-0.210	-0.164	-0.287	-0.220	-0.175	0.401	-0.954	0.322	-0.665	-0.025	-0.085	-0.855	1.234
29	-0.372	-0.191	-0.186	-0.282	-0.191	-0.057	0.485	-1.128	0.385	-0.772	-0.036	-0.128	-1.006	1.467
30	-0.368	-0.214	-0.194	-0.362	-0.156	-0.073	0.468	-1.264	0.351	-0.870	-0.061	-0.058	-0.942	1.755
31	-0.036	-0.116	0.067	-0.070	-0.017	-0.107	0.591	0.192	0.404	0.174	-0.019	-0.017	-1.025	-0.453
32	0.036	-0.045	0.078	-0.013	-0.031	-0.077	0.442	0.299	0.320	0.249	-0.002	0.007	-0.780	-0.551

* Data was in error

TABLE 4. CONTINUED

8465 Pound Vehicle — Fwd. c.g.

REC	Z90R REAL	Z90R IMAG	Z90L REAL	Z90L IMAG	Z140R REAL	Z140R IMAG	Z140L REAL	Z140L IMAG	Z200R REAL	Z200R IMAG	Z200L REAL	Z200L IMAG
1	0.013	0.022	0.003	-0.026	0.041	0.020	0.032	-0.021	0.124	0.065	0.083	-0.064
2	0.009	0.025	-0.016	-0.031	0.033	0.022	0.018	-0.030	0.124	0.067	0.058	-0.082
3	-0.023	-0.001	-0.039	-0.075	-0.004	-0.013	-0.003	-0.082	0.098	0.040	0.043	-0.192
4	-0.007	-0.011	-0.054	-0.104	0.030	-0.032	-0.012	-0.117	0.167	0.013	-0.003	-0.279
5	-0.011	-0.003	-0.096	-0.115	-0.012	-0.052	-0.043	-0.136	0.240	0.022	-0.081	-0.327
6	-0.008	-0.038	-0.137	-0.147	0.038	-0.058	-0.073	-0.167	0.260	-0.018	-0.140	-0.371
7	-0.015	-0.023	-0.033	-0.048	0.008	0.028	-0.006	-0.036	0.069	0.106	0.014	-0.098
8	-0.009	-0.013	-0.036	-0.109	0.033	-0.026	0.005	-0.113	0.146	0.028	0.036	-0.245
9	-0.015	0.011	-0.058	-0.118	-0.004	-0.029	-0.010	-0.126	0.155	0.066	0.018	-0.278
10	-0.019	[illegible]	-0.045	-0.092	-0.016	0.013	-0.001	-0.094	0.124	0.064	0.035	-0.216
11	0.024	0.023	-0.040	-0.150	0.054	0.012	-0.000	-0.146	0.203	0.143	0.003	-0.328
12	0.049	-0.034	0.021	-0.024	0.054	-0.047	0.036	-0.035	0.112	-0.096	0.053	-0.042
13	0.018	-0.030	-0.012	-0.047	0.029	-0.049	0.006	-0.066	0.101	-0.084	0.014	-0.123
14	0.033	-0.046	0.049	-0.034	0.042	-0.042	-0.007	-0.069	0.060	-0.065	0.130	-0.008
15	0.049	-0.016	0.028	0.032	0.039	-0.018	0.018	0.031	0.062	-0.084	0.002	0.088
16	0.058	-0.033	0.047	0.046	0.047	-0.042	0.036	0.033	0.052	-0.146	0.030	0.107
17	0.015	0.001	0.034	0.057	-0.007	0.007	0.011	0.061	-0.049	-0.037	-0.093	0.155
18	-0.021	0.033	-0.041	-0.073	0.009	0.034	-0.007	-0.058	0.083	0.137	0.018	-0.156
19	-0.011	0.015	-0.008	-0.063	0.008	0.026	0.018	-0.045	0.046	0.113	0.069	-0.102
20	0.026	0.035	0.010	-0.106	0.052	0.035	0.038	-0.102	0.135	0.169	0.073	-0.256
21	-0.086	-0.033	-0.093	-0.064	-0.095	-0.043	-0.103	-0.075	-0.123	-0.038	-0.179	-0.139
22	-0.074	0.044	0.074	0.000	-0.071	0.067	0.066	0.034	-0.226	0.170	0.228	0.059
23	0.036	-0.007	0.086	-0.051	0.054	0.010	0.107	-0.022	0.057	0.094	0.220	-0.030
24	-0.010	0.040	-0.030	-0.028	0.021	0.034	0.005	-0.024	0.116	0.100	0.055	-0.091
25	-0.142	-0.073	-0.309	-0.386	-0.041	-0.106	-0.183	-0.394	0.294	0.006	-0.216	-0.808
26	-0.122	-0.183	-0.198	-0.388	-0.047	-0.204	-0.112	-0.388	0.159	-0.103	-0.108	-0.695
27	-0.093	-0.167	-0.231	-0.234	-0.055	-0.205	-0.170	-0.285	0.182	-0.272	-0.274	-0.526
28	-0.082	-0.137	-0.196	-0.337	-0.009	-0.175	-0.113	-0.355	0.232	-0.103	-0.139	-0.677
29	-0.073	-0.122	-0.234	-0.381	-0.006	-0.177	-0.137	-0.429	0.330	-0.072	-0.200	-0.860
30	-0.121	-0.169	-0.217	-0.410	-0.043	-0.217	-0.122	-0.459	0.211	-0.145	-0.115	-0.910
31	0.024	0.048	0.063	-0.137	0.063	0.068	0.111	-0.095	0.122	0.293	0.258	-0.221
32	0.090	0.090	0.074	-0.065	0.097	0.082	0.095	-0.033	0.170	0.238	0.179	-0.103

TABLE 4. CONTINUED

8465 Pound vehicle							Fwd. c.g.					
REC	Z260R		Z260L		Z396R		Z396L		ZLONG		ZLATR	
	REAL	IMAG	REAL	IMAG	REAL	IMAG	REAL	IMAG	REAL	IMAG	REAL	IMAG
1	0.210	0.038	0.200	0.015	0.232	0.089	0.216	0.058	0.091	-0.012	-0.063	0.056
2	0.191	0.027	0.169	-0.012	0.225	0.075	0.180	0.033	0.079	0.009	0.070	-0.017
3	0.157	-0.075	0.154	-0.137	-0.127	0.122	0.168	-0.112	0.063	-0.042	0.055	-0.083
4	0.204	-0.161	0.172	-0.227	-0.026	-0.308	0.216	-0.208	0.084	-0.080	0.054	-0.129
5	0.213	-0.190	0.175	-0.274	-0.041	-0.305	0.232	-0.252	0.100	-0.091	0.042	-0.149
6	0.175	-0.231	0.147	-0.338	0.211	-0.232	0.137	-0.354	0.094	-0.123	0.023	-0.174
7	0.101	0.056	0.033	0.091	0.108	0.130	0.122	0.002	0.045	0.021	0.003	-0.038
8	0.204	-0.119	0.197	-0.179	-0.226	-0.085	0.230	-0.127	0.090	-0.066	0.068	-0.109
9	0.195	-0.105	0.185	-0.188	0.238	-0.026	0.177	-0.146	0.085	-0.055	0.063	-0.114
10	0.172	-0.068	0.169	-0.130	0.208	0.001	0.143	-0.075	0.078	-0.039	0.059	-0.089
11	0.232	-0.062	0.213	-0.159	0.288	0.044	0.227	-0.094	0.109	-0.033	0.068	-0.112
12	0.173	-0.117	0.153	-0.099	0.178	-0.078	-0.147	-0.063	0.069	-0.067	0.059	-0.052
13	0.134	-0.155	0.126	-0.176	0.165	-0.117	0.131	-0.132	0.050	-0.083	0.036	-0.089
14	0.180	-0.065	0.195	-0.028	0.068	0.110	0.203	0.035	0.077	-0.040	0.003	-0.093
15	0.071	-0.020	0.048	0.019	0.066	-0.043	0.016	0.128	0.029	-0.017	0.019	0.014
16	0.084	-0.073	0.073	-0.009	0.063	-0.119	0.138	0.042	0.039	-0.045	0.031	-0.001
17	-0.052	0.065	-0.042'	0.116	-0.066	0.105	-0.004	0.153	-0.031	0.032	-0.020	0.065
18	0.126	0.041	0.110	-0.030	0.149	0.104	0.082	-0.023	0.056	0.018	0.046	-0.028
19	0.118	0.038	0.130	0.025	0.138	0.134	0.136	0.023	0.050	0.028	0.058	-0.006
20	0.191	0.007	0.214	-0.084	0.158	0.070	0.237	-0.083	0.100	0.002	0.081	-0.070
21	-0.218	-0.142	-0.234	-0.179	-0.186	-0.175	-0.167	-0.228	-0.121	-0.073	-0.129	-0.085
22	-0.063	0.199	0.043	0.206	-0.111	0.208	0.119	0.267	-0.037	0.109	0.042	0.084
23	0.232	0.080	0.284	0.066	0.166	0.178	0.346	0.155	0.114	0.039	0.139	0.016
24	0.176	0.038	0.172	0.000	0.177	0.104	0.151	0.048	0.071	0.023	0.067	-0.012
25	0.168	-0.429	0.190	-0.796	0.188	-0.270	0.398	-0.864	0.087	-0.241	-0.016	-0.379
26	0.097	-0.573	0.168	-0.772	0.171	-0.424	0.291	-0.713	0.046	-0.299	-0.014	-0.397
27	-0.004	-0.588	-0.027	-0.761	-0.007	-0.417	-0.057	-0.627	-0.006	-0.333	-0.081	-0.353
28	0.147	-0.540	0.157	-0.777	0.240	-0.443	0.311	-0.742	0.065	-0.298	-0.007	-0.386
29	0.203	-0.606	0.172	-0.928	0.245	-0.599	0.287	-0.879	0.103	-0.343	-0.003	-0.464
30	0.136	-0.679	0.144	-1.020	0.155	-0.498	0.328	-0.775	0.073	-0.401	-0.001	-0.520
31	0.297	0.143	0.431	0.045	0.251	0.241	0.533	0.082	0.158	0.075	0.174	-0.018
32	0.272	0.169	0.341	0.143	0.231	0.224	0.349	0.222	0.142	0.091	0.143	0.029

TABLE 4. CONTINUED

8465 Pound vehicle									Fwd. c.g.			
REC	ZCOLL		Y50		Y90		Y140		Y220B		Y220T	
	REAL	IMAG	REAL	IMAG	REAL	IMAG	REAL	IMAG	REAL	IMAG	REAL	IMAG
1	0.086	-0.020	-0.034	0.053	-0.013	0.041	-0.006	0.027	0.018	0.012	-0.060	0.049
2	0.067	-0.027	-0.068	0.056	-0.023	0.046	-0.008	0.031	0.035	0.014	-0.074	0.082
3	0.049	-0.101	-0.052	0.076	-0.021	0.058	-0.009	0.037	0.027	0.016	-0.085	0.097
4	0.039	-0.146	-0.069	0.065	-0.024	0.051	-0.010	0.033	0.046	0.012	-0.089	0.132
5	0.023	-0.166	-0.099	0.064	-0.031	0.050	-0.014	0.028	0.061	0.005	-0.141	0.172
6	0.001	-0.208	-0.136	0.141	-0.051	0.090	-0.022	0.050	-0.069	-0.038	-0.266	0.322
7	0.032	-0.015	-0.068	0.089	-0.027	0.065	-0.008	0.039	0.029	0.019	-0.120	0.037
8	0.062	-0.138	-0.050	0.090	-0.018	0.069	-0.006	0.045	0.034	0.016	-0.101	0.105
9	0.052	-0.137	-0.061	0.079	-0.019	0.069	-0.004	0.048	0.045	0.030	-0.142	0.125
10	0.053	-0.107	-0.069	0.081	-0.023	0.063	-0.010	0.045	0.035	0.022	-0.130	0.105
11	0.066	-0.139	-0.065	0.078	-0.024	0.084	-0.013	0.059	0.040	0.048	-0.186	0.075
12	0.067	-0.065	-0.002	0.093	0.004	0.048	0.006	0.030	0.019	-0.011	-0.011	-0.044
13	0.037	-0.100	0.009	0.085	0.007	0.057	0.005	0.039	0.018	0.002	-0.047	0.005
14	0.099	-0.032	0.009	0.109	0.003	0.054	0.001	0.031	0.003	-0.017	-0.064	-0.034
15	0.025	0.012	-0.034	0.080	-0.016	0.028	-0.010	0.012	0.001	-0.036	0.059	-0.056
16	0.042	-0.006	-0.049	0.061	-0.025	0.018	-0.012	0.006	0.002	-0.033	0.080	-0.051
17	-0.025	0.070	-0.013	0.054	-0.013	0.020	-0.010	0.007	-0.011	-0.028	0.015	-0.069
18	0.039	-0.038	-0.046	0.096	-0.019	0.072	-0.006	0.042	0.028	0.022	-0.164	0.010
19	0.050	-0.011	-0.059	0.075	-0.025	0.060	-0.010	0.033	0.020	0.017	-0.120	-0.013
20	0.093	-0.077	0.018	0.047	0.005	0.054	-0.004	0.034	-0.015	0.034	-0.170	0.068
21	-0.133	-0.094	-0.015	0.035	-0.011	0.022	-0.011	0.013	-0.005	-0.005	-0.030	0.002
22	0.039	0.094	0.047	0.070	-0.012	0.042	-0.010	0.017	-0.056	-0.015	-0.106	-0.202
23	0.153	0.014	-0.008	0.052	-0.016	0.042	-0.012	0.026	-0.018	0.003	-0.112	-0.041
24	0.070	-0.024	-0.048	[illegible]	-0.013	0.042	-0.005	0.026	0.032	0.023	[illegible]	0.089
25	-0.058	-0.416	0.037	0.106	0.017	0.146	0.002	0.118	0.017	0.123	-0.416	0.704
26	-0.044	-0.468	0.023	0.223	0.006	0.170	-0.011	0.112	0.001	0.033	-0.431	0.234
27	-0.125	-0.396	0.041	0.213	0.014	0.122	0.003	0.074	0.019	-0.016	-0.105	0.280
28	-0.031	-0.432	-0.013	0.143	-0.005	0.127	-0.011	0.095	0.022	0.051	-0.312	0.370
29	-0.069	-0.564	-0.064	0.137	-0.026	0.143	-0.017	0.118	0.054	0.087	-0.267	0.628
30	-0.038	-0.590	-0.014	0.252	-0.012	0.191	-0.013	0.122	0.015	0.036	-0.311	0.565
31	0.189	-0.029	0.062	0.119	0.000	0.100	-0.022	0.068	-0.061	0.035	-0.269	0.052
32	0.167	0.023	-0.075	0.159	-0.041	0.102	-0.020	0.056	0.016	-0.001	-0.184	-0.077

TABLE 4. CONTINUED

8465 Pound vehicle							Fwd. c.g.					
REC	Y300		Y380		Y440		Y490		Y517		X140	
	REAL	IMAG	REAL	IMAG	REAL	IMAG	REAL	IMAG	REAL	IMAG	REAL	IMAG
1	0.026	-0.045	-0.009	-0.067	-0.082	-0.108	-0.135	-0.114	-0.271	-0.103	0.010	0.012
2	0.046	-0.037	-0.013	-0.049	-0.103	-0.077	-0.206	-0.059	-0.356	0.014	0.018	0.011
3	0.047	-0.041	-0.027	0.011	-0.082	0.045	-0.194	0.059	-0.336	0.055	0.023	0.015
4	0.045	-0.056	-0.024	-0.039	-0.161	0.024	-0.225	0.206	-0.663	0.039	0.030	0.009
5	0.043	-0.081	-0.087	-0.065	-0.326	0.017	-0.256	0.168	-0.888	0.324	0.033	0.009
6	0.040	-0.079	-0.176	0.085	-0.503	0.347	-0.764	0.433	-1.233	1.107	0.027	0.023
7	0.031	-0.030	-0.051	-0.021	-0.186	0.023	-0.246	0.027	-0.420	-0.075	0.003	0.017
8	0.046	-0.051	0.008	-0.018	-0.094	0.048	-0.197	0.023	-0.353	0.036	0.028	0.015
9	0.056	-0.045	-0.021	-0.018	-0.116	0.020	-0.232	-0.019	-0.400	-0.065	0.028	0.020
10	0.052	-0.043	-0.009	-0.020	-0.124	0.019	-0.277	0.047	-0.442	0.022	0.024	0.015
11	0.026	-0.044	-0.057	-0.059	-0.225	-0.058	-0.319	-0.016	-0.579	-0.045	0.019	0.021
12	0.027	-0.052	-0.047	-0.059	0.052	-0.089	0.020	-0.098	-0.076	0.040	-0.005	0.011
13	0.030	-0.046	0.065	-0.057	0.061	-0.052	-0.057	-0.030	-0.139	0.017	0.007	0.009
14	0.023	-0.070	0.024	-0.100	0.002	-0.157	0.033	-0.122	-0.085	0.048	-0.004	0.021
15	-0.001	-0.061	0.013	-0.103	0.030	-0.140	0.032	-0.103	-0.053	0.029	-0.011	-0.016
16	0.001	-0.052	0.028	-0.110	0.057	-0.180	0.038	-0.127	0.004	-0.010	-0.014	-0.013
17	-0.003	-0.041	0.001	-0.087	0.065	-0.159	0.000	-0.102	0.022	-0.062	-0.015	-0.010
18	0.025	-0.051	-0.058	-0.045	-0.210	-0.041	-0.282	-0.087	-0.403	-0.096	0.003	0.021
19	0.034	-0.025	-0.049	-0.046	-0.216	0.054	-0.324	-0.032	-0.294	-0.129	0.002	0.024
20	-0.048	-0.036	-0.103	-0.021	-0.178	0.022	-0.072	-0.024	0.123	-0.005	0.011	0.012
21	-0.002	-0.032	0.022	-0.023	0.055	0.051	0.018	0.025	0.012	0.012	0.015	-0.010
22	-0.019	-0.083	-0.036	-0.210	-0.145	-0.371	-0.027	-0.252	0.088	-0.157	-0.014	0.016
23	-0.010	-0.047	-0.061	-0.084	-0.141	-0.118	-0.110	-0.102	0.182	0.154	0.001	0.011
24	0.046	-0.028	-0.011	-0.051	-0.096	-0.083	-0.197	-0.102	-0.346	-0.069	0.020	0.014
25	-0.060	0.035	-0.238	0.401	-0.399	0.881	-0.367	0.608	-0.232	0.819	0.069	0.039
26	-0.086	-0.029	-0.272	0.219	-0.594	0.636	-0.553	0.520	-0.364	1.233	0.043	0.035
27	-0.078	-0.008	-0.100	0.327	-0.082	0.898	-0.155	0.905	0.338	1.691	0.053	-0.002
28	-0.035	-0.007	-0.202	0.182	-0.473	0.541	-0.416	0.313	-0.418	0.969	0.046	0.016
29	-0.039	0.017	-0.257	0.316	-0.496	0.888	-0.501	0.566	-0.417	1.104	0.062	0.001
30	-0.073	-0.022	-0.292	0.402	-0.541	1.162	-0.563	1.134	-0.039	1.815	0.062	0.007
31	-0.095	-0.081	-0.249	-0.113	-0.413	-0.130	-0.263	-0.046	-0.009	0.057	0.016	0.047
32	0.011	-0.117	-0.147	-0.184	-0.432	-0.218	-0.441	-0.082	-0.470	0.202	0.001	0.028

TABLE 4. CONTINUED

8465 Pound vehicle Fwd. c.g.

REC	X180T REAL	X180T IMAG	X540 REAL	X540 IMAG	X200R REAL	X200R IMAG	X200L REAL	X200L IMAG	X190R REAL	X190R IMAG	X220L REAL	X220L IMAG
1	-0.044	-0.067	-0.596	-0.175	0.046	-0.017	0.007	0.041	0.028	-0.024	-0.001	0.009
2	-0.069	-0.061	-0.532	-0.135	0.063	-0.021	-0.001	0.044	0.024	-0.027	-0.001	0.006
3	-0.089	-0.070	-0.502	0.122	0.066	-0.037	0.011	0.057	0.026	-0.039	0.008	0.019
4	-0.121	-0.070	-0.715	0.374	0.087	-0.052	0.015	0.036	0.024	-0.061	0.010	0.018
5	-0.174	-0.090	-0.674	0.476	0.099	-0.062	0.014	0.065	0.023	-0.073	0.016	0.020
6	-0.225	-0.118	-0.523	0.576	0.112	-0.089	-0.007	0.119	0.041	-0.099	0.003	0.038
7	-0.079	-0.135	-0.297	-0.082	0.004	-0.051	-0.014	0.063	0.020	-0.033	-0.003	0.012
8	-0.100	-0.092	-0.678	0.203	0.078	-0.046	0.014	0.065	0.033	-0.054	0.010	0.020
9	-0.118	-0.123	-0.619	0.173	0.083	-0.037	0.011	0.067	0.025	-0.064	0.012	0.020
10	-0.110	-0.094	-0.527	0.093	0.081	-0.035	0.007	0.062	0.033	-0.047	0.010	0.020
11	-0.105	-0.145	-0.684	0.047	0.072	-0.034	0.010	0.073	0.029	-0.080	0.002	0.027
12	0.070	-0.022	-0.469	0.145	0.012	-0.024	-0.002	0.034	0.036	-0.020	-0.011	0.021
13	0.015	-0.056	-0.454	0.320	0.018	-0.037	0.017	0.036	0.033	-0.036	-0.002	0.020
14	0.067	-0.126	-0.502	-0.019	0.020	-0.016	0.001	0.052	0.031	-0.030	-0.014	0.027
15	0.079	0.053	-0.150	-0.033	-0.016	-0.041	-0.006	0.002	0.009	-0.004	-0.009	-0.010
16	0.107	0.051	-0.221	-0.006	-0.012	-0.028	-0.022	-0.017	0.008	0.003	-0.015	-0.007
17	0.123	0.024	0.053	-0.197	-0.025	-0.018	-0.016	-0.001	0.007	0.009	-0.012	-0.007
18	-0.097	-0.167	-0.328	-0.059	-0.051	-0.018	-0.003	0.069	0.025	-0.036	-0.001	0.016
19	-0.047	-0.147	-0.324	-0.119	[illegible]	-0.004	-0.020	0.057	0.029	-0.030	-0.006	0.015
20	-0.107	-0.143	-0.543	-0.008	0.021	-0.032	0.035	0.064	0.025	-0.058	0.009	0.015
21	-0.049	0.025	0.345	0.464	0.011	-0.054	0.016	0.021	-0.030	-0.056	0.020	0.001
22	0.112	-0.178	-0.004	-0.538	0.003	0.007	-0.038	0.055	0.025	0.003	-0.006	0.015
23	0.041	-0.165	-0.660	-0.307	0.033	-0.004	0.005	0.059	0.041	-0.022	-0.008	0.014
24	-0.122	-0.096	-0.479	-0.180	0.062	-0.011	0.010	0.041	0.017	-0.033	0.006	0.008
25	-0.637	-0.132	-0.975	1.336	0.146	-0.125	0.088	0.159	-0.022	-0.192	0.056	0.052
26	-0.315	-0.265	-0.847	1.341	0.107	-0.117	0.046	0.152	0.056	-0.171	0.035	0.071
27	-0.166	-0.043	-0.333	1.509	0.058	-0.176	0.076	0.112	0.019	-0.143	0.047	0.040
28	-0.315	-0.140	-0.877	1.332	0.105	-0.121	0.053	0.111	0.038	-0.158	0.033	0.045
29	-0.396	-0.028	-1.023	1.605	0.145	-0.162	0.061	0.114	0.031	-0.168	0.040	0.030
30	-0.310	-0.025	-0.996	1.817	0.141	-0.211	0.061	0.167	0.062	-0.190	0.050	0.048
31	-0.129	-0.280	-0.017	-0.422	0.058	-0.016	0.028	0.121	0.064	-0.066	0.011	0.035
32	-0.033	-0.229	-0.785	-0.580	0.074	-0.030	-0.044	0.112	0.056	-0.048	-0.004	0.025

TABLE 4. CONTINUED

REC	9075 Pound vehicle Z50 REAL	Z50 IMAG	Z100T REAL	Z100T IMAG	Z210T REAL	Z210T IMAG	Z340 REAL	Z340 IMAG	Z400 REAL	Z400 IMAG	Z460 REAL	Z460 IMAG	Fwd. c.g. Z540 REAL	Z540 IMAG
1	-0.085	-0.002	-0.014	-0.014	-0.062	-0.017	0.297	0.005	0.198	0.027	-0.046	0.021	-0.592	-0.034
2	-0.147	-0.011	-0.054	-0.017	-0.114	-0.028	0.239	0.036	0.168	0.051	-0.028	0.024	-0.497	-0.089
3	-0.174	-0.026	-0.078	-0.045	-0.097	-0.048	0.220	-0.113	0.007	-0.155	-0.015	0.042	-0.410	0.156
4	-0.148	-0.013	-0.066	-0.057	-0.139	-0.043	0.290	-0.248	0.217	-0.137	-0.009	0.030	-0.605	0.336
5	-0.169	-0.021	-0.081	-0.057	-0.129	-0.016	0.310	-0.251	0.227	-0.128	-0.025	0.072	-0.657	0.497
6	-0.230	-0.078	-0.124	-0.088	-0.175	-0.002	0.294	-0.341	0.215	-0.212	0.041	0.050	-0.426	0.574
7	-0.145	-0.086	-0.043	-0.058	-0.116	-0.069	0.193	0.069	0.118	0.076	-0.045	0.042	-0.392	-0.077
8	-0.174	-0-066	-0.077	-0.057	-0.111	-0.061	-0.220	-0.087	-0.110	0.108	-0.033	0.012	-0.441	0.029
9	-0.170	-0.073	-0.072	-0.068	-0.203	-0.103	0.143	0.274	0.217	-0.003	-0.031	0.003	-0 545	-0.076
10	-0.152	-0.062	-0.060	-0.049	-0.074	-0.054	0.233	-0.038	0.154	-0.004	-0.028	-0.026	-0.425	0.003
11	-0.154	-0.050	-0.060	-0.055	-0.114	-0.112	0.005	-0.257	0.163	-0.001	-0.022	0.028	-0.453	-0.003
12	-0.03[illegible]	-0.031	0.015	-0.040	0.018	-0.049	0.129	0.234	-0.114	0.122	-0.036	0.013	-0.447	0.047
13	-0.035	-0.010	0.020	-0.036	0.028	-0.049	0.265	-0.093	-0.164	-0.056	-0.042	-0.003	-0.436	0.115
14	-0.017	-0.069	0.027	-0.051	0.003	-0.062	0.266	0.004	0.168	0.012	-0.047	-0.003	-0.489	-0.015
15	0.075	0.044	0.072	0.023	0.088	-0.018	0.146	0.061	0.089	0.062	0.004	0.035	-0.226	-0.073
16	0.092	0.029	0.038	0.028	0.090	-0.001	-0.012	0.146	-0.025	0.106	-0.004	0.014	0.017	-0.166
17	0.056	0.018	0.036	0.029	0.063	-0.038	0.087	0.166	0.056	0.123	-0.018	0.019	-0.133	-0.255
18	0.066	0.014	0.029	0.028	0.049	-0.011	-0.030	0.158	-0.036	0.103	-0.014	-0.006	0.062	-0.272
19	0.099	-0.057	0.070	-0.006	0.068	-0.070	-0.010	0.156	-0.009	0.110	-0.017	-0.014	-0.003	-0.245
20	-0.021	-0.117	0.056	-0.090	0.003	-0.126	0.367	0.081	0.242	0.062	-0.037	-0.029	-0.660	-0.223
21	-0.106	-0.059	-0.104	-0.081	-0.147	-0.052	-0.221	-0.267	-0.134	-0.191	-0.010	-0.002	0.245	0.426
22	-0.101	-0.068	-0.066	-0.086	-0.108	-0.093	-0.044	-0.251	-0.022	-0.163	-0.007	-0.001	0.005	0.332
23	0.005	-0.051	0.062	-0.026	0.002	-0.075	0.299	0.158	0.217	0.118	-0.005	-0.039	-0.546	-0.368
24	-0.178	-0.114	-0.096	-0.181	-0.077	-0.085	0.258	-0.704	0.224	-0.495	0.067	-0.048	-0.453	0.985
25	-0.225	-0.199	-0.099	-0.251	-0.160	-0.104	0.372	-0.828	0.318	-0.546	0.046	-0.064	-0.719	1.061
26	-0.272	-0.249	-0.117	-0.248	-0.282	-0.188	0.507	-0.490	0.370	-0.305	0.039	-0.013	-0.914	0.623
27	-0.065	-0.126	0.008	-0.200	-0.012	-0.094	0.400	-0.659	0.329	-0.411	0.095	0.035	-0.572	0.999
28	-0.378	-0.198	-0.184	-0.249	-0.373	-0.120	0.519	-0.630	0.416	-0.425	0.030	-0.006	-0.907	0.892
29	-0.500	-0.309	-0.271	-0.359	-0.320	0.032	0.583	-0.070	0.433	-0.716	0.021	-0.068	-1.009	1.426
30	-0.359	-0.310	-0.183	-0.363	-0.242	-0.107	0.461	-1.044	0.327	-0.719	0.001	-0.094	-0.863	1.367
31	-0.111	-0.125	0.009	-0.091	-0.103	-0.127	0.584	0.094	0.420	0.096	-0.008	-0.013	-0.996	-0.268
32	-0.059	-0.026	0.023	0.001	-0.058	-0.045	0.397	0.312	0.268	0.246	-9.013	0.009	-0.692	-0.581

TABLE 4. CONTINUED

9075 Pound vehicle												Fwd. c.g.
REC	Z90R		Z90L		Z140R		Z140L		Z200R		Z200L	
	REAL	IMAG	REAL	IMAG	REAL	IMAG	REAL	IMAG	REAL	IMAG	REAL	IMAG
1	-0.014	0.005	-0.005	-0.027	0.024	0.002	0.025	-0.023	0.113	0.027	0.108	-0.082
2	-0.043	0.008	-0.040	-0.035	0.005	0.006	0.002	-0.029	0.102	0.061	0.076	-0.091
3	-0.051	-0.011	-0.063	-0.068	-0.009	-0.020	-0.017	-0.067	0.092	0.006	0.037	-0.202
4	-0.032	-0.019	-0.058	-0.088	0.006	-0.041	-0.016	-0.101	-0.113	-0.043	0.013	-0.297
5	-0.035	-0.010	-0.068	-0.097	0.007	-0.032	-0.020	-0.108	0.148	0.009	0.004	-0.328
6	-0.058	-0.049	-0.102	-0.146	-0.001	-0.064	-0.040	-0.155	0.060	0.140	-0.032	-0.432
7	-0.063	-0.008	-0.036	-0.079	-0.022	0.005	0.006	-0.054	0.018	0.114	0.110	-0.124
8	-0.056	-0.018	-0.068	-0.085	-0.009	-0.016	-0.016	-0.073	0.099	0.055	0.044	-0.185
9	-0.038	0.011	-0.080	-0.120	-0.001	0.013	-0.027	-0.106	0.174	0.145	0.005	-0.304
10	-0.042	-0.019	-0.050	-0.074	-0.002	-0.020	-0.006	-0.063	0.103	0.041	0.057	-0.156
11	-0.051	0.007	-0.061	-0.105	-0.010	-0.008	-0.013	-0.097	0.108	0.108	0.054	-0.274
12	0.017	-0.016	0.006	-0.034	0.036	-0.018	0.028	-0.032	0.058	0.116	0.099	-0.060
13	-0.031	-0.005	0.006	-0.030	0.041	-0.026	0.027	-0.035	-0.000	-0.148	0.096	-0.086
14	0.023	-0.026	0.014	-0.049	0.040	-0.021	0.035	-0.033	0.109	-0.000	0.113	-0.047
15	0.053	0.014	0.053	0.043	0.051	0.005	0.044	0.037	0.065	-0.042	0.069	0.095
16	0.032	0.015	0.032	0.040	0.014	0.026	0.014	0.047	-0.012	0.015	-0.001	0.120
17	0.033	0.016	0.035	0.043	0.028	0.023	0.028	0.051	0.034	0.017	0.040	0.136
18	0.009	0.014	0.030	0.036	-0.003	0.022	0.014	0.042	0.057	0.024	0.027	0.118
19	0.018	-0.024	0.058	0.010	-0.000	-0.006	0.036	0.030	-0.087	-0.016	0.091	0.144
20	0.015	-0.025	0.046	-0.075	0.041	-0.008	0.078	-0.053	0.084	0.091	0.022	-0.083
21	-0.097	-0.041	-0.088	-0.078	-0.097	-0.046	-0.091	-0.081	-0.164	-0.060	-0.159	-0.192
22	-0.060	-0.045	-0.067	-0.082	-0.050	-0.049	-0.055	-0.088	-0.046	-0.058	-0.088	-0.221
23	0.027	0.009	0.060	-0.027	0.038	0.018	0.076	-0.003	0.052	0.093	0.204	-0.002
24	-0.040	-0.132	-0.126	-0.194	-0.012	-0.161	-0.083	-0.230	0.188	-0.242	-0.156	-0.572
25	-0.070	-0.160	-0.137	-0.273	-0.015	-0.182	-0.077	-0.296	0.189	-0.217	-0.092	-0.691
26	-0.092	-0.137	-0.114	-0.279	-0.021	-0.134	-0.039	-0.263	0.157	-0.037	0.065	-0.615
27	0.009	-0.139	-0.044	-0.189	0.028	-0.168	-0.022	-0.224	0.188	-0.246	-0.055	-0.525
28	-0.142	-0.110	-0.189	-0.278	-0.049	-0.128	-0.090	-0.278	0.184	-0.063	-0.013	-0.708
29	-0.197	-0.206	-0.260	-0.401	-0.091	-0.229	-0.133	-0.412	0.218	-0.205	-0.063	-0.998
30	-0.150	-0.238	-0.186	-0.380	-0.065	-0.255	-0.099	-0.388	0.159	-0.269	-0.039	-0.893
31	0.007	-0.001	0.011	-0.130	0.059	0.013	0.074	-0.099	0.187	0.220	0.267	-0.253
32	0.013	0.076	0.026	-0.038	0.041	0.076	0.064	-0.007	0.120	0.269	0.221	-0.063

TABLE 4. CONTINUED

9075 Pound vehicle							Fwd. c.g.					
REC	Z260R		Z260L		Z396R		Z396L		ZLONG		ZLATR	
	REAL	IMAG	REAL	IMAG	REAL	IMAG	REAL	IMAG	REAL	IMAG	REAL	IMAG
1	0.183	-0.010	0.190	-0.028	0.202	0.032	0.201	0.024	0.031	0.071	0.082	-0.022
2	0.150	0.011	0.161	-0.007	0.156	0.066	0.142	0.033	0.064	0.003	0.068	-0.018
3	0.125	-0.082	0.127	-0.123	0.055	0.142	-0.045	-0.139	0.048	-0.044	0.046	-0.068
4	0.142	-0.166	0.143	-0.222	-0.039	-0.219	0.216	-0.185	0.057	-0.085	0.046	-0.119
5	0.159	-0.171	0.167	-0.225	-0.016	-0.226	0.199	-0.229	0.066	-0.078	0.049	-0.120
6	0.120	-0.210	0.160	-0.295	0.146	-0.163	0.126	-0.326	0.069	-0.110	0.046	-0.159
7	0.108	0.036	0.137	0.013	0.136	0.110	0.004	0.102	0.043	0.017	0.006	-0.063
8	0.130	-0.044	0.137	-0.091	0.141	0.041	-0.080	0.127	0.058	-0.026	0.056	-0.058
9	0.006	-0.158	0.172	-0.101	0.205	0.048	0.081	0.196	0.073	-0.021	0.049	-0.074
10	-0.094	0.190	0.153	-0.073	0.161	0.036	-0.011	0.133	0.059	-0.022	0.061	-0.044
11	0.135	-0.061	0.148	-0.124	0.173	0.082	0.140	0.073	0.059	-0.034	0.053	-0.079
12	-0.119	0.136	0.004	-0.171	0.165	-0.016	-0.136	0.124	0.068	-0.027	0.068	-0.029
13	0.175	-0.079	0.165	-0.084	-0.165	-0.040	-0.147	-0.068	0.072	-0.040	0.066	-0.043
14	0.173	-0.010	0.070	0.165	0.163	0.012	0.183	0.010	-0.053	0.051	-0.069	-0.031
15	0.111	0.010	0.104	0.049	0.070	-0.022	0.107	0.120	0.045	0.005	0.044	0.021
16	-0.004	0.096	-0.006	0.107	-0.000	0.064	-0.000	0.130	-0.006	0.038	-0.008	0.054
17	0.044	0.083	0.056	0.121	0.130	0.067	0.027	0.177	0.028	0.044	0.028	0.066
18	-0.036	0.101	-0.015	0.118	0.029	0.085	-0.050	0.122	-0.015	0.043	-0.007	0.057
19	-0.006	0.073	0.007	0.110	-0.014	0.072	0.024	0.118	-0.016	0.035	0.007	0.061
20	0.202	0.033	0.268	0.017	0.218	0.069	0.251	0.038	0.100	-0.002	0.121	-0.035
21	-0.189	-0.150	-0.180	-0.192	-0.119	-0.139	-0.136	-0.197	-0.106	-0.075	-0.111	-0.093
22	-0.059	-0.152	-0.065	-0.196	-0.034	-0.141	-0.015	-0.191	-0.037	-0.078	-0.040	-0.099
23	0.178	0.096	0.228	0.094	0.157	0.123	0.257	0.084	0.090	0.043	0.100	0.028
24	0.065	-0.465	0.083	-0.527	0.100	-0.439	0.207	-0.409	0.027	-0.248	-0.019	-0.277
25	0.107	-0.510	0.162	-0.619	0.152	-0.446	0.319	-0.500	0.047	-0.271	0.011	-0.318
26	0.184	-0.351	0.271	-0.429	0.252	-0.262	0.426	-0.292	0.078	-0.175	0.063	-0.249
27	0.140	-0.454	0.152	-0.488	0.244	-0.391	0.365	-0.366	0.053	-0.249	0.020	-0.272
28	0.133	-0.400	0.245	-0.543	0.241	-0.316	0.497	-0.408	0.073	-0.211	0.039	-0.282
29	0.144	-0.610	0.285	-0.833	0.073	-0.478	0.496	-0.730	0.070	-0.336	0.033	-0.407
30	0.086	-0.636	0.197	-0.792	0.127	-0.524	0.372	-0.614	0.046	-0.341	0.014	-0.398
31	0.301	0.043	0.399	-0.021	0.289	0.108	0.504	0.071	0.157	0.014	0.157	-0.032
32	0.229	0.184	0.277	0.152	0.210	0.232	0.311	0.265	0.114	0.091	0.125	0.053

TABLE 4. CONTINUED

9075 Pound vehicle									Fwd. c.g.			
	ZCOLL		Y50		Y90		Y140		Y220B		Y220T	
REC	REAL	IMAG	REAL	IMAG	REAL	IMAG	REAL	IMAG	REAL	IMAG	REAL	IMAG
1	0.074	-0.032	-0.032	0.026	-0.013	0.022	-0.004	0.017	-0.018	0.012	-0.109	0.129
2	0.057	-0.023	-0.041	0.034	-0.015	0.029	-0.006	0.020	0.032	0.003	-0.155	0.148
3	0.034	-0.084	-0.045	0.024	-0.018	0.023	-0.008	0.018	0.030	0.001	-0.109	0.196
4	0.028	-0.135	-0.064	0.038	-0.031	0.025	-0.015	0.014	0.034	-0.013	-0.096	0.209
5	0.031	-0.136	-0.053	0.043	-0.030	0.028	-0.022	0.009	0.024	-0.028	-0.134	0.261
6	0.025	-0.181	-0.071	0.046	-0.047	0.033	-0.038	0.015	0.013	-0.023	-0.274	0.413
7	0.052	-0.021	-0.033	0.062	-0.014	0.041	-0.004	0.019	0.001	-0.023	-0.237	0.072
8	0.042	-0.067	-0.036	0.026	-0.015	0.026	-0.006	0.020	0.029	0.002	-0.176	0.169
9	0.042	-0.093	-0.020	0.036	-0.011	0.041	-0.012	0.020	0.002	-0.021	-0.245	0.227
10	0.047	-0.058	-0.028	0.044	-0.012	0.035	-0.005	0.021	0.001	-0.028	-0.151	0.166
11	0.044	-0.098	-0.032	0.029	-0.018	0.037	-0.011	0.021	-0.018	0.016	-0.216	0.128
12	0.067	-0.036	0.014	0.067	0.004	0.040	0.004	0.029	-0.002	-0.015	-0.043	-0.011
13	0.071	-0.050	-0.004	0.073	0.002	0.043	0.002	0.028	-0.001	-0.018	-0.035	0.005
14	0.006	-0.082	0.019	0.075	0.011	0.045	0.004	0.029	-0.004	-0.015	-0.080	0.003
15	0.057	0.023	-0.029	0.067	-0.016	0.037	-0.012	0.026	-0.005	-0.007	0.038	-0.090
16	-0.003	0.060	-0.023	0.052	-0.013	0.029	-0.013	0.021	-0.003	-0.003	0.032	-0.078
17	0.036	0.063	-0.020	0.060	-0.013	0.034	-0.009	0.022	-0.003	-0.005	0.038	-0.067
18	-0.007	0.063	-0.013	0.073	-0.009	0.039	-0.006	0.027	-0.006	-0.010	0.008	-0.082
19	0.013	0.057	0.012	0.080	0.001	0.043	0.003	0.028	-0.004	-0.007	-0.048	-0.168
20	0.113	-0.025	0.017	0.040	0.004	0.032	-0.001	0.013	-0.010	-0.006	-0.166	0.043
21	-0.117	-0.096	-0.015	0.022	-0.010	0.015	-0.009	0.007	-0.007	-0.015	0.064	0.058
22	-0.053	-0.108	-0.024	0.015	-0.012	0.015	-0.011	0.009	-0.003	-0.014	-0.028	0.072
23	0.119	0.029	0.015	0.042	0.003	0.030	0.003	0.014	-0.002	-0.015	-0.145	0.013
24	-0.064	-0.294	-0.053	0.128	-0.041	0.069	-0.039	0.038	-0.000	-0.050	-0.075	0.207
25	-0.027	-0.360	0.003	0.095	-0.023	0.063	-0.036	0.045	-0.016	-0.015	-0.205	0.299
26	0.034	-0.274	0.058	0.119	0.006	0.076	-0.020	0.038	-0.030	-0.037	-0.404	0.305
27	-0.017	-0.290	-0.066	0.135	-0.040	0.082	-0.036	0.052	0.008	-0.039	-0.097	0.163
28	0.017	-0.330	0.111	0.091	0.026	0.080	-0.015	0.046	-0.051	-0.020	-0.394	0.523
29	-0.012	-0.482	0.130	0.134	0.028	0.099	-0.017	0.070	-0.056	-0.010	-0.377	0.839
30	-0.024	-0.494	0.087	0.146	0.011	0.088	-0.021	0.056	-0.046	-0.037	-0 375	0.511
31	0.161	-0.066	0.098	0.064	0.029	0.049	0.003	0.023	-0.027	-0.016	-0.317	0.168
32	0.156	0.055	0.013	0.051	-0.014	0.044	-0.009	0.024	0.016	-0.012	-0.182	0.070

TABLE 4. CONTINUED

9075 Pound vehicle							Fwd. c.g.					
REC	Y300		Y380		Y440		Y490		Y517		X140	
	REAL	IMAG	REAL	IMAG	REAL	IMAG	REAL	IMAG	REAL	IMAG	REAL	IMAG
1	0.026	-0.050	-0.047	-0.085	0.154	-0.144	-0.220	-0.135	-0.364	-0.082	0.018	0.009
2	0.035	-0.053	-0.051	-0.068	-0.171	-0.073	-0.231	0.004	-0.380	0.130	0.022	0.008
3	0.034	-0.056	-0.049	-0.061	-0.156	-0.052	-0.241	-0.033	-0.331	0.013	0.023	0.012
4	0.023	-0.084	-0.091	-0.050	-0.305	0.012	-0.365	0.139	-0.641	0.134	0.038	0.007
5	-0.011	-0.123	-0.156	-0.126	-0.398	-0.064	-0.353	0.208	-0.718	0.298	0.034	0.005
6	-0.053	-0.100	-0.314	-0.014	-0.620	0.148	-0.430	0.262	-0.937	0.670	0.030	0.009
7	0.034	-0.076	-0.063	-0.122	-0.234	-0.137	-0.360	-0.147	-0.521	-0.154	0.008	0.016
8	0.035	-0.064	-0.034	-0.072	-0.144	-0.061	-0.205	-0.050	-0.329	0.035	0.030	0.017
9	-0.015	-0.011	-0.137	-0.141	-0.310	-0.161	-0.347	-0.114	-0.358	0.063	0.032	0.022
10	0.033	-0.061	-0.044	-0.058	-0.152	-0.014	-0.272	0.014	-0.343	0.116	0.022	0.013
11	0.022	-0.094	-0.056	-0.142	-0.178	-0.184	-0.324	-0.081	-0.530	0.023	0.023	0.018
12	0.018	-0.041	0.006	-0.046	-0.011	-0.049	0.037	-0.077	-0.067	0.104	0.004	0.005
13	0.018	-0.046	-0.015	-0.044	-0.066	-0.015	-0.097	0.014	-0.101	0.179	0.005	0.005
14	0.014	-0.047	-0.006	-0.055	-0.066	0.006	-0.090	-0.051	-0.014	0.105	0.004	0.013
15	0.003	-0.023	0.024	-0.053	0.023	-0.098	0.014	-0.092	0.001	-0.065	-0.014	-0.013
16	-0.006	-0.014	0.008	-0.043	0.056	-0.031	0.018	-0.085	0.053	-0.057	-0.018	-0.010
17	0.005	-0.020	-0.004	-0.079	0.080	-0.034	0.057	-0.142	0.030	-0.066	-0.011	-0.004
18	0.005	-0.015	0.022	-0.052	0.060	-0.049	0.064	-0.071	0.061	-0.069	-0.020	-0.004
19	0.027	-0.009	0.038	-0.034	0.062	-0.070	0.020	-0.077	-0.033	-0.114	-0.023	0.006
20	0.016	-0.058	-0.026	-0.061	-0.109	-0.073	-0.043	-0.083	-0.043	0.027	0.007	0.018
21	-0.001	-0.038	0.011	-0.014	0.010	0.075	-0.010	0.040	-0.009	-0.007	0.014	-0.009
22	0.001	-0.044	0.002	-0.011	-0.004	0.042	0.006	0.045	0.017	0.035	0.019	0.004
23	0.014	-0.059	-0.027	-0.071	-0.080	-0.132	-0.011	-0.001	-0.046	0.016	0.003	0.015
24	-0.114	-0.103	-0.395	0.094	-0.705	0.384	-0.529	0.544	-0.439	1.348	0.039	-0.014
25	-0.112	-0.093	-0.351	0.020	-0.735	0.293	-0.383	0.280	-0.322	1.097	0.037	-0.011
26	-0.107	-0.142	-0.361	-0.074	-0.727	0.067	-0.583	0.297	-0.461	0.716	0.042	0.021
27	-0.091	-0.090	-0.306	0.044	-0.573	0.285	-0.474	0.631	-0.430	1.032	0.021	-0.009
28	-0.159	-0.114	-0.405	0.043	-0.684	0.410	-0.511	0.469	-0.194	1.065	0.056	0.011
29	-0.217	-0.081	-0.567	0.265	-1.011	0.816	-0.565	1.083	-0.089	1.904	0.057	0.003
30	-0.183	-0.082	-0.475	0.205	-0.803	0.656	-0.483	0.797	-0.059	1.593	0.050	-0.000
31	-0.071	-0.134	-0.233	-0.141	-0.428	-0.144	-0.290	-0.016	-0.025	0.195	0.032	0.036
32	0.027	-0.119	-0.081	-0.193	-0.271	-0.321	-0.309	-0.193	-0.400	0.048	0.015	0.024

TABLE 4. CONTINUED

	9075 Pound vehicle								Fwd. c.g.			
REC	X180T		X540		X200R		X200L		X190R		X220L	
	REAL	IMAG	REAL	IMAG	REAL	IMAG	REAL	IMAG	REAL	IMAG	REAL	IMAG
1	-0.130	-0.076	-0.535	-0.070	-0.002	-0.068	-0.005	0.036	0.009	-0.039	0.005	0.009
2	-0.173	-0.104	-0.430	-0.121	0.085	-0.031	-0.007	0.051	-0.002	-0.047	0.012	0.008
3	-0.181	-0.096	-0.359	0.134	0.085	-0.040	0.002	0.069	0.011	-0.075	0.010	0.011
4	-0.224	-0.088	-0.558	0.311	0.106	-0.068	0.003	0.085	-0.009	-0.078	0.017	0.014
5	-0.235	-0.092	-0.603	0.415	0.098	-0.079	0.008	0.096	0.006	-0.083	0.019	0.016
6	-0.280	-0.162	-0.444	0.535	0.120	-0.083	-0.014	0.128	0.032	-0.118	0.016	0.023
7	-0.147	-0.205	-0.332	-0.089	0.076	-0.025	-0.019	0.083	0.022	-0.063	-0.001	0.020
8	-0.181	-0.156	-0.384	0.029	0.087	-0.037	0.004	0.085	0.007	-0.061	0.013	0.015
9	-0.288	-0.227	-0.499	-0.063	0.087	-0.064	0.016	0.118	-0.022	-0.104	0.021	0.027
10	-0.154	-0.122	-0.376	-0.004	0.079	-0.038	-0.002	0.081	0.030	-0.071	0.008	0.014
11	-0.179	-0.206	-0.413	-0.013	0.078	-0.051	0.004	0.102	0.014	-0.082	0.015	0.019
12	0.019	-0.043	-0.436	0.134	0.023	-0.035	-0.013	0.041	0.030	-0.022	-0.005	0.010
13	0.026	-0.045	-0.431	0.100	0.023	-0.040	-0.018	0.046	0.034	-0.025	-0.000	0.009
14	0.002	-0.092	-0.475	-0.018	0.033	-0.032	-0.022	0.061	0.040	-0.033	-0.001	0.013
15	0.100	0.042	-0.255	-0.122	-0.013	-0.027	-0.020	-0.004	0.030	0.012	-0.017	-0.010
16	0.143	0.032	-0.018	-0.211	-0.019	-0.016	-0.032	-0.007	0.025	0.023	-0.018	-0.009
17	0.068	-0.007	-0.142	-0.276	-0.010	-0.012	-0.025	-0.000	0.015	0.020	-0.015	-0.005
18	0.112	0.001	0.141	-0.260	-0.017	-0.019	-0.035	0.009	0.010	0.018	-0.020	-0.001
19	0.188	-0.079	-0.031	-0.257	-0.015	0.005	-0.053	0.019	0.035	0.008	-0.024	0.005
20	-0.027	-0.252	-0.629	-0.198	0.051	-0.020	-0.016	0.086	0.039	-0.074	0.004	0.023
21	-0.133	-0.028	0.271	0.440	0.027	-0.064	0.022	0.049	-0.036	-0.073	0.017	0.001
22	-0.132	-0.101	0.016	0.351	0.029	-0.059	0.036	0.064	-0.044	-0.084	0.017	0.011
23	0.027	-0.161	-0.536	-0.340	0.041	-0.019	-0.023	0.062	0.045	-0.043	0.001	0.016
24	-0.137	-0.052	-0.522	1.015	0.099	-0.146	0.012	0.145	0.045	-0.125	0.030	0.015
25	-0.243	-0.098	-0.79[illegible]	1.091	0.103	-0.133	0.023	0.144	0.045	-0.140	0.03[illegible]	0.082
26	-0.387	-0.345	-0.977	0.643	0.143	-0.105	0.008	0.178	0.037	-0.161	0.041	0.050
27	-0.037	-0.062	-0.727	0.980	0.080	-0.132	-0.006	0.131	0.056	-0.111	0.007	0.021
28	-0.560	-0.253	-0.975	0.884	0.133	-0.148	0.051	0.196	-0.012	-0.199	0.054	0.039
29	-0.559	-0.107	-1.080	1.510	0.176	-0.205	0.034	0.267	0.018	-0.231	0.056	0.051
30	-0.371	-0.164	-0.880	1.443	0.140	-0.181	0.030	0.230	0.053	-0.204	0.044	0.042
31	-0.223	-0.330	-0.966	-0.257	0.094	-0.062	-0.004	0.148	0.040	-0.108	0.028	0.035
32	-0.113	-0.219	-0.679	-0.612	0.101	-0.052	-0.051	0.095	0.037	-0.056	0.002	0.020

TABLE 4. CONTINUED

9500 Pound vehicle								Fwd. c.g.						
REC	Z50		Z100T		Z210T		Z340		Z400		Z460		Z540	
	REAL	IMAG	REAL	IMAG	REAL	IMAG	REAL	IMAG	REAL	IMAG	REAL	IMAG	REAL	IMAG
1	-0.080	-0.010	-0.002	-0.011	-0.055	-0.030	0.312	0.026	0.210	0.052	-0.032	0.038	-0.528	-0.034
2	-0.094	-0.011	-0.014	-0.013	-0.065	-0.025	0.312	0.033	0.214	0.053	-0.012	0.037	[illegible]	-0.062
3	-0.170	-0.013	-0.073	-0.022	-0.082	-0.026	0.108	0.218	0.166	0.008	-0.010	0.038	-0.438	0.046
4	-0.131	-0.071	-0.066	-0.061	-0.095	-0.067	0.179	-0.090	-0.008	-0.139	-0.060	0.002	-0.442	0.115
5	-0.210	-0.021	-0.105	-0.053	-0.152	-0.055	0.300	-0.245	0.215	-0.101	-0.033	0.080	-0.664	0.449
6	-0.194	-0.049	-0.125	-0.061	-0.181	-0.061	0.237	-0.199	0.183	-0.102	0.058	0.087	-0.282	0.405
7	-0.176	0.011	-0.070	0.002	-0.149	-0.129	0.171	0.008	0.130	0.055	-0.024	0.070	-0.362	0.083
8	-0.178	-0.025	-0.082	-0.023	-0.125	-0.073	0.217	-0.013	0.154	0.025	-0.033	0.018	-0.485	-0.041
9	-0.225	-0.018	-0.116	-0.032	-0.164	-0.089	0.017	-0.235	0.172	0.009	-0.013	0.028	-0.448	0.029
10	-0.219	-0.069	-0.104	-0.047	-0.151	-0.072	0.224	-0.002	0.169	0.023	-0.001	0.023	-0.437	-0.013
11	-0.185	-0.054	-0.090	-0.054	-0.153	-0.133	0.228	-0.073	0.067	0.167	-0.020	0.040	-0.478	0.051
12	-0.028	-0.026	0.015	-0.042	0.022	-0.060	0.215	-0.079	-0.003	-0.145	-0.028	0.009	-0.401	0.105
13	0.003	-0.059	0.032	-0.051	0.013	-0.062	0.280	-0.046	0.157	-0.011	-0.022	0.003	-0.440	0.050
14	-0.018	-0.070	0.013	-0.061	0.004	-0.098	0.098	0.178	0.105	-0.005	-0.042	-0.001	-0.371	-0.006
15	0.046	0.046	0.040	0.017	0.042	0.006	0.060	0.040	0.033	0.036	-0.013	0.002	-0.160	-0.080
16	0.047	0.040	-0.007	-0.006	0.036	0.012	-0.076	-0.029	-0.045	-0.014	-0.011	0.007	0.039	0.024
17	0.015	0.008	0.009	-0.015	0.024	-0.029	0.029	-0.052	0.024	-0.028	-0.016	-0.001	-0.092	0.067
18	-0.137	0.004	-0.044	-0.097	-0.105	-0.106	0.266	-0.103	0.170	-0.047	-0.048	0.019	-0.542	0.144
19	-0.158	0.014	-0.046	-0.006	-0.017	-0.134	0.193	0.020	0.147	0.051	-0.033	0.060	-0.426	0.038
20	-0.118	-0.099	-0.064	-0.016	0.120	-0.062	0.173	-0.011	0.131	-0.009	-0.018	0.045	-0.382	0.089
21	-0.124	0.092	-0.110	0.031	-0.101	0.081	-0.245	-0.105	-0.145	-0.072	-0.001	-0.003	0.261	0.138
22	0.018	-0.016	-0.026	0.041	0.030	-0.049	-0.245	0.287	-0.160	0.183	0.007	-0.004	0.370	-0.455
23	-0.045	-0.072	0.018	-0.065	0.053	-0.057	0.269	-0.066	0.185	-0.029	-0.022	0.008	-0.499	0.069
24	-0.188	-0.140	-0.097	-0.202	-0.113	-0.080	0.337	-0.689	0.318	-0.473	0.157	-0.007	-0.472	1.051
25	-0.595	-0.265	-0.319	[illegible]	-0.514	0.051	0.669	-0.554	0.527	-0.334	0.092	0.055	-1.102	0.871
26	-0.443	-0.306	-0.258	-0.329	-0.393	-0.104	0.388	-0.756	0.371	-0.514	0.093	-0.032	-0.649	1.061
27	-0.376	-0.130	-0.255	-0.201	-0.213	0.003	0.146	-0.807	0.149	-0.594	0.085	-0.126	-0.223	1.038
28	-0.499	-0.304	-0.251	-0.323	-0.467	-0.099	0.596	-0.513	0.493	-0.307	0.121	0.073	-1.004	0.817
29	-0.350	-0.246	-0.205	-0.322	-0.182	0.049	0.401	-1.021	0.325	-0.716	0.117	-0.061	-0.666	1.425
30	-0.461	-0.432	-0.246	-0.429	-0.452	-0.086	0.500	-0.800	0.412	-0.549	0.079	-0.061	-0.784	1.036
31	-0.067	-0.055	0.015	-0.010	-0.073	-0.046	0.422	0.224	0.308	0.200	-0.021	0.050	-0.779	-0.364
32	-0.075	-0.091	0.023	-0.055	-0.071	-0.097	0.458	0.120	0.354	0.119	0.033	0.031	-0.796	-0.203

TABLE 4. CONTINUED

9500 Pound vehicle							Fwd. c.g.					
REC	Z90R		Z90L		Z140R		Z140L		Z200R		Z200L	
	REAL	IMAG	REAL	IMAG	REAL	IMAG	REAL	IMAG	REAL	IMAG	REAL	IMAG
1	-0.006	0.004	-0.005	-0.017	-0.001	-0.032	0.029	-0.015	0.125	0.052	0.053	0.100
2	-0.014	-0.007	-0.014	-0.018	-0.003	-0.026	-0.002	-0.024	0.114	0.056	-0.075	0.073
3	-0.052	-0.013	-0.062	-0.032	-0.007	-0.022	-0.014	-0.031	0.110	0.023	0.060	-0.085
4	-0.049	-0.049	-0.048	-0.063	-0.016	-0.049	-0.015	-0.064	0.102	0.001	0.072	-0.107
5	-0.073	-0.033	-0.080	-0.081	-0.023	-0.053	-0.030	-0.092	0.062	0.126	0.090	-0.289
6	-0.064	-0.044	-0.086	-0.088	-0.013	-0.054	-0.035	-0.095	0.171	-0.012	0.044	-0.280
7	-0.062	0.018	-0.062	-0.016	-0.024	0.015	-0.020	-0.017	0.057	0.046	0.039	-0.094
8	-0.066	-0.008	-0.077	-0.046	-0.020	-0.012	-0.027	-0.042	0.115	0.081	0.041	-0.113
9	-0.088	0.006	-0.103	-0.061	-0.029	-0.004	-0.048	-0.063	0.129	0.112	0.012	-0.195
10	-0.092	-0.024	-0.098	-0.065	-0.034	-0.015	-0.039	-0.048	0.090	0.088	0.031	-0.107
11	-0.079	-0.020	-0.077	-0.086	-0.028	-0.027	-0.027	-0.081	0.114	0.075	0.080	-0.198
12	0.012	-0.031	0.009	-0.034	0.028	-0.037	0.028	-0.036	0.123	-0.022	0.094	-0.024
13	0.028	-0.039	0.026	-0.043	0.040	-0.031	0.041	-0.031	0.052	0.098	-0.092	-0.035
14	-0.001	-0.044	0.011	-0.051	0.016	-0.039	0.027	-0.038	0.002	-0.108	-0.132	-0.064
15	0.031	0.029	0.013	0.022	0.024	0.017	0.012	0.020	0.031	0.019	-0.019	0.065
16	.0.010	0.019	-0.000	0.008	-0.006	0.002	-0.018	-0.003	-0.025	-0.039	-0.061	-0.048
17	0.003	-0.009	0.009	-0.008	-0.000	-0.017	0.005	-0.014	0.001	-0.058	0.021	-0.023
18	-0.029	-0.045	-0.034	-0.094	0.005	-0.040	0.005	-0.084	0.102	0.052	[illegible]	-0.172
19	-0.049	0.012	-0.046	-0.020	-0.014	0.006	-0.010	-0.017	0.095	0.063	0.059	-0.089
20	-0.057	0.017	-0.058	-0.019	-0.024	0.003	-0.017	-0.022	0.061	0.049	0.039	-0.089
21	-0.094	0.042	-0.108	0.032	-0.092	0.016	-0.111	0.009	-0.093	-0.061	-0.218	-0.084
22	-0.044	0.022	-0.016	0.038	-0.061	0.048	-0.036	0.065	-0.180	0.031	-0.072	0.160
23	0.007	-0.020	0.008	-0.074	0.029	-0.020	0.036	-0.063	0.079	0.078	0.137	0.139
24	-0.044	-0.155	-0.123	-0.202	-0.003	-0.171	-0.067	-0.227	0.263	-0.246	-0.064	-0.561
25	-0.222	-0.089	-0.287	-0.333	-0.052	-0.081	-0.129	-0.307	0.284	0.116	0.072	-0.815
26	-0.206	-0.181	-0.234	-0.331	-0.102	-0.177	-0.138	-0.321	0.158	-0.132	-0.019	-0.750
27	-0.171	-0.150	-0.222	-0.210	-0.101	-0.170	-0.155	-0.243	0.165	-0.255	-0.171	-0.611
28	-0.192	-0.119	-0.237	-0.335	-0.061	-0.094	-0.104	-0.308	0.251	0.093	0.075	-0.763
29	-0.138	-0.209	-0.213	-0.310	-0.052	-0.231	-0.119	-0.342	0.298	-0.298	-0.100	-0.815
30	-0.219	-0.234	-0.229	-0.422	-0.103	-0.196	-0.117	-0.391	0.161	-0.128	0.048	-0.894
31	0.017	0.023	0.007	-0.042	0.060	0.032	0.050	-0.014	0.149	0.177	0.187	-0.049
32	0.016	-0.014	0.016	-0.072	0.058	-0.004	0.062	-0.047	0.142	0.144	0.192	-0.086

TABLE 4. CONTINUED

9500 Pound vehicle							Fwd. c.g.					
REC	Z260R		Z260L		Z396R		Z396L		ZLONG		ZLATR	
	REAL	IMAG	REAL	IMAG	REAL	IMAG	REAL	IMAG	REAL	IMAG	REAL	IMAG
1	0.186	-0.010	0.209	-0.007	0.192	0.053	0.230	0.058	0.085	-0.017	0.013	-0.091
2	0.181	-0.010	0.195	-0.007	0.189	0.042	0.244	0.076	-0.069	-0.038	-0.075	-0.042
3	0.133	-0.052	0.142	-0.066	0.151	0.021	0.154	0.028	0.054	-0.035	0.059	-0.036
4	0.098	-0.080	0.106	-0.096	0.006	-0.155	-0.012	-0.127	0.032	-0.055	0.036	-0.056
5	0.129	-0.202	0.164	-0.211	0.153	-0.147	0.142	0.249	0.048	-0.102	0.050	-0.122
6	0.084	-0.162	0.134	-0.177	0.028	-0.119	0.239	-0.102	0.040	-0.085	0.035	-0.101
7	0.090	0.002	-0.094	-0.041	0.090	0.075	-0.095	0.077	0.012	0.032	0.041	-0.014
8	0.005	-0.121	0.134	-0.052	0.148	0.042	0.181	0.037	0.051	-0.025	0.051	-0.035
9	0.103	-0.053	0.133	-0.084	0.127	0.021	0.182	0.029	0.040	-0.034	0.039	-0.060
10	0.114	-0.014	0.006	-0.146	0.116	0.047	0.191	0.012	0.045	-0.019	0.048	-0.028
11	0.106	-0.076	0.135	-0.104	0.151	0.027	0.187	-0.003	0.040	-0.049	0.048	-0.072
12	0.137	-0.073	0.150	-0.079	0.004	-0.140	0.074	0.147	0.060	-0.047	0.063	-0.046
13	0.006	-0.171	0.002	-0.189	0.065	0.126	0.080	0.199	0.061	-0.030	-0.005	-0.071
14	0.125	-0.056	0.005	-0.142	0.036	0.078	0.146	0.006	0.050	-0.036	0.062	-0.033
15	0.039	0.024	0.036	0.030	0.044	0.045	0.023	0.061	0.018	0.012	0.011	0.010
16	-0.063	-0.030	-0.069	-0.024	-0.050	-0.029	-0.049	0.010	-0.030	-0.012	-0.040	-0.015
17	0.022	-0.037	0.019	-0.040	0.007	-0.077	0.032	-0.040	0.003	-0.018	0.002	-0.023
18	0.149	-0.087	0.176	-0.127	0.139	-0.024	0.196	-0.067	0.064	-0.053	0.063	-0.076
19	0.101	-0.020	0.124	-0.025	0.110	0.074	0.107	0.007	0.040	-0.008	0.047	-0.019
20	0.051	-0.031	0.105	-0.051	0.163	-0.061	0.101	-0.015	0.033	-0.018	0.040	-0.033
21	-0.195	-0.034	-0.206	-0.078	-0.147	-0.036	-0.115	-0.088	-0.111	-0.015	-0.115	-0.026
22	-0.154	0.189	-0.147	0.193	-0.178	0.199	-0.149	0.203	-0.092	0.099	-0.073	0.106
23	0.156	-0.044	0.162	-0.079	0.172	0.018	0.221	0.053	0.078	-0.029	0.075	-0.058
24	0.035	-0.506	0.153	-0.526	0.093	-0.495	0.385	-0.313	0.031	-0.272	0.005	-0.269
25	0.183	-0.376	0.375	-0.520	0.217	-0.253	0.604	-0.311	0.126	-0.185	0.083	-0.269
26	0.016	-0.481	0.171	-0.596	0.090	-0.412	0.465	-0.503	0.011	-0.254	-0.011	-0.305
27	-0.099	-0.488	0.009	-0.607	-0.043	-0.496	0.304	-0.531	-0.036	-0.269	-0.060	-0.291
28	0.156	-0.370	0.318	-0.469	0.167	-0.266	0.579	-0.350	0.106	-0.177	0.055	-0.245
29	0.016	-0.652	0.166	-0.757	0.064	-0.694	0.389	-0.547	0.039	-0.342	-0.009	-0.372
30	0.072	-0.510	0.239	-0.649	0.125	-0.432	0.623	-0.466	0.036	-0.266	0.031	-0.334
31	0.259	0.090	0.302	0.095	0.260	0.174	0.329	0.220	0.143	0.047	0.135	0.031
32	0.241	0.025	0.323	0.015	0.249	0.097	0.419	0.142	0.134	0.002	0.137	-0.013

TABLE 4. CONTINUED

9500 Pound vehicle								Fwd. c.g.				
	ZCOLL		Y50		Y90		Y140		Y220B		Y220T	
REC	REAL	IMAG	REAL	IMAG	REAL	IMAG	REAL	IMAG	REAL	IMAG	REAL	IMAG
1	0.087	-0.027	-0.014	-0.013	-0.008	-0.006	-0.010	-0.005	0.007	-0.016	-0.094	0.129
2	0.004	-0.082	-0.020	-0.014	-0.015	-0.006	-0.010	-0.004	0.007	-0.023	-0.111	0.136
3	0.050	-0.052	-0.023	-0.012	-0.017	-0.006	-0.014	-0.006	0.007	-0.025	-0.144	0.165
4	0.030	-0.071	-0.023	0.020	-0.016	0.008	-0.014	0.003	0.014	-0.030	-0.138	0.130
5	0.036	-0.141	-0.001	-0.029	-0.014	-0.024	-0.020	-0.031	-0.002	-0.068	-0.167	0.241
6	0.020	-0.119	-0.015	0.034	-0.021	-0.007	-0.030	-0.022	-0.013	-0.084	-0.240	0.306
7	0.033	-0.018	-0.025	0.013	-0.017	0.008	-0.013	0.001	0.000	-0.017	-0.116	0.156
8	0.042	-0.047	-0.018	-0.016	-0.018	-0.007	-0.017	-0.011	0.008	-0.032	-0.192	0.193
9	0.030	-0.070	-0.019	0.001	-0.020	-0.000	-0.020	-0.013	-0.003	-0.046	-0.235	0.229
10	0.039	-0.041	-0.020	-0.001	-0.017	0.001	-0.014	-0.003	0.009	-0.031	-0.215	0.185
11	0.037	-0.089	-0.022	0.010	-0.026	0.004	-0.021	-0.010	0.001	-0.046	-0.227	0.148
12	0.070	-0.054	0.025	0.031	0.005	0.023	-0.005	0.017	-0.010	-0.008	-0.044	0.011
13	0.075	-0.035	0.063	0.037	0.022	0.027	0.004	0.023	-0.008	-0.010	-0.076	0.016
14	0.066	-0.040	0.053	0.052	0.018	0.032	0.007	0.027	-0.013	0.001	-0.094	-0.009
15	0.018	0.016	-0.023	0.066	-0.017	0.044	-0.013	0.031	-0.010	-0.001	0.074	-0.018
16	-0.041	-0.019	-0.014	0.052	-0.013	0.039	-0.009	0.026	-0.005	-0.000	0.075	-0.003
17	0.004	-0.023	-0.018	0.070	-0.013	0.042	-0.009	0.028	-0.003	0.002	0.035	-0.024
18	0.062	-0.089	0.042	-0.007	0.017	0.002	0.005	-0.005	-0.005	-0.023	-0.160	0.170
19	0.040	-0.024	-0.036	-0.007	-0.025	-0.006	-0.022	-0.009	0.001	-0.028	-0.131	0.146
20	0.031	-0.033	-0.040	-0.001	-0.032	0.001	-0.021	-0.004	0.001	-0.024	-0.096	0.164
21	-0.137	-0.019	-0.099	-0.021	-0.059	-0.000	-0.047	0.004	-0.028	-0.003	0.087	0.115
22	-0.081	0.109	0.004	0.109	-0.004	0.076	-0.002	0.053	-0.005	0.022	-0.011	-0.246
23	0.084	-0.063	0.0[illegible]8	-0.002	0.026	0.001	0.012	-0.004	-0.001	-0.024	-0.173	0.152
24	-0.031	-0.321	0.108	0.159	0.159	0.020	-0.024	0.006	-0.050	-0.128	-0.121	0.236
25	0.049	-0.319	0.384	0.242	0.242	0.156	0.051	0.078	-0.070	-0.031	-0.478	0.916
26	-0.054	-0.361	0.259	0.159	0.159	0.085	0.012	0.055	-0.083	-0.025	-0.432	0.524
27	-0.119	-0.325	0.212	0.134	0.134	0.051	-0.021	0.038	-0.117	-0.048	-0.159	0.456
28	0.039	-0.326	0.313	0.233	0.233	0.118	0.031	0.075	-0.075	-0.030	-0.485	0.694
29	-0.063	-0.448	0.251	0.260	0.260	0.072	-0.011	0.065	-0.110	-0.075	-0.209	0.646
30	-0.019	-0.413	0.260	0.333	0.333	0.076	-0.001	0.110	-0.102	-0.026	-0.577	0.701
31	0.141	0.014	0.132	0.046	0.046	0.067	0.039	0.011	0.025	-0.028	-0.163	0.201
32	0.146	-0.023	0.083	0.066	0.066	0.036	0.014	0.008	0.012	-0.045	-0.201	0.151

TABLE 4. CONTINUED

9500 Pound vehicle							Fwd. c.g.					
REC	Y300		Y380		Y440		Y490		Y517		X140	
	REAL	IMAG	REAL	IMAG	REAL	IMAG	REAL	IMAG	REAL	IMAG	REAL	IMAG
1	-0.014	-0.079	-0.098	-0.140	-0.241	-0.230	-0.273	-0.243	-0.318	-0.225	0.024	0.005
2	-0.030	-0.084	-0.152	-0.130	-0.335	-0.195	-0.357	-0.120	-0.394	0.009	0.023	0.008
3	-0.018	-0.087	-0.119	-0.105	-0.248	-0.119	-0.279	-0.049	-0.282	0.095	0.007	0.025
4	-0.004	-0.080	-0.101	-0.084	-0.257	-0.068	-0.342	-0.011	-0.582	0.110	0.018	0.010
5	-0.046	-0.173	-0.204	-0.209	-0.460	-0.227	-0.410	0.082	-0.664	0.332	-0.033	-0.015
6	-0.104	-0.178	-0.329	-0.153	-0.622	-0.087	-0.445	0.163	-0.850	0.734	0.002	-0.027
7	-0.028	-0.072	-0.148	-0.086	-0.337	-0.050	-0.415	-0.003	-0.453	0.075	0.016	0.001
8	-0.024	-0.112	-0.159	-0.150	-0.351	-0.190	-0.409	-0.149	-0.467	0.024	0.026	0.004
9	-0.059	-0.144	-0.218	-0.158	-0.449	-0.151	-0.480	-0.054	-0.523	0.283	0.029	0.005
10	-0.037	-0.104	-0.189	-0.114	-0.397	-0.074	-0.429	-0.001	-0.459	0.172	0.029	0.006
11	-0.040	-0.134	-0.195	-0.152	-0.424	-0.149	-0.518	-0.005	-0.619	0.135	0.026	0.003
12	-0.029	-0.132	-0.085	-0.033	-0.134	-0.021	-0.130	0.106	-0.110	0.008	0.003	0.008
13	-0.053	-0.026	-0.120	-0.016	-0.175	0.034	-0.077	0.067	0.136	0.110	0.017	0.002
14	-0.013	-0.035	-0.044	-0.051	-0.061	-0.092	-0.081	0.041	-0.115	0.023	0.008	0.008
15	-0.024	-0.026	-0.021	-0.016	-0.017	-0.052	0.000	-0.018	0.062	-0.087	0.003	-0.010
16	-0.008	-0.011	0.015	-0.008	0.030	-0.039	0.021	-0.046	0.039	-0.076	-0.005	-0.009
17	-0.000	-0.004	-0.010	-0.002	0.029	-0.011	-0.012	0.022	0.004	-0.021	-0.001	-0.008
18	-0.037	-0.079	-0.100	-0.077	-0.188	-0.061	-0.093	-0.073	-0.011	-0.084	0.025	0.002
19	-0.028	-0.094	-0.176	-0.143	-0.394	-0.242	-0.409	-0.208	-0.514	-0.056	0.015	0.006
20	-0.047	-0.080	-0.203	-0.083	-0.434	-0.026	-0.546	-0.045	-0.614	0.058	0.021	0.001
21	-0.056	0.005	-0.067	0.042	-0.058	0.122	-0.071	0.040	0.028	-0.054	0.005	-0.029
22	0.003	0.026	0.020	0.003	0.048	-0.035	0.038	-0.041	0.062	-0.139	-0.019	0.006
23	-0.032	-0.072	-0.080	-0.090	-0.174	-0.056	-0.101	-0.098	0.053	-0.052	0.019	0.002
24	-0.282	-0.251	-0.745	-0.256	-1.132	-0.049	-0.703	0.411	-0.464	1.546	0.031	-0.052
25	-0.270	-0.244	-0.691	-0.213	-1.239	-0.047	-0.776	0.216	-0.176	0.992	0.044	-0.058
26	-0.287	-0.111	-0.620	-0.033	-1.018	0.212	-0.622	0.235	-0.087	1.076	0.031	-0.057
27	-0.327	-0.055	-0.627	0.240	-0.726	0.599	-0.295	0.921	0.459	1.710	0.010	-0.059
28	-0.269	-0.235	-0.695	-0.208	-1.116	-0.118	-0.795	0.323	-0.231	0.982	0.038	-0.045
29	-0.385	-0.199	-0.880	0.064	-1.268	0.455	-0.661	0.506	0.140	1.844	0.036	-0.074
30	-0.326	-0.160	-0.754	-0.029	-1.293	0.347	-0.884	0.479	-0.173	1.715	0.045	-0.077
31	-0.001	-0.137	-0.110	-0.205	-0.244	-0.329	-0.227	-0.189	-0.246	0.038	0.027	0.013
32	-0.059	-0.143	-0.268	-0.175	-0.526	-0.193	-0.554	0.009	-0.364	0.312	0.031	0.011

TABLE 4. CONTINUED

9500 Pound vehicle							Fwd. c.g.					
	X180T		X540		X200R		X200L		X190R		X220L	
REC	REAL	IMAG	REAL	IMAG	REAL	IMAG	REAL	IMAG	REAL	IMAG	REAL	IMAG
1	-0.122	-0.090	-0.549	-0.090	0.067	-0.041	-0.001	0.030	0.023	-0.043	0.011	0.007
2	-0.127	-0.095	-0.557	-0.113	0.076	-0.048	-0.007	0.041	0.022	-0.041	0.011	0.008
3	-0.159	-0.124	-0.406	-0.008	0.077	-0.064	0.006	0.054	0.013	-0.057	0.001	0.018
4	-0.096	-0.126	-0.387	0.110	0.062	-0.049	-0.028	0.064	0.029	-0.066	0.009	0.013
5	-0.250	-0.148	-0.595	0.353	0.103	-0.112	-0.016	0.087	0.008	-0.111	0.028	0.011
6	-0.212	-0.171	-0.304	0.324	0.095	-0.105	-0.039	0.107	0.040	-0.108	0.024	0.012
7	-0.188	-0.104	-0.302	0.016	0.076	-0.040	0.005	0.051	0.003	-0.055	0.011	0.007
8	-0.194	-0.160	-0.434	-0.069	0.097	-0.072	-0.004	0.065	0.016	-0.078	0.014	0.011
9	-0.270	-0.195	-0.417	-0.027	0.092	-0.109	0.011	0.094	-0.000	-0.105	0.023	0.016
10	-0.220	-0.191	-0.403	-0.043	0.110	-0.077	-0.000	0.080	0.010	-0.089	0.016	0.011
11	-0.202	-0.212	-0.435	0.028	0.091	-0.096	-0.011	0.096	0.018	-0.096	0.021	0.019
12	0.034	-0.053	-0.383	0.082	0.024	-0.054	-0.004	0.028	0.044	-0.032	0.009	0.005
13	0.025	-0.063	-0.455	0.026	0.050	-0.054	0.009	0.051	0.049	-0.045	0.014	0.006
14	0.036	-0.120	-0.340	-0.008	0.024	-0.029	-0.023	0.037	0.044	-0.038	0.006	0.008
15	0.018	0.066	-0.133	-0.102	0.013	-0.042	0.006	0.008	-0.000	-0.001	-0.002	-0.006
16	0.040	0.069	0.038	0.010	-0.010	-0.035	-0.008	0.022	-0.001	-0.002	-0.001	-0.005
17	0.012	0.024	-0.102	0.055	0.013	-0.025	-0.013	0.010	0.005	-0.002	-0.005	-0.005
18	-0.176	-0.218	-0.486	0.113	0.051	-0.069	0.024	0.065	0.008	-0.098	0.021	0.013
19	-0.174	-0.139	-0.341	-0.004	0.062	-0.048	-0.010	0.051	0.003	-0.062	0.008	0.008
20	-0.192	-0.101	-0.290	0.023	0.076	-0.059	-0.001	0.045	-0.001	-0.061	0.011	0.003
21	-0.155	0.111	0.268	0.130	-0.016	-0.062	0.034	0.004	-0.092	-0.039	0.006	-0.025
22	0.171	-0.069	0.381	-0.440	-0.002	0.035	-0.035	0.010	0.019	0.029	-0.014	0.002
23	-0.113	-0.136	-0.482	0.036	0.054	-0.069	0.010	0.056	0.037	-0.066	0.016	0.012
24	-0.200	-0.104	-0.618	0.990	0.088	-0.187	-0.041	0.103	0.057	-0.162	0.038	-0.000
25	-0.866	-0.273	-1.194	0.759	0.168	-0.190	0.004	0.083	-0.071	-0.273	0.063	-0.016
26	-0.550	-0.277	-0.766	1.004	0.104	-0.186	0.007	0.082	-0.019	-0.246	0.048	-0.023
27	-0.384	-0.057	-0.365	1.082	0.023	-0.200	0.013	0.095	-0.036	-0.188	0.043	-0.023
28	-0.740	-0.383	-1.123	0.764	0.145	-0.179	0.006	0.107	-0.039	-0.283	0.060	-0.011
29	-0.400	-0.028	-0.845	1.462	0.090	-0.260	0.011	0.112	0.022	-0.232	0.060	-0.019
30	-0.669	-0.335	-0.890	0.963	0.153	-0.219	0.015	0.096	-0.011	-0.310	0.062	-0.033
31	-0.186	-0.198	-0.755	-0.429	0.120	-0.046	-0.031	0.064	0.027	-0.080	0.020	0.015
32	-0.197	-0.248	-0.813	-0.253	0.129	-0.070	-0.036	0.084	0.049	-0.097	0.022	0.015

TABLE 4. CONTINUED

9500 Pound vehicle								Aft c.g.						
REC	Z50		Z100T		Z210T		Z340		Z400		Z460		Z540	
	REAL	IMAG	REAL	IMAG	REAL	IMAG	REAL	IMAG	REAL	IMAG	REAL	IMAG	REAL	IMAG
1	-0.109	-0.058	-0.028	-0.035	-0.096	-0.065	0.208	0.073	0.183	0.073	-0.043	0.024	-0.574	-0.151
2	-0.124	-0.052	-0.044	-0.021	-0.119	-0.077	0.277	0.117	0.191	0.122	-0.021	0.049	-0.547	-0.189
3	-0.230	-0.095	-0.123	-0.063	-0.149	-0.082	0.247	0.004	0.158	0.015	-0.023	0.024	-0.458	-0.059
4	-0.149	-0.084	-0.067	-0.076	-0.089	-0.082	0.275	-0.105	-0.171	-0.075	-0.054	0.013	-0.603	0.099
5	-0.188	-0.082	-0.110	-0.084	-0.169	-0.075	0.251	-0.149	0.002	-0.195	-0.026	0.070	-0.546	0.266
6	-0.216	-0.090	-0.139	-0.091	-0.200	-0.048	0.282	-0.188	0.001	-0.234	0.031	0.094	-0.477	0.400
7	-0.174	-0.072	-0.078	-0.043	-0.164	-0.077	0.173	0.096	0.120	0.108	-0.029	0.048	-0.398	-0.151
8	-0.223	-0.136	-0.116	-0.093	-0.157	-0.149	0.276	-0.027	0.200	0.016	-0.037	0.017	-0.563	-0.047
9	-0.242	-0.110	-0.127	-0.100	-0.186	-0.131	0.315	-0.123	-0.208	-0.091	-0.063	0.028	-0.665	0.138
10	-0.180	-0.137	-0.090	-0.087	-0.110	-0.110	0.257	0.016	0.178	0.033	-0.029	0.020	-0.501	-0.124
11	-0.209	-0.157	-0.110	-0.091	-0.157	-0.186	0.243	0.063	0.168	0.082	-0.037	0.032	-0.513	-0.196
12	-0.015	-0.043	0.028	-0.042	-0.012	-0.060	0.311	0.020	0.203	0.015	-0.023	0.023	-0.468	-0.017
13	-0.022	-0.057	0.026	-0.049	0.014	-0.058	0.287	0.002	0.186	0.018	0.001	0.027	-0.479	0.002
14	-0.039	-0.053	0.020	-0.039	-0.017	-0.072	0.284	0.067	0.186	0.063	-0.040	-0.009	-0.542	-0.175
15	0.022	0.028	0.016	0.014	0.018	0.024	0.000	0.004	0.009	0.009	-0.001	0.006	-0.039	0.003
16	0.035	-0.031	0.018	-0.028	0.039	-0.117	0.031	0.064	0.019	0.029	-0.005	-0.027	-0.096	-0.159
17	-0.009	-0.053	-0.002	-0.031	0.049	-0.107	0.067	0.058	0.046	0.049	-0.017	-0.013	-0.169	-0.179
18	-0.030	-0.109	-0.030	-0.050	-0.046	-0.096	-0.001	0.150	-0.015	0.110	-0.047	-0.014	-0.080	-0.323
19	-0.127	-0.093	-0.035	-0.066	-0.018	-0.074	0.174	0.093	0.096	0.070	-0.062	0.011	-0.416	-0.110
20	0.017	-0.134	0.041	-0.057	-0.028	-0.107	0.256	0.213	0.177	0.149	-0.002	-0.035	-0.439	-0.467
21	-0.215	-0.058	-0.153	-0.081	-0.149	-0.054	-0.038	-0.268	-0.026	-0.174	-0.014	0.005	-0.017	0.391
22	-0.251	-0.023	-0.190	-0.073	-0.184	-0.008	-0.091	-0.322	-0.044	-0.207	-0.005	0.013	0.046	0.509
23	0.028	-0.088	0.045	-0.035	-0.026	-0.084	0.263	0.241	0.177	0.192	-0.026	-0.018	-0.467	-0.497
24	-0.206	-0.201	-0.135	-0.238	-0.104	-0.073	0.294	-0.647	0.285	-0.420	0.094	-0.015	-0.486	0.955
25	-0.576	-0.499	-0.309	-0.465	-0.576	-0.015	0.819	-0.309	0.620	-0.146	0.055	0.138	-1.409	0.616
26	-0.393	-0.550	-0.220	-0.498	-0.456	-0.215	0.597	-0.366	0.469	-0.181	0.087	0.094	-0.999	0.586
27	-0.405	-0.213	-0.312	-0.276	-0.177	-0.035	0.232	-0.735	0.205	-0.505	0.050	0.006	-0.445	1.121
28	-0.513	-0.427	-0.267	-0.400	-0.497	-0.125	0.727	-0.354	0.578	-0.171	0.047	0.112	-1.309	0.596
29	-0.500	-0.353	-0.311	-0.384	-0.340	0.031	0.570	-0.758	0.463	-0.475	0.089	0.014	-1.030	1.090
30	-0.416	-0.392	-0.222	-0.419	-0.318	-0.069	0.587	-0.750	0.440	-0.470	0.057	-0.015	-1.000	1.058
31	0.131	-0.112	0.107	-0.072	0.063	-0.175	0.246	0.349	0.141	0.260	-0.057	-0.027	-0.464	-0.720
32	-0.279	-0.345	-0.102	-0.245	0.180	-0.579	0.519	0.065	0.363	0.093	-0.063	0.023	-1.049	-0.228

TABLE 4. CONTINUED

9500 Pound vehicle							Aft c.g.					
REC	Z90R		Z90L		Z140R		Z140L		Z200R		Z200L	
	REAL	IMAG	REAL	IMAG	REAL	IMAG	REAL	IMAG	REAL	IMAG	REAL	IMAG
1	-0.035	-0.021	-0.019	-0.034	0.001	-0.019	0.016	-0.019	0.055	0.043	-0.108	-0.041
2	-0.044	-0.018	-0.036	-0.027	-0.003	-0.012	0.003	-0.011	0.055	0.061	-0.080	-0.035
3	-0.108	-0.052	-0.101	-0.071	-0.050	-0.038	-0.044	-0.049	0.058	0.028	0.063	-0.097
4	-0.063	-0.067	-0.049	-0.080	-0.016	-0.067	-0.009	-0.076	-0.000	-0.097	0.114	-0.147
5	-0.090	-0.065	-0.074	-0.100	-0.041	-0.065	-0.027	-0.097	0.017	0.070	0.101	-0.243
6	-0.097	-0.070	-0.099	-0.127	-0.041	-0.076	-0.042	-0.119	0.120	-0.001	0.061	-0.329
7	-0.091	-0.015	-0.061	-0.052	-0.045	0.002	-0.018	-0.031	-0.003	0.074	0.100	-0.115
8	-0.105	-0.074	-0.103	-0.112	-0.044	-0.059	-0.042	-0.086	0.084	0.036	0.074	-0.182
9	-0.112	-0.064	-0.115	-0.122	-0.045	-0.062	-0.052	-0.113	0.121	0.046	0.069	-0.262
10	-0.085	-0.078	-0.067	-0.096	-0.034	-0.056	-0.019	-0.066	0.049	0.023	0.093	-0.106
11	-0.111	-0.072	-0.091	-0.111	-0.051	-0.048	-0.037	-0.075	0.028	0.078	0.091	-0.144
12	0.020	-0.029	0.015	-0.035	0.040	-0.027	0.031	-0.019	0.111	-0.002	-0.005	-0.107
13	0.019	-0.035	0.010	-0.041	0.037	-0.029	0.031	-0.026	0.108	0.006	-0.056	0.061
14	0.015	-0.025	0.003	-0.036	0.039	-0.020	0.031	-0.020	0.092	0.032	0.034	0.077
15	0.018	0.018	0.009	0.015	0.013	0.010	0.001	0.012	0.018	-0.001	-0.013	0.015
16	0.010	-0.016	0.021	-0.018	0.008	-0.002	0.010	-0.005	-0.021	0.011	0.025	0.026
17	-0.011	-0.019	0.006	-0.042	-0.007	-0.009	0.008	-0.020	-0.033	0.040	0.053	-0.033
18	-0.038	-0.032	-0.005	-0.054	-0.027	-0.007	-0.003	-0.020	-0.103	0.062	0.045	-0.014
19	-0.059	-0.038	-0.045	-0.047	-0.026	-0.019	-0.009	-0.019	0.032	0.060	0.084	-0.026
20	0.024	-0.034	0.041	-0.071	0.044	-0.002	0.055	-0.027	0.035	0.127	0.140	-0.012
21	-0.133	-0.050	-0.138	-0.079	-0.101	-0.060	-0.106	-0.087	-0.036	-0.087	-0.095	-0.225
22	-0.168	-0.033	-0.168	-0.069	-0.136	-0.046	-0.133	-0.087	-0.077	-0.099	-0.123	-0.258
23	0.041	-0.005	0.050	-0.033	0.053	0.011	0.062	-0.001	0.068	0.127	0.141	0.017
24	-0.080	-0.196	-0.141	-0.234	-0.038	-0.209	-0.088	-0.248	0.228	-0.229	-0.076	-0.541
25	-0.238	-0.205	-0.313	-0.479	-0.076	-0.119	-0.150	-0.391	0.264	0.254	0.108	-0.876
26	-0.174	-0.282	-0.230	-0.483	-0.074	-0.194	-0.119	-0.392	0.180	0.068	0.042	-0.785
27	-0.204	-0.213	-0.269	-0.272	-0.118	-0.212	-0.188	-0.286	0.200	-0.248	-0.176	-0.650
28	-0.201	-0.207	-0.276	-0.417	-0.064	-0.150	-0.128	-0.347	0.265	0.142	0.106	-0.749
29	-0.218	-0.260	-0.294	-0.398	-0.098	-0.233	-0.172	-0.380	0.286	-0.158	-0.067	-0.843
30	-0.186	-0.286	-0.222	-0.415	-0.070	-0.265	-0.111	-0.392	0.253	-0.188	0.070	-0.803
31	0.052	-0.010	0.122	-0.057	0.052	0.015	0.104	-0.008	-0.079	0.153	0.293	0.046
32	-0.136	-0.160	-0.077	-0.252	-0.046	-0.101	0.006	-0.174	0.037	0.130	0.305	-0.239

TABLE 4. CONTINUED

9500 Pound vehicle							Aft c.g.					
REC	Z260R		Z260L		Z396R		Z396L		ZLONG		ZLATR	
	REAL	IMAG	REAL	IMAG	REAL	IMAG	REAL	IMAG	REAL	IMAG	REAL	IMAG
1	0.156	0.012	0.188	0.017	0.162	0.059	0.190	0.089	0.021	0.059	0.027	0.071
2	0.156	0.031	0.193	0.050	0.174	0.090	0.222	0.162	0.065	0.005	0.069	0.013
3	-0.079	0.101	0.074	0.139	0.029	0.138	0.173	0.063	0.041	-0.029	0.046	-0.027
4	0.153	-0.119	0.173	-0.123	-0.009	-0.193	0.185	0.024	0.051	-0.076	0.058	-0.072
5	0.097	-0.150	0.140	-0.151	0.124	-0.103	0.228	0.004	0.029	-0.082	0.040	-0.092
6	0.089	-0.181	0.161	-0.175	0.097	-0.150	0.133	0.277	0.032	-0.096	0.036	-0.111
7	0.080	0.033	0.120	0.030	0.087	0.124	0.111	0.074	0.021	0.014	0.040	-0.000
8	0.140	-0.059	0.176	-0.070	0.171	0.010	0.216	0.035	0.046	-0.051	0.050	-0.055
9	0.152	-0.123	0.176	-0.139	-0.008	-0.200	0.074	0.204	0.054	-0.075	0.050	-0.090
10	0.065	0.119	0.082	0.153	0.170	0.023	0.185	0.077	0.044	-0.031	0.058	-0.029
11	0.129	-0.008	0.161	-0.009	0.154	0.074	0.167	0.098	0.038	-0.021	0.049	-0.026
12	0.186	-0.016	0.196	-0.014	0.199	-0.003	0.226	0.064	0.076	-0.019	0.012	-0.078
13	0.183	-0.016	0.085	0.191	0.166	-0.005	0.222	0.024	0.078	-0.018	0.010	-0.077
14	0.181	0.013	0 197	0.028	0.178	0.038	0.201	0.092	-0.061	0.054	0.084	-0.001
15	0.010	0.007	0.003	0.007	0.019	0.020	0.025	-0.010	0.003	0.009	0.005	0.008
16	0.026	0.032	0.020	0.047	0.016	0.027	-0.005	0.031	0.006	0.013	0.004	0.015
17	0.017	0.019	0.048	0.024	-0.001	0.035	0.066	0.038	0.011	0.009	0.018	0.004
18	-0.002	0.093	0.005	0.086	-0.088	0.126	-0.022	0.097	-0.015	0.040	-0.001	0.032
19	0.114	0.046	0.123	0.048	0.056	0.055	0.114	0.061	0.039	0.012	0.050	0.023
20	0.153	0.116	0.193	0.124	0.160	0.154	0.189	0.151	0.083	0.046	0.081	0.036
21	-0.078	-0.160	-0.080	-0.209	-0.049	-0.121	-0.024	-0.224	-0.064	-0.009	-0.064	-0.101
22	-0.125	-0.191	-0.111	-0.236	-0.080	-0.190	-0.072	-0.238	-0.093	-0.092	-0.089	-0.109
23	0.187	0.134	0.205	0.135	0.172	0.170	0.199	0.174	0.094	0.063	0.092	0.046
24	0.036	-0.467	0.136	-0.473	0.187	-0.364	0.380	-0.281	0.021	-0.251	-0.010	-0.256
25	0.262	-0.292	0.459	-0.365	0.352	-0.205	0.556	-0.109	0.140	-0.130	0.078	-0.225
26	0.124	-0.363	0.313	-0.389	0.266	-0.261	0.534	-0.041	0.067	-0.177	0.030	-0.244
27	-0.037	-0.502	0.063	-0.595	0.000	-0.446	0.337	-0.451	-0.028	-0.278	-0.062	-0.299
28	0.257	-0.326	0.418	-0.371	0.304	-0.240	0.569	-0.121	0.133	-0.160	0.086	-0.231
29	0.114	-0.523	0.279	-0.640	0.092	-0.442	0.498	-0.358	0.058	-0.298	0.011	-0.339
30	0.137	-0.537	0.315	-0.628	0.195	-0.312	0.593	-0.328	0.077	-0.309	0.048	-0.351
31	0.138	0.158	0.196	0.192	0.084	0.236	0.178	0.273	0.067	0.078	0.095	0.066
32	0.250	-0.062	0.352	-0.043	0 244	0.034	0.431	0.128	0.109	-0.040	0.140	-0.081

TABLE 4. CONTINUED

9500 Pound vehicle							Aft c.g.					
REC	ZCOLL		Y50		Y90		Y140		Y220B		Y220F	
	REAL	IMAG	REAL	IMAG	REAL	IMAG	REAL	IMAG	REAL	IMAG	REAL	IMAG
1	-0.066	-0.035	0.026	-0.031	0.010	-0.017	0.007	-0.013	0.016	-0.022	-0.227	0.142
2	0.066	0.000	0.020	-0.028	0.010	-0.014	0.002	-0.016	0.023	-0.031	-0.252	0.117
3	0.035	-0.042	0.047	-0.027	0.020	-0.018	0.011	-0.014	0.020	-0.036	-0.248	0.154
4	0.051	-0.101	-0.010	-0.046	-0.010	-0.021	0.008	-0.013	0.020	-0.034	-0.184	0.135
5	0.029	-0.108	-0.025	-0.015	-0.012	-0.013	-0.008	-0.027	0.011	-0.064	-0.260	0.199
6	0.020	-0.131	0.026	0.039	-0.013	-0.003	-0.026	-0.024	-0.014	-0.091	-0.289	0.306
7	0.033	-0.034	0.010	0.019	0.002	0.007	0.002	-0.008	0.017	-0.031	-0.280	0.120
8	0.041	-0.072	0.003	-0.079	-0.006	-0.036	0.011	-0.020	0.012	-0.048	-0.276	0.159
9	0.043	-0.109	-0.035	-0.018	-0.008	-0.015	0.000	-0.018	0.011	-0.057	-0.245	0.219
10	0.046	-0.046	-0.047	-0.018	-0.004	-0.021	0.006	-0.009	0.019	-0.033	-0.259	0.147
11	0.042	-0.042	-0.001	-0.084	-0.005	-0.041	0.021	-0.020	0.030	-0.041	-0.316	0.094
12	0.081	-0.019	0.032	0.104	0.053	0.008	0.026	0.006	0.003	-0.025	-0.103	0.023
13	0.009	-0.086	0.087	0.024	0.042	0.021	0.021	0.014	-0.000	-0.015	-0.092	0.029
14	-0.067	0.058	0.080	0.021	0.041	0.023	0.022	0.014	0.008	-0.019	-0.141	0.038
15	0.002	0.009	-0.001	0.047	0.001	0.031	-0.001	0.020	-0.004	-0.002	0.016	-0.007
16	0.009	0.012	0.024	0.084	0.010	0.054	0.004	0.034	0.004	0.003	0.004	-0.046
17	0.017	-0.001	0.047	0.041	0.022	0.028	0.016	0.017	0.006	-0.003	-0.073	-0.007
18	-0.002	0.033	0.065	0.069	0.040	0.047	0.031	0.025	0.021	-0.011	-0.175	-0.079
19	0.043	0.013	0.032	-0.017	0.011	-0.013	0.008	-0.013	0.009	-0.022	-0.198	0.045
20	0.098	0.025	0.099	0.016	0.053	0.017	0.033	0.009	0.018	-0.016	-0.258	0.039
21	-0.086	-0.112	0.001	-0.033	-0.009	-0.012	-0.010	-0.004	-0.013	-0.013	-0.017	0.122
22	-0.104	-0.129	0.006	-0.017	-0.007	-0.003	-0.006	-0.001	-0.014	-0.011	-0.047	0.146
23	0.096	0.042	0.086	0.002	0.047	0.009	0.028	0.002	0.020	-0.019	-0.241	0.044
24	-0.041	-0.280	0.143	0.153	0.030	0.062	-0.018	0.019	-0.070	-0.101	-0.121	0.229
25	0.075	-0.293	0.426	0.411	0.219	0.248	0.118	0.136	0.015	-0.039	-0.618	0.861
26	0.019	-0.298	0.261	0.440	0.119	0.246	0.053	0.127	-0.002	-0.070	-0.619	0.452
27	-0.100	-0.334	0.253	0.154	0.079	0.082	0.006	0.047	-0.094	-0.060	-0.136	0.438
28	0.066	-0.289	0.338	0.313	0.173	0.181	0.087	0.091	0.014	-0.069	-0.566	0.671
29	-0.023	-0.402	0.353	0.270	0.152	0.152	0.051	0.084	-0.054	-0.069	-0.345	0.815
30	0.026	-0.396	0.277	0.264	0.111	0.149	0.030	0.081	-0.058	-0.065	-0.447	0.622
31	0.083	0.062	0.189	0.125	0.109	0.088	0.078	0.056	0.047	-0.002	-0.274	-0.244
32	0.108	-0.107	0.124	0.076	0.050	0.037	0.031	0.009	0.014	-0.051	-0.533	0.110

TABLE 4. CONTINUED

9500 Pound vehicle							Aft c.g.					
REC	Y300		Y380		Y440		Y490		Y517		X140	
	REAL	IMAG	REAL	IMAG	REAL	IMAG	REAL	IMAG	REAL	IMAG	REAL	IMAG
1	0.015	-0.094	-0.058	-0.177	-0.154	-0.302	-0.176	-0.305	-0.203	-0.275	0.016	0.014
2	0.019	-0.118	-0.076	-0.224	-0.246	-0.375	-0.331	-0.269	-0.419	-0.066	0.019	0.020
3	0.013	-0.118	-0.074	-0.175	-0.192	-0.241	-0.234	-0.153	-0.273	0.079	0.020	0.013
4	0.030	-0.114	-0.021	-0.176	-0.133	-0.270	-0.218	-0.214	-0.380	-0.051	0.020	0.011
5	-0.020	-0.192	-0.187	-0.267	-0.464	-0.359	-0.500	-0.057	-0.890	0.123	0.024	0.008
6	-0.102	-0.246	-0.356	-0.313	-0.681	-0.345	-0.458	0.096	-0.921	0.599	-0.021	0.022
7	0.016	-0.127	-0.096	-0.208	-0.282	-0.296	-0.350	-0.266	-0.415	-0.182	0.006	0.013
8	-0.005	-0.153	-0.078	-0.221	-0.193	-0.297	-0.217	-0.181	-0.245	0.091	0.025	0.010
9	-0.012	-0.184	-0.097	-0.257	-0.260	-0.331	-0.324	-0.212	-0.409	0.092	0.026	0.003
10	0.011	-0.114	-0.089	-0.164	-0.230	-0.231	-0.284	-0.148	-0.326	0.019	0.021	0.013
11	0.049	-0.148	0.008	-0.248	-0.097	-0.376	-0.253	-0.246	-0.411	-0.002	0.019	0.021
12	-0.027	-0.072	-0.090	-0.099	-0.134	-0.141	-0.121	0.012	-0.109	0.136	0.014	0.003
13	-0.030	-0.052	-0.069	-0.070	-0.126	-0.051	-0.068	0.043	0.123	0.127	0.015	0.002
14	-0.018	-0.072	-0.079	-0.100	-0.137	-0.146	-0.123	-0.073	-0.022	0.151	0.015	0.006
15	-0.016	-0.025	-0.005	-0.035	-0.010	-0.037	-0.002	-0.032	0.010	-0.006	0.000	-0.002
16	0.009	-0.019	0.033	-0.040	0.062	-0.036	0.048	-0.040	0.005	-0.035	-0.008	0.003
17	0.019	-0.035	0.039	-0.068	0.039	-0.081	0.028	-0.034	-0.006	0.006	-0.006	0.009
18	0.046	-0.051	0.069	-0.072	0.031	-0.123	0.054	-0.067	0.001	-0.029	-0.008	0.016
19	0.021	-0.107	-0.009	-0.213	-0.052	-0.345	-0.080	-0.406	-0.163	-0.366	0.007	0.009
20	0.026	-0.065	-0.008	-0.102	-0.046	-0.173	-0.003	-0.098	-0.016	0.012	0.016	0.019
21	-0.038	-0.028	-0.058	0.020	-0.084	0.054	-0.035	0.051	0.046	-0.009	0.011	-0.017
22	-0.028	-0.[illegible]	-0.051	0.005	-0.085	0.052	-0.022	0.014	0.045	0.038	0.005	-0.022
23	0.038	-0.083	0.028	-0.135	0.029	-0.221	0.018	-0.128	-0.003	-0.048	0.016	0.018
24	-0.301	-0.228	-0.675	-0.153	-1.115	0.016	-0.598	0.484	-0.355	1.442	0.027	-0.047
25	-0.146	-0.396	-0.567	-0.616	-1.125	-0.702	-0.945	-0.055	-0.685	1.093	0.055	-0.060
26	-0.156	-0.401	-0.602	-0.588	-1.229	-0.596	-1.012	0.017	-0.821	1.300	0.053	-0.069
27	-0.313	-0.136	-0.596	0.088	-0.838	0.443	-0.461	0.749	0.454	1.474	0.013	-0.063
28	-0.136	-0.383	-0.558	-0.559	-1.105	-0.660	-1.030	-0.079	-0.704	0.966	0.053	-0.048
29	-0.314	-0.232	-0.758	-0.102	-1.252	0.344	-0.893	0.803	-0.223	1.932	0.030	-0.074
30	-0.280	-0.213	-0.695	-0.116	-1.210	0.155	-0.887	0.706	-0.263	1.719	0.038	-0.067
31	0.082	-0.087	0.055	-0.203	0.046	-0.366	0.061	-0.339	-0.040	-0.199	-0.001	0.038
32	-0.017	-0.205	-0.185	-0.400	-0.492	-0.624	-0.536	-0.458	-0.589	-0.101	0.035	0.017

TABLE 4. CONCLUDED

9500 Pound vehicle								Aft c.g.				
REC	X180T		X540		X200R		X200L		X190R		X220L	
	REAL	IMAG	REAL	IMAG	REAL	IMAG	REAL	IMAG	REAL	IMAG	REAL	IMAG
1	-0.125	-0.183	-0.518	-0.171	-0.053	0.054	-0.003	0.046	0.032	-0.054	0.010	0.014
2	-0.156	-0.205	-0.493	-0.243	-0.075	0.071	-0.011	0.051	0.021	-0.062	0.008	0.016
3	-0.181	-0.228	-0.421	-0.079	0.108	-0.042	-0.003	0.077	0.020	-0.088	0.010	0.017
4	-0.102	-0.161	-0.545	0.078	0.086	-0.038	-0.019	0.060	0.037	-0.079	0.007	0.013
5	-0.182	-0.215	-0.499	0.210	0.116	-0.062	-0.043	0.081	0.038	-0.105	0.014	0.017
6	-0.248	-0.245	-0.465	0.288	0.113	-0.096	-0.028	0.102	0.040	-0.131	0.027	0.014
7	-0.152	-0.235	-0.342	-0.182	0.088	-0.022	-0.028	0.085	0.029	-0.078	0.001	0.024
8	-0.200	-0.285	-0.521	-0.065	0.095	-0.057	0.007	0.093	0.035	-0.122	0.017	0.017
9	-0.238	-0.259	-0.593	0.106	0.095	-0.085	0.000	0.101	0.024	-0.126	0.013	0.018
10	-0.135	-0.241	-0.451	-0.128	0.107	-0.026	-0.015	0.078	0.050	-0.906	0.010	0.019
11	-0.156	-0.352	-0.452	-0.200	0.001	-0.119	-0.009	0.094	0.038	-0.110	0.012	0.023
12	-0.010	-0.083	-0.477	-0.067	0.061	-0.054	-0.005	0.063	0.046	-0.037	0.012	0.008
13	0.001	-0.074	-0.468	-0.030	0.052	-0.052	0.005	0.055	0.042	-0.031	0.006	0.008
14	-0.008	-0.134	-0.505	-0.185	0.063	-0.044	0.002	0.062	0.047	-0.048	0.007	0.010
15	0.006	0.034	-0.032	-0.007	-0.002	-0.025	0.003	0.012	-0.004	-0.002	0.003	-0.000
16	0.051	-0.046	-0.089	-0.149	0.008	-0.015	-0.014	0.033	0.026	-0.006	-0.005	0.007
17	0.024	-0.109	-0.147	-0.159	0.020	-0.007	-0.014	0.041	0.025	-0.017	-0.006	0.015
18	0.038	-0.184	-0.030	-0.292	0.033	-0.004	-0.031	0.081	0.036	-0.045	-0.008	0.024
19	-0.094	-0.149	-0.340	-0.112	0.052	-0.007	0.005	0.043	0.020	-0.036	0.003	0.017
20	-0.009	-0.256	-0.423	-0.426	0.065	-0.014	-0.008	0.080	0.044	-0.057	0.008	0.015
21	-0.184	-0.055	0.013	0.395	0.019	-0.078	0.027	0.044	-0.054	-0.086	0.008	-0.007
22	-0.229	-0.015	0.055	0.503	0.024	-0.084	0.019	0.047	-0.065	-0.076	0.010	-0.013
23	-0.014	-0.220	-0.438	-0.481	0.060	-0.010	-0.007	0.069	0.047	-0.045	0.007	0.014
24	-0.158	-0.110	-0.577	0.899	0.075	-0.187	-0.004	0.121	0.041	-0.139	0.037	-0.006
25	-0.796	-0.469	-1.438	0.383	0.242	-0.186	0.005	0.102	-0.011	-0.279	0.052	-0.006
26	-0.525	-0.563	-1.068	0.408	0.202	-0.186	-0.013	0.110	0.038	-0.274	0.050	-0.010
27	-0.306	-0.112	-0.541	1.064	0.020	-0.210	0.015	0.117	0.005	-0.190	0.032	-0.024
28	-0.683	-0.476	-1.367	0.422	0.214	-0.190	-0.002	0.124	0.004	-0.263	0.038	-0.001
29	-0.558	-0.182	-1.104	0.986	0.140	-0.253	-0.000	0.147	0.008	-0.265	0.049	-0.026
30	-0.470	-0.240	-1.091	0.982	0.161	-0.227	-0.007	0.119	0.054	-0.231	0.045	-0.027
31	0.266	-0.353	-0.428	-0.657	0.091	0.014	-0.090	0.093	0.134	-0.066	-0.008	0.027
32	-0.155	-0.616	-0.957	-0.243	0.156	-0.032	-0.021	0.098	0.092	-0.174	0.017	0.029

GROUND VIBRATION TEST SYSTEM

The shake testing was done in Kaman's full size shake test rig. A shake test system including suspension of the test vehicle was designed and fabricated such that the shaking system could be used for both the single point and/or direct shake (calibration testing) and the combination of shaker inputs (ground flying).

It was anticipated that the major sources of the two-per-rev vibratory excitation forces were the main rotor forces and torque moment, the control forces and the horizontal stabilizer force. Thus, if direct shaking techniques are used, the test vehicle should be shaken at these points. However, it is virtually impossible to shake the vehicle at the control reaction points. Therefore, to determine control loads and/or other unanticipated excitation forces such as rotor-fuselage interference (wake effects), modal accelerations testing (single point shaking) must be done. Thus, other locations for shaking on the test vehicle must be selected to obtain good response. Figure 7 shows the anticipated location for force inputs to do direct force shake and modal acceleration testing for the calibration.

For the calibration testing those forces and moments will be applied separately; however, for ground flying they will be applied simultaneously with the proper phase and magnitude. Therefore a ground vibration system was designed to do both calibration testing and ground flying. Figure 8 shows a schematic of the ground flying system.

It is seen from this design that the ground flying shaking system for forces applied at the hub has the capability of applying a vertical force, a lateral force, and two longitudinal forces to produce both a vibratory torque and longitudinal force. It is further seen that the excitation system is designed to have long attachment rods from the shaker to the hub to prevent any interaction of the forces. Therefore the system had

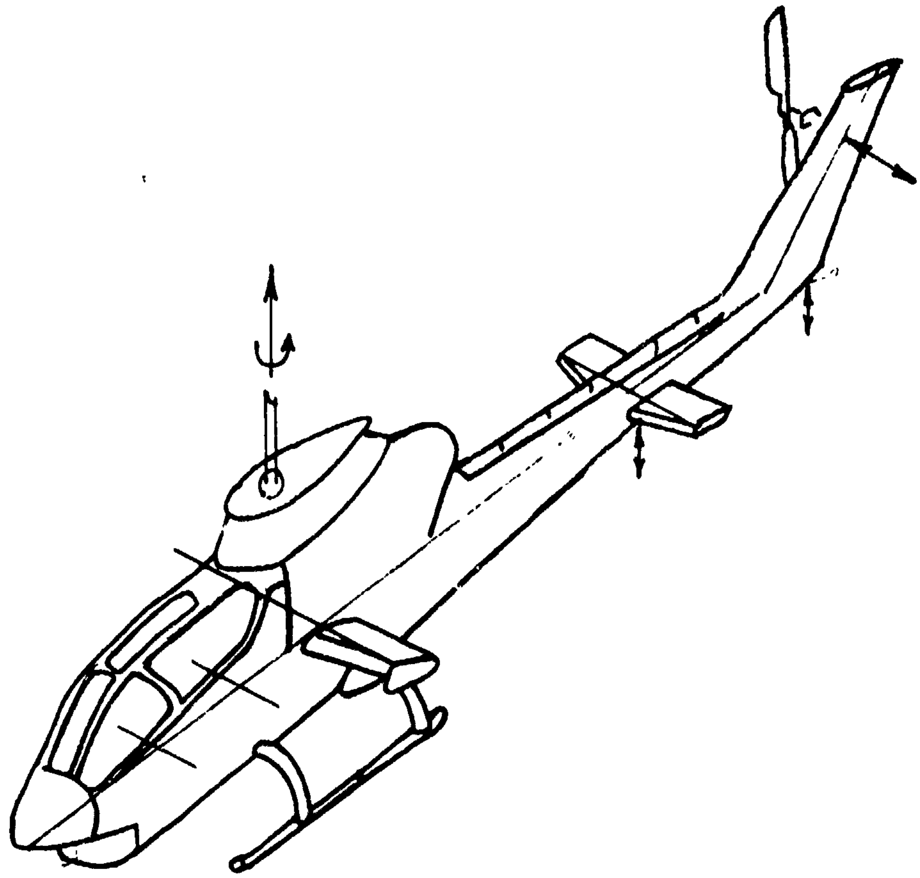

Figure 7. Shaker location points.

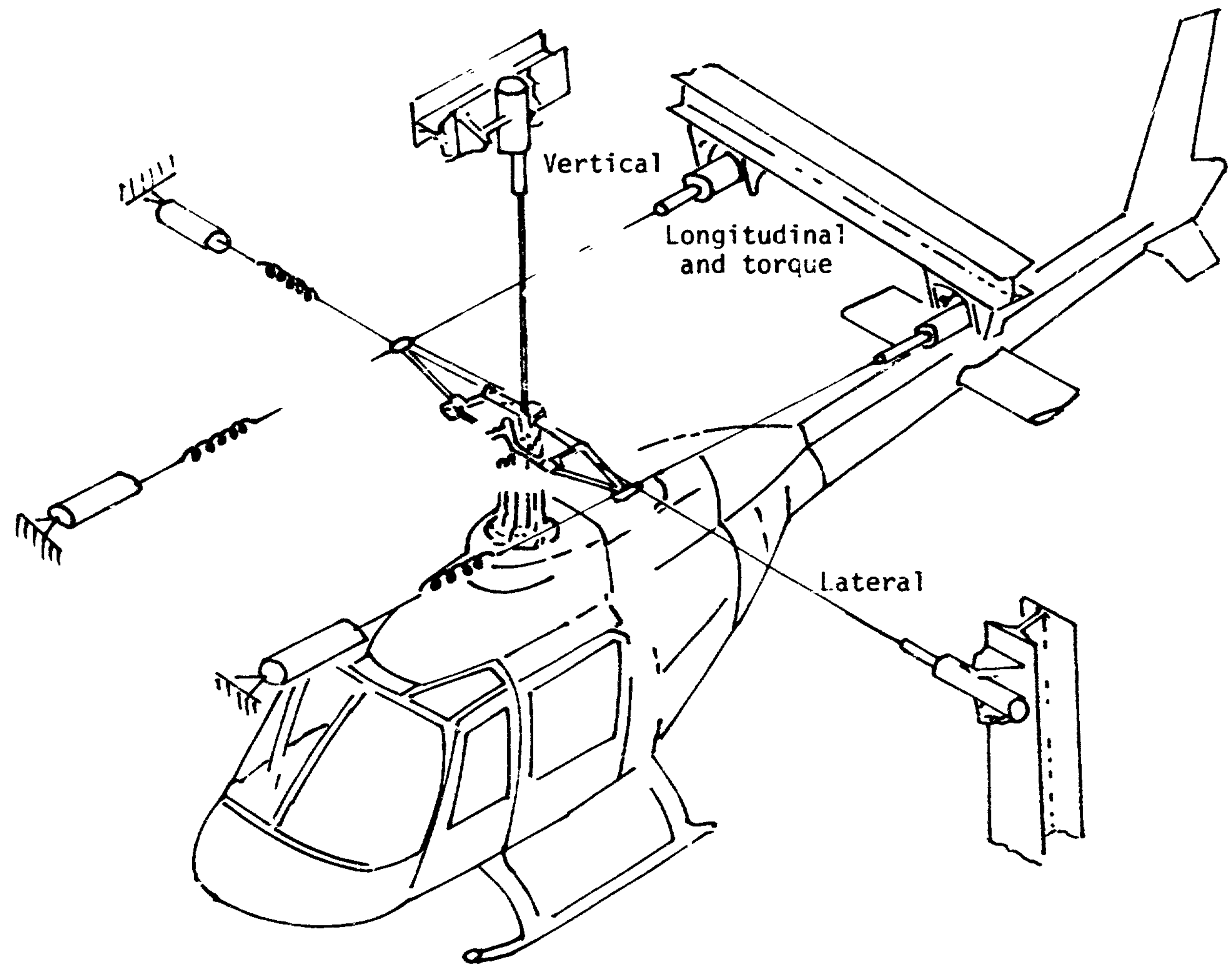

Figure 8. Schematic of the ground flying system.

to be preloaded with soft bungee to prevent any compression in the rods.

Since the rotor forces that are determined are in the shaft, then both for the shake test to calibrate the system and for ground flying, the hub mass and suspension system should be designed as light as possible. This is achieved as shown schematically in Figure 9 in which the hub of the AH-1G hub is used in conjunction with a light triangular member attached such that moments can be applied. This hub shake test attachment is also used to suspend the helicopter on soft bungee to duplicate the free-free boundary condition. Figure 10 is a photograph of the suspension system.

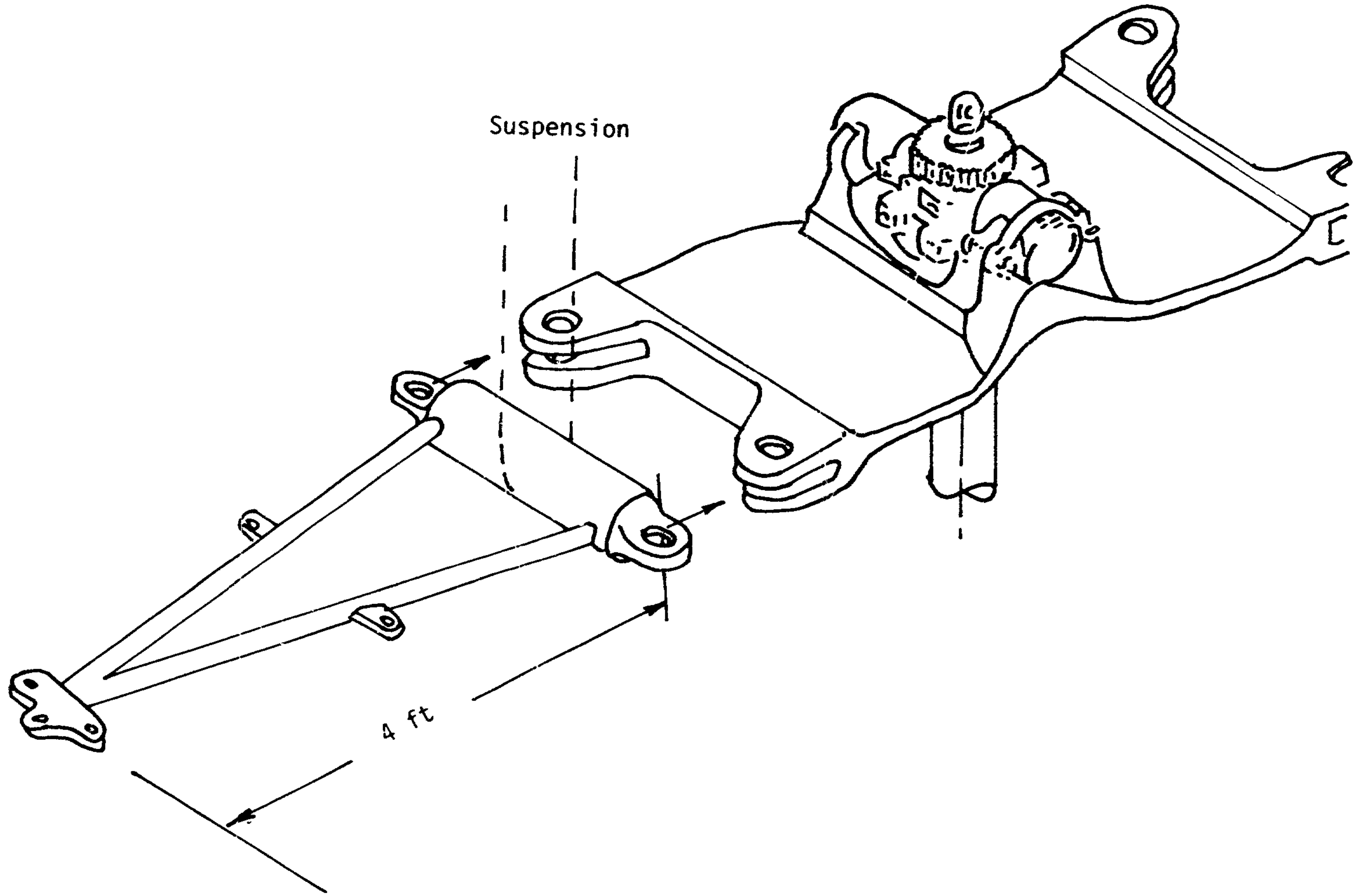

Figure 9. Suspension and nub hardware.

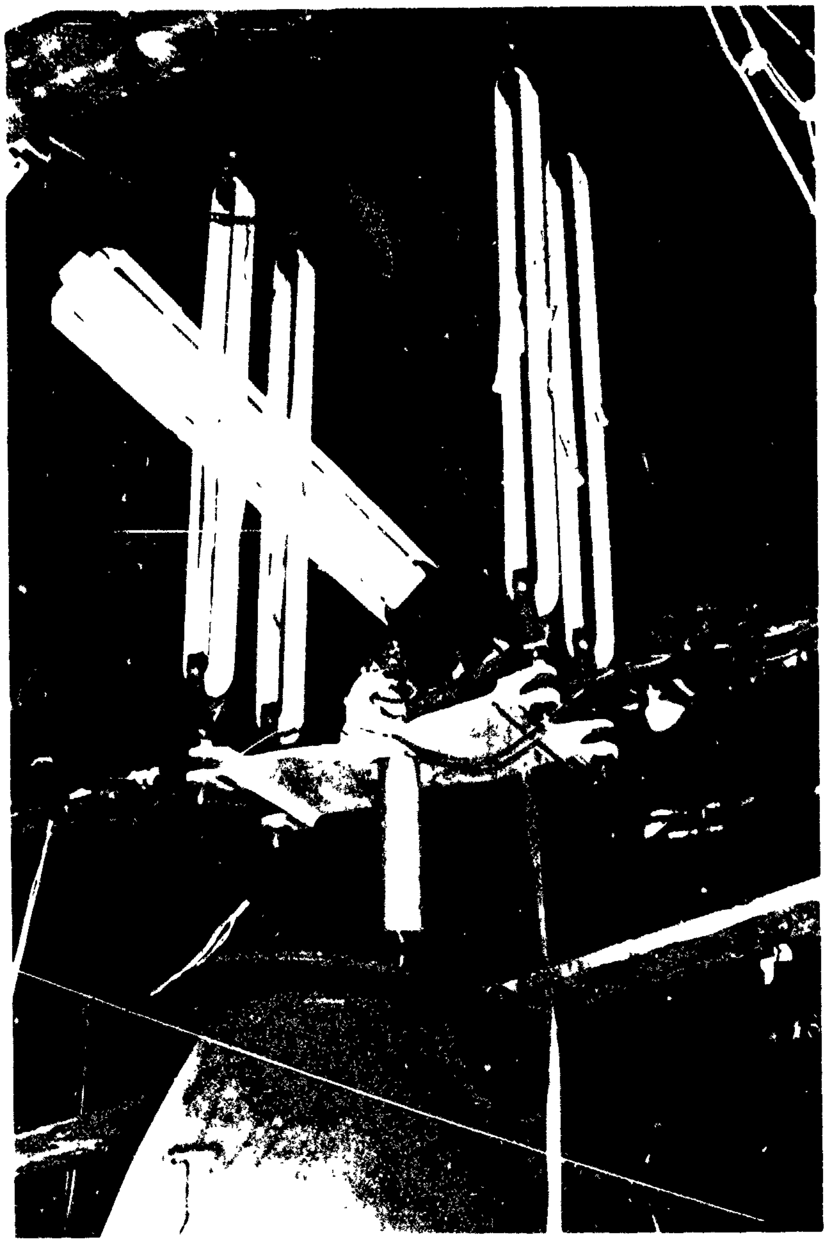

Figure 10. Photograph of the AH-1G suspension system.

TECHNIQUES AND PROCEDURES FOR VIBRATION TESTING OF THE AH-1G HELICOPTER

The development of effective techniques for shaking the AH-1G and analyzing the acquired vibration data constituted a major part of the research work associated with testing. The validity of the methods employed rests heavily upon the consistency between the measured structural mobilities and the theoretical models for which these mobilities are derived. This consistency is critical since the measured mobilities are used not only to obtain the global modal parameters of the test vehicle but also to derive mobilities which were not measured directly.

Digital signal analyzers have made it possible to measure the response of structures to any physically realizable excitation. However, the interpretation of measured structure to specified excitation forces is subject to the mathematical model used in the process of analyzing the data. The model may be more or less sophisticated, depending on the test data. The dynamic testing of a structure like the helicopter poses a number of specific problems. These problems are associated with: (1) the size and complexity of structure; (2) the nonuniform distribution of mass, stiffness and damping; and (3) the correct application of linear vibration theory to the process of data acquisition and analysis.

It has been implied that the techniques adopted for the structural dynamic testing are closely related with the theory underlying the vibration analysis. A discussion of the specific test procedures must necessarily be preceded by a brief summary of the theoretical considerations. This chapter addresses: (1) the theory of the generalized linear structure; (2) the principal characteristics of acceleration mobility data; (3) testing procedures for global parameters and the estimation of these parameters; (4) testing procedures for obtaining mode shapes and the method of calculating mode shapes; and (5) methods for deriving mobilities from modal data.

THEORY OF THE GENERALIZED LINEAR STRUCTURE

The dynamic properties of any structure can always be characterized by a relationship between a selected set of motion coordinates and the set of externally applied forces; i.e.,

$$\begin{Bmatrix} \text{Motion} \\ \text{Vector} \end{Bmatrix} = \begin{vmatrix} \text{Character of} \\ \text{Structure} \end{vmatrix} \times \begin{Bmatrix} \text{Force} \\ \text{Vector} \end{Bmatrix} \tag{1}$$

The character of the structure implied in equation (1) will be termed mobility. If the motion vector is a vector of (displacements/velocities/accelerations), the character of the structure is termed (displacement/velocity/acceleration) mobilities, respectively.

The central phenomenon of vibration theory is cyclic oscillation, hence the quantities that go into equation (1) are generally sought in the frequency domain. For example, in acceleration measurements,

$$\{\ddot{y}(\omega)\} = [\ddot{Y}(\omega)]\{f(\omega)\} \tag{2}$$

where $\{\ddot{y}(\omega)\}$ is the Fourier transform of the accelerations; $[\ddot{Y}(\omega)]$ is the acceleration mobility matrix; and $\{f(\omega)\}$ is the Fourier transform of the vector of generalized forces, compatible with the selected set of coordinates.

From a measurement standpoint, the jkth element of the matrix $[\ddot{Y}(\omega)]$ relates the acceleration measured along the jth coordinate when the only force acting on the structure is that applied along the kth coordinate; i.e.,

$$\ddot{y}_j(\omega) = \ddot{Y}_{jk}(\omega)\ f_k(\omega) \qquad \text{when } f_{i \neq k} = 0 \tag{3}$$

Linear vibration response of a structure may be characterized by the following conditions: (1) the response of the structure to random forcing is stationary in time (i.e., forced vibrations are steady); (2) the elements of the matrix $[\ddot{Y}(\omega)]$ are functions of frequency only, and depend on neither the motion coordinates nor the forcing vector; and (3) the

mobility matrix $[\ddot{Y}(\omega)]$ is symmetric; i.e., $Y_{jk} = Y_{kj}$.

The foregoing conditions have specific practical implications in vibration testing and analysis. The first condition is necessary for any structure to survive continuous operation under arbitrary dynamic excitation. The second condition more or less stipulates the type of shake test data that is adequate for analysis based on a linear model of the structure. If the mobility functions measured for different force levels are not the same, the assumption of linearity is not satisfied. This is usually the case when only part of the structure may be participating in the response. As the force level is increased, more and more of the relevant motion coordinates of the structure start to participate in the response. The range of linear response is reached only when the measured mobility remains unchanged with changing force levels. The third requirement is that of reciprocity. If the shaking and measurement stations are interchanged, the same mobility should be recorded, otherwise the $[\ddot{Y}]$ matrix will not be symmetric, as required by the linear model.

It is important to note that in the foregoing characterization of a linear system, no assumptions are made about the nature of the damping mechanisms occurring in the structures. All the conditions required for linear modeling can be verified in the process of the actual shake test of the structure.

The relationship between the Fourier transform of the force vector and that of the displacement vector of a steadily vibrating undamped multiple degree of freedom system can be written as

$$\left(- \omega^2 [M] + [K]\right)\{y(\omega)\} = f(\omega) \tag{4}$$

where [M] and [K] are real, symmetric mass and stiffness matrices, respectively. Thus, the displacement mobility matrix for an undamped system is

simply

$$[Y(\omega)]_U = \left(-\omega^2 [M] + [K] \right)^{-1} \tag{5}$$

The presence of damping in its most general form can be modeled by introducing a frequency-dependent complex damping matrix into equation (5):

$$[Y(\omega)]_D = \left(-\omega^2 [M] + [K] + [D^R(\omega)] + i[D^I(\omega)] \right)^{-1} \tag{6}$$

It is to be carefully noted that this analytical development has meaning only in the frequency domain for the general case of damping. This is mainly because the physical quantities that can be used to characterize the arbitrary damping of a structure are related to the energy dissipated per cycle of oscillation. In cases where the time domain, force/motion relationship, representing the damping mechanism is known, the damped equations of motion can be developed in the time domain and then Fourier transformed into the frequency domain. However, taking the inverse Fourier transform of the frequency domain equations that may adequately describe an arbitrarily damped system may not yield a time domain system of equations that makes physical sense. In other words, arbitrary damping mechanisms may not be susceptible to a time domain description. Mathematical models developed from time domain equations of motion usually fail to identify global characteristics of structures with significant damping.

In general, the elements of $[D^R(\omega)]$ are small compared to those of the $[K]$ matrix. Also, in order for reciprocity conditions to be met and for energy to be dissipated, the damping matrix must be symmetric and nonnegative definite over the entire frequency range.

For a damped system, then

$$\left([K] + i[D(\omega)] - \omega^2 [M] \right) \{y(\omega)\} - \{f(\omega)\} \tag{7}$$

Consider the complex, frequency-dependent characteristic value problem:

$$\left([K] + i[D(\omega)]\right)\{\phi\} = \lambda(\omega)[M]\ \{\phi\} \tag{8}$$

where $\{\phi\} = \{\phi^R\} + i\{\phi^I\}$ is the complex characteristic vector which can be assumed to be frequency independent; $\lambda(\omega) = \lambda^R(\omega) + i\lambda^I(\omega)$ is the frequency dependent complex eigenvalue.

If combinations of $\left(\lambda_j(\omega),\ \{\phi\}_j\right)$ and $\left(\lambda_k(\omega),\ \{\phi\}_k\right)$ exist which satisfy equation (8), then

$$\{\phi\}_k^T \left([K] + i[D(\omega)]\right)\{\phi\}_j = \lambda_j(\omega)\{\phi\}_k^T\ [M]\{\phi\}_j \tag{9}$$

and

$$\{\phi\}_j^T \left([K] + i[D(\omega)]\right)\{\phi\}_k = \lambda_k(\omega)\{\phi\}_j^T\ [M]\{\phi\}_k \tag{10}$$

$\{\phi\}^T$ denotes the transpose of $\{\phi\}$. By virtue of the symmetry of the [K], [M] and $[D(\omega)]$ matrices, equations (9) and (10) lead to the following orthogonality relationships:

$$\{\phi\}_j^T\ [M]\ \{\phi\}_k = m_j\ \delta_{jk} \tag{11}$$

and

$$\{\phi\}_j^T \left([K] + i[D(\omega)]\right)\{\phi\}_k = \left(k_j + id_j(\omega)\right)\ \delta_{jk} \tag{12}$$

where

$$m_j = \{\phi\}_j^T\ [M]\ \{\phi\}_j \tag{13}$$

$$k_j = \{\phi\}_j^T\ [K]\ \{\phi\}_j \tag{14}$$

$$d_j(\omega) = \{\phi\}_j^T\ [D(\omega)]\ \{\phi\}_j \tag{15}$$

$$\delta_{jk} = \begin{matrix} 0 & j \neq k \\ 1 & j = k \end{matrix} \tag{16}$$

It follows that

$$\{\phi\}_j^T \left([K] - \omega^2 [M] + i[D(\omega)]\right) \{\phi\}_k = \left(k_j - \omega^2 m_j + i d_j(\omega)\right) \delta_{jk}$$

$$= \left(\lambda_j(\omega) - \omega^2 m_j\right) \delta_{jk} \tag{17}$$

If the vectors $\{\phi\}_j$ exist, it can easily be verified that only the imaginary parts of $\lambda_j(\omega)$ need be frequency dependent, so that

$$\lambda_j(\omega) = \lambda_j^R + i\ \lambda_j^I\ (\omega) \tag{18}$$

Indeed, by post-multiplying the transpose of equation (8) by $\{\phi\}_j^*$, which is the complex conjugate of $\{\phi\}_j$, the following equation is obtained:

$$\{\phi\}_j^T \left([K] - i[D(\omega)]\right) \{\phi\}_j^* = \lambda_j(\omega)\ \{\phi\}_j^T\ [M]\ \{\phi\}_j^* \tag{19}$$

Similarly, the complex conjugate of equation (8) can be premultiplied by $\{\phi\}_j^T$ to get

$$\{\phi\}_j^T \left([K] - i[D(\omega)]\right) \{\phi\}_j^* = \lambda_j^*(\omega)\ \{\phi\}_j^T\ [M]\ \{\phi\}_j^* \tag{20}$$

From equations (19) and (20),

$$\lambda_j\ (\omega) + \lambda_j^*(\omega) = 2\ \{\phi\}_j^T\ [K]\ \{\phi\}_j^* / \{\phi\}_j^T\ [M]\ \{\phi\}_j^* \tag{21}$$

and

$$\lambda_j\ (\omega) - \lambda_j^*(\omega) = 2i\ \{\phi\}_j^T\ [D(\omega)]\ \{\phi\}_j^* / \{\phi\}_j^T\ [M] \{\phi\}_j^* \tag{22}$$

The right side of equation (21) is a frequency independent quantity. However, the right side of equation (22) is frequency dependent, establishing the validity of the claim made in equation (18).

A complex L x N modal matrix $[\Phi]$ can be defined such that its jth column is the L x 1 vector $\{\phi\}_j$; j = 1, 2, ...N, where L is the number of coordinates chosen to describe the system and N is the number of modes of the system. In principle, N is infinitely large; in practice, over a given frequency range, only a finite number of system modes are necessary.

Equation (7) can be rewritten to give

$$\{y(\omega)\} = [\Phi]\left[[\Phi]^T\left([K] - \omega^2 [M] + i[D(\omega)]\right)[\Phi]\right]^{-1}[\Phi]^T\{f(\omega)\} \qquad (23)$$

and, using the orthogonality relationships, leads to the results,

$$\{y(\omega)\} = [\Phi]\left[\frac{1}{\left[(\lambda_j^R - \omega^2) + i\lambda_j^I(\omega)\right] m_j}\right][\Phi]^T \{f(\omega)\} \qquad (24)$$

By definition, $\{y(\omega)\} = [Y(\omega)]\{f(\omega)\}$; hence

$$[Y(\omega)] = \sum_{n=1}^{N}\left[\frac{\{\phi\}_n \{\phi\}_n^T}{m_n}\right]\frac{1}{(\lambda_n^R - \omega^2) + i\,\lambda_n^I(\omega)} \qquad (25)$$

λ_n^R and $\lambda_n^I(\omega)$ have units of (frequency)^2, and from physical considerations, both λ_n^R and $\lambda_n^I(\omega)$ are positive. It is therefore possible to define

$$\lambda_n^R \equiv \Omega_n^2 \qquad (26)$$

and

$$\lambda_n^I(\omega) \equiv g_n(\omega)\Omega_n^2 \qquad (27)$$

The matrix of modal acceleration coefficients of the nth mode is defined as

$$[A]_n \equiv \frac{1}{m_n}\{\phi\}_n\{\phi\}_n^T \qquad (28)$$

The acceleration mobility matrix and the displacement mobility matrix are related by

$$[\ddot{Y}(\omega)] = -\omega^2 [Y(\omega)] \tag{29}$$

Making use of equations (26), (27), (28) and (29), the j kth acceleration mobility can be written as

$$\ddot{Y}_{jk}(\omega) = -\sum_{n=1}^{N} A_{jkn} \frac{\omega^2/\Omega_n^{\,2}}{(1 - \omega^2/\Omega_n^{\,2}) + ig_n(\omega)} \tag{30}$$

In the most general case, the dependence of $g_n(\omega)$ on frequency may not be known. However, it is expedient to take advantage of the fact that the $ig_n(\omega)$ term in equation (30) is dominant only in the frequency range where $\omega^2/\Omega_n^{\,2} \simeq 1$, i.e., near the natural frequency of the nth mode. Thus, any suitable representation of $g_n(\omega)$ which matches the correct value in the neighborhood of $\omega = \Omega_n$ may be assumed.

The general form of the j kth element of the acceleration mobility matrix can be written as

$$\ddot{Y}_{jk} = \ddot{Y}^R_{jk} + i\ddot{Y}^I_{jk} = E^R_{jk} + iE^I_{jk} - \sum_{n=1}^{N} A_{jkn} \frac{\omega^2/\Omega_n^{\,2}}{(1 - \omega^2/\Omega^2_{\,n}) + ig_n(\omega)} \tag{31}$$

where $E^R_{jk} + iE^I_{jk}$ represents the rigid body acceleration coefficients. In most cases, E^I_{jk} is very small compared to the rest of the terms in the series. It is often neglected; $A_{jkn} = A^R_{jkn} + iA^I_{jkn}$ is the j kth complex element of the matrix of modal accelerations for the nth mode; Ω_n and g_n are the natural frequencies and damping coefficients of the nth mode, respectively; ω is frequency.

CHARACTERISTICS OF ACCELERATION MOBILITY DATA

Mode frequency functions

The real and imaginary parts of $\ddot{Y}_{jk}$ can be written as

$$\ddot{Y}^R_{jk} = E^R_{jk} - \sum_{n=1}^{N} \left[A^R_{jkn}\, \ddot{F}^R_n (\omega) - A^I_{jkn}\, \ddot{F}^I_n (\omega) \right] \tag{32}$$

and

$$\ddot{Y}^I_{jk} = E^I_{jk} - \sum_{n=1}^{N} \left[A^I_{jkn}\, \ddot{F}^R_n (\omega) + A^R_{jkn}\, \ddot{F}^I_n (\omega) \right] \tag{33}$$

or

$$\ddot{Y}_{jk} = E^R_{jk} + iE^I_{jk} - \sum_{n=1}^{N} A_{jkn}\, \ddot{F}_n (\omega) \tag{34}$$

where the mode frequency functions are defined as

$$\ddot{F}^R_n (\omega) \equiv \frac{\omega^2/\Omega_n^{\,2}\ (\omega^2/\Omega_n^{\,2} - 1)}{(\omega^2/\Omega_n^{\,2} - 1)^2 + g_n^{\,2}} \tag{35}$$

$$\ddot{F}^I_n (\omega) \equiv \frac{g_n\ \omega^2/\Omega_n^{\,2}}{(\omega^2/\Omega_n^{\,2} - 1)^2 + g_n^{\,2}} \tag{36}$$

and

$$\ddot{F}_n (\omega) = \ddot{F}^R_n (\omega) + i\ddot{F}^I_n (\omega) \tag{37}$$

Equations (32), (33) and (34) represent the measured acceleration mobility as a linear combination of the mode functions. It is therefore important to acquire a familiarity with the basic characteristics of the

mode functions of damped systems and the essential features of their linear combinations. Plots of $\ddot{F}^R(\omega)$ and $\ddot{F}^I(\omega)$ as functions of frequency ratio for three values of the damping coefficient are shown in Figure 11. The polar plots of the complex $F(\omega)$ functions are shown in Figure 12.

The $\ddot{F}^R(\omega)$ function is characterized by two peaks at

$$\omega_{1n} = \Omega_n\sqrt{1 + g_n^2 - g_n\sqrt{1 + g_n^2}} \tag{38}$$

and

$$\omega_{2n} = \Omega_n\sqrt{1 + g_n^2 + g_n\sqrt{1 + g_n^2}}\ ; \tag{39}$$

while the $\ddot{F}^I(\omega)$ function has only one peak at $\omega_{3n} = {}_n\sqrt{1 + g_n^2}$.
Note that

$$\frac{\omega_{2n}^2 - \omega_{1n}^2}{\Omega_n^2} = 2g_n\sqrt{1 + g_n^2} \tag{40}$$

which increases with increasing damping.

From the plots in Figure 11, it is seen that linear combinations of $\ddot{F}^R$ and $\ddot{F}^I$ vary rapidly in the vicinity of the natural frequency and are either negligible or slowly varying with frequency in the regions away from the natural frequency.

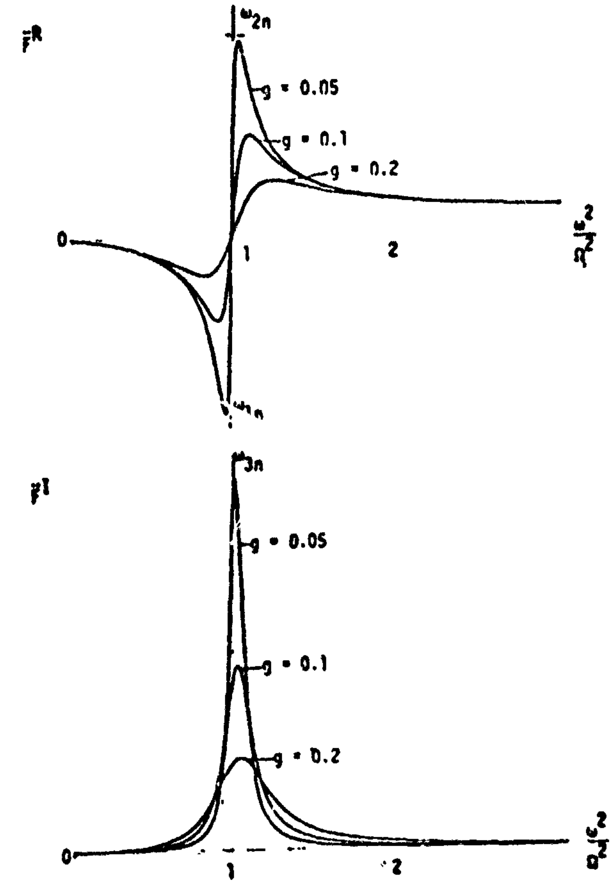

Figure 11. Real ($\ddot{F}^R$) and imaginary ($\ddot{F}^I$) parts of the complex "Mode" function $\ddot{F}(\omega)$.

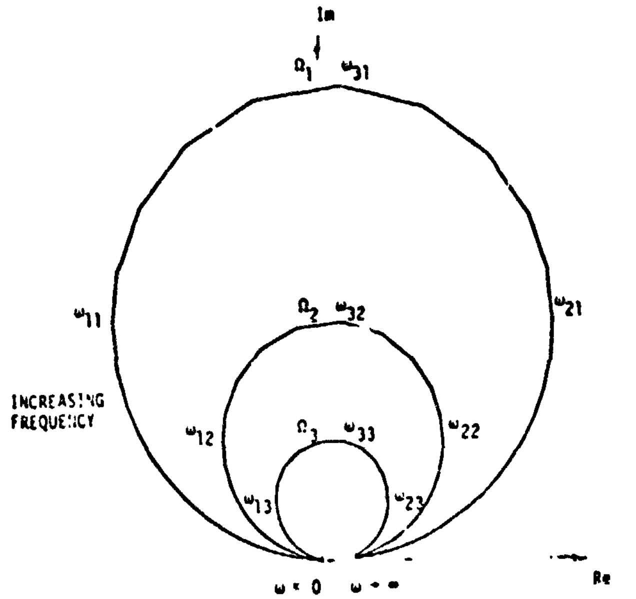

Figure 12. Polar plot of the complex $\ddot{F}(\omega)$ function.

Separated Modes - Equation (31) carries the basic implication that the effects of the structure's modes occurring at different frequencies on the measured mobility are addicive in the frequency domain. If a mode occurs at a frequency in the neighborhood of which the contributions from the other modes of the structure are either negligible or are weakly varying with frequency, such a mode is said to be well separated. The nature of the measured mobility in this frequency range will be dominated by that particular mode.

Classical Modes - In the case of a classical mode, i.e., when the system mode shape is the same for the damped system as it would be for the undamped system the A_{jkn} is a real number, i.e., $A^I_{jkn} = 0$, and the real part of the measured acceleration mobility will show two turning points for each separated mode and the imaginary part will show a single turning point only. For a classical mode, equation (40) can be approximated to give an estimate of the damping coefficient: $g_n \approx (\omega_{2n} - \omega_{1n})/\Omega_n$.

Figures 13 and 14 show acceleration mobility measurements obtained from a helicopter structure. Two close, but distinguishable modes are present. The dominant mode can be seen to be very nearly classical, with double turning points in the real and a single turning point in the imaginary mobilities.

Complex Modes - For the general case of nonclassical or complex modes, both A^R_{jkn} and A^I_{jkn} are significant. The measured real and imaginary mobilities of a well separated mode contain linear combinations of both $F^R(\omega)$ and $F^I(\omega)$ in proportions given in equations (32) and (33). In particular, if $A^I_{jkn} >> A^R_{jkn}$, the imaginary part of the acceleration mobility will show two turning points, while the real part will show a single turning point only. Figures 15 and 16 show an example of this occurrence in the data measured from the AH-1G (the shaking coordinate was vertical at the tail, and the measurement coordinate was vertical at the nose) between 40 and 50 Hz.

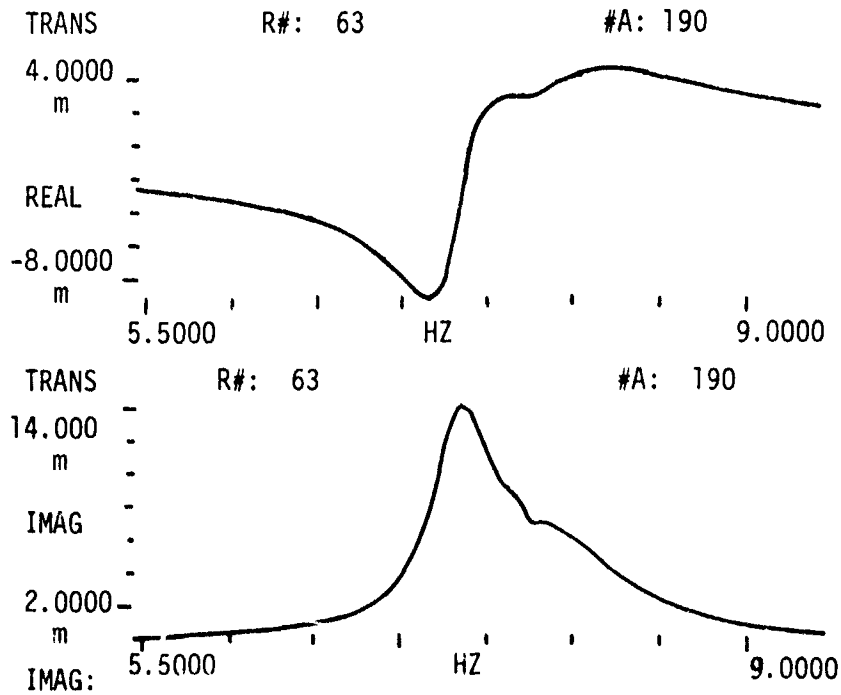

Figure 13. Measured acceleration mobility of a helicopter between 5.5 and 10 Hz. (Shaking vertically at the tail, measuring vertical acceleration at the nose.)

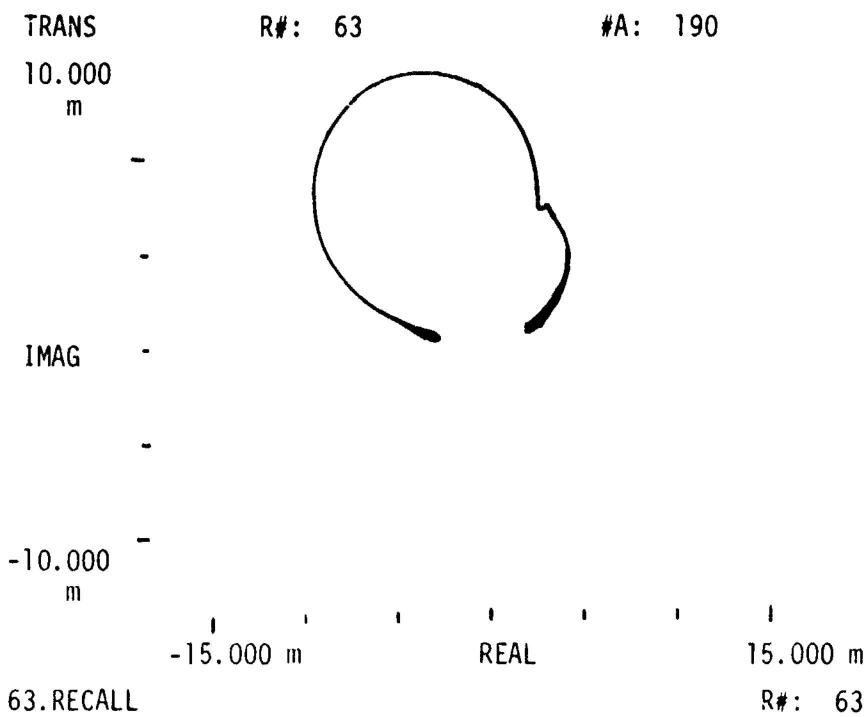

Figure 14. Data of Figure 13 plotted on the Argand Plane.

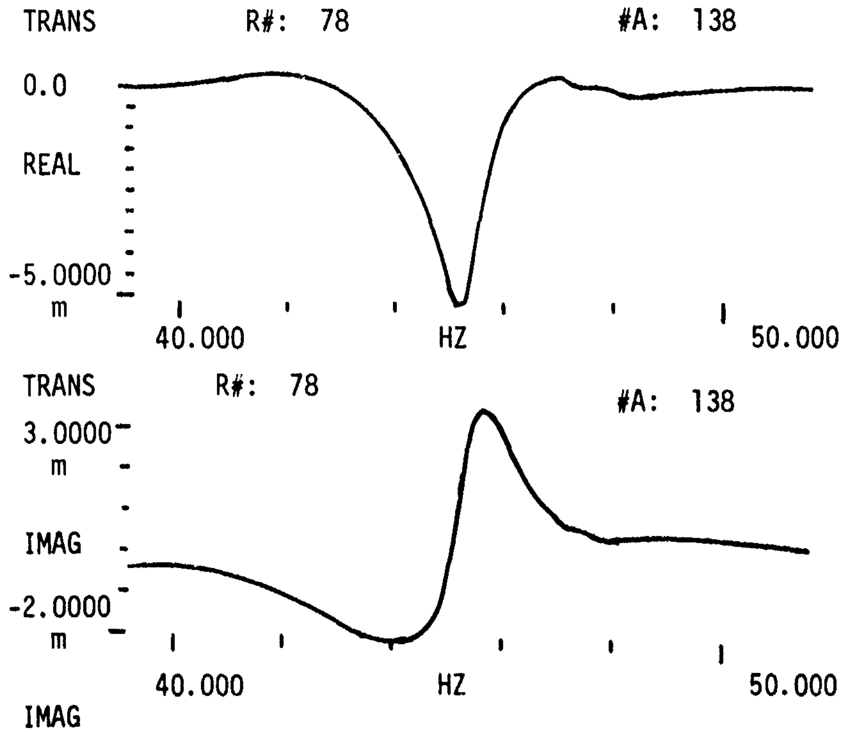

Figure 15. Measured acceleration mobility of a helicopter between 38 Hz and 52 Hz. (Shaking vertically at the tail, measuring vertical acceleration at the nose.)

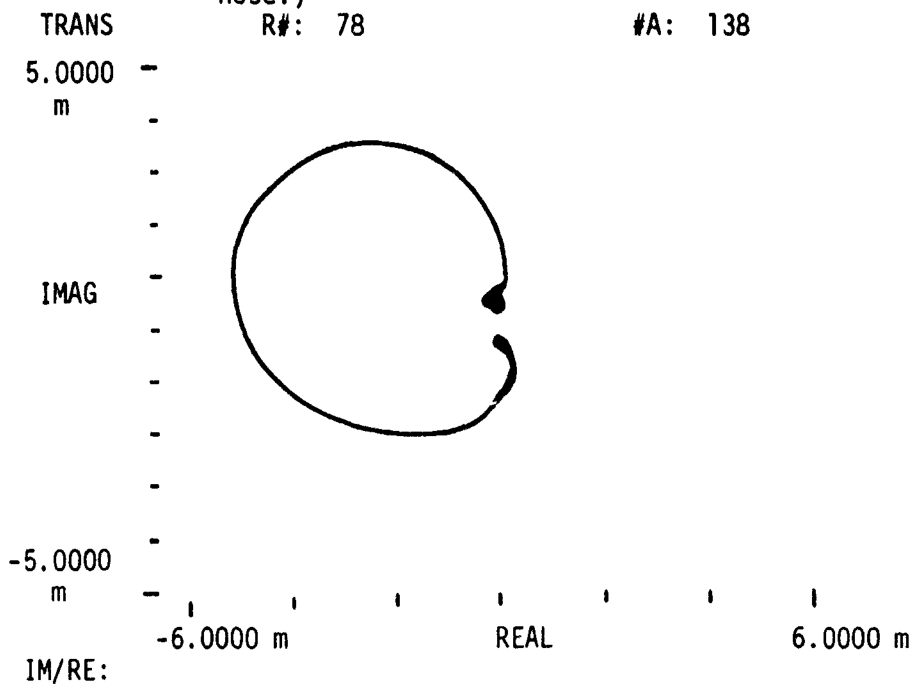

Figure 16. Data of Figure 15 plotted on the Argand Plane.

Coupled Modes - System modes occurring in frequency ranges such that their mutual contributions to the measured mobility in this frequency range are rapidly varying functions of frequency are said to be coupled.

Mode Clusters - A mode cluster (or a cluster of modes) is characterized by a group of system modes which are coupled together by virtue of the proximity of their resonances. Mode clusters are usually separated by regions of negligible or slowly varying mobility values in the frequency domain.

Mode clusters generally have the appearance of single modes in wide band, low frequency resolution mobility measurements. Higher resolution data usually helps to reveal the modal content of a particular mode cluster. Figure 17 shows broad band (0-200 Hz) mobility of a helicopter vertical tail shake, measuring vertical acceleration at the nose. Between mode clusters, measured mobility is seen vary slowly close to the zero value. In fact, what appears to be a single mode in the 0-10 Hz frequency range is actually a cluster of two modes, as Figures 13 and 14 (which are higher resolution measurement of the same mobility in the 5-10 Hz range) show.

Identification of mode clusters is useful in determining which modes should be included when truncating equation (31), since the contributions of the remaining modes are either negligible or frequency independent. It also helps in identifying frequency segments for higher resolution data acquisition.

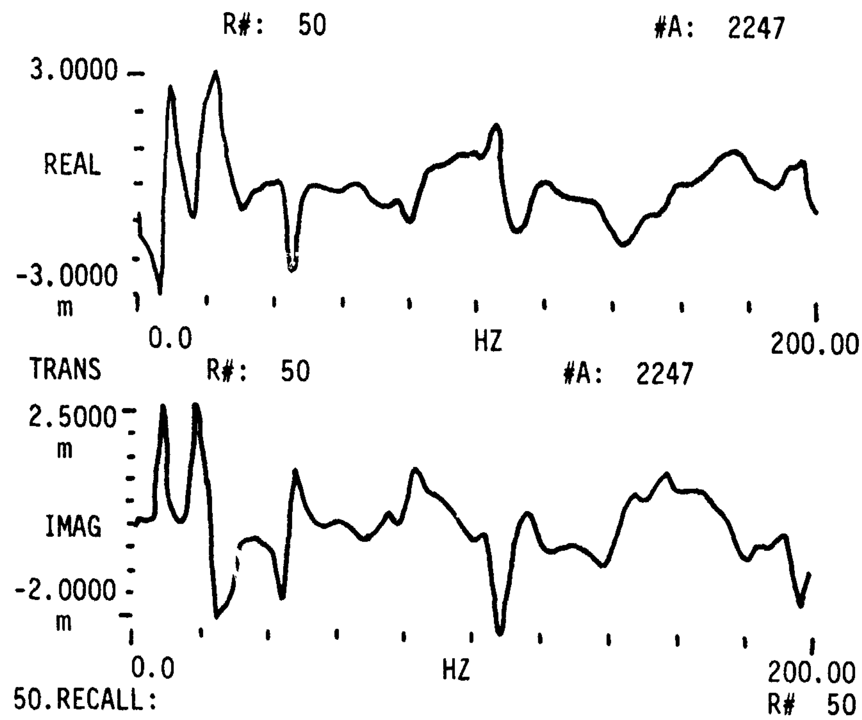

Figure 17. Measured acceleration mobility of a helicopter between 2 and 200 Hz. (Shaking vertically at the tail, measuring vertical acceleration at the nose.)

SHAKE TESTING FOR GLOBAL PARAMETERS

Each elastic mode of the structure is characterized by a natural frequency Ω_n and a damping coefficient g_n which are global properties of the structure. These are the only constants that enter into the mode frequency functions. They are the same for a given mode, regardless of the response coordinate. The first stage of modal testing is to determine the global parameters of the dominant elastic modes which occur inside the frequency range of interest.

The experimental data required for determining the global parameters are the continuous frequency plots of a number of mobilities which are considered to represent the global vibrational behavior of the structure. For a selected set of shaking locations, e.g., tail vertical, tail rotor or gearbox lateral, the transfer functions between the response coordinates and the shaking coordinates are measured over the determined frequency range. Typical response coordinates for such measurements are (1) nose vertical, (2) wing (right and/or left) vertical, (3) center of gravity vertical, (4) tail vertical, and (5) horizontal stabilizer vertical.

The test setup for measuring frequency-dependent mobility functions is shown in Figure 18. The helicopter is suspended as a free body by soft rubber bungee chords. The configuration shown has the shaker located vertically at the tail and the response accelerometer at the horizontal stabilizer vertical. Signals for driving the electromagnetic shaker originate from the signal generator. A gage installed at the point of force application generates voltage signals which are proportional to the applied force. These signals are inputs to the dual channel digital signal analyzer. The accelerometer at the response coordinate generates voltage signals proportional to the response acceleration, which are also inputs to the digital signal analyzer.

The signal analyzer is capable of sampling the time domain force and response signals, digitizing these samples and computing the real-time

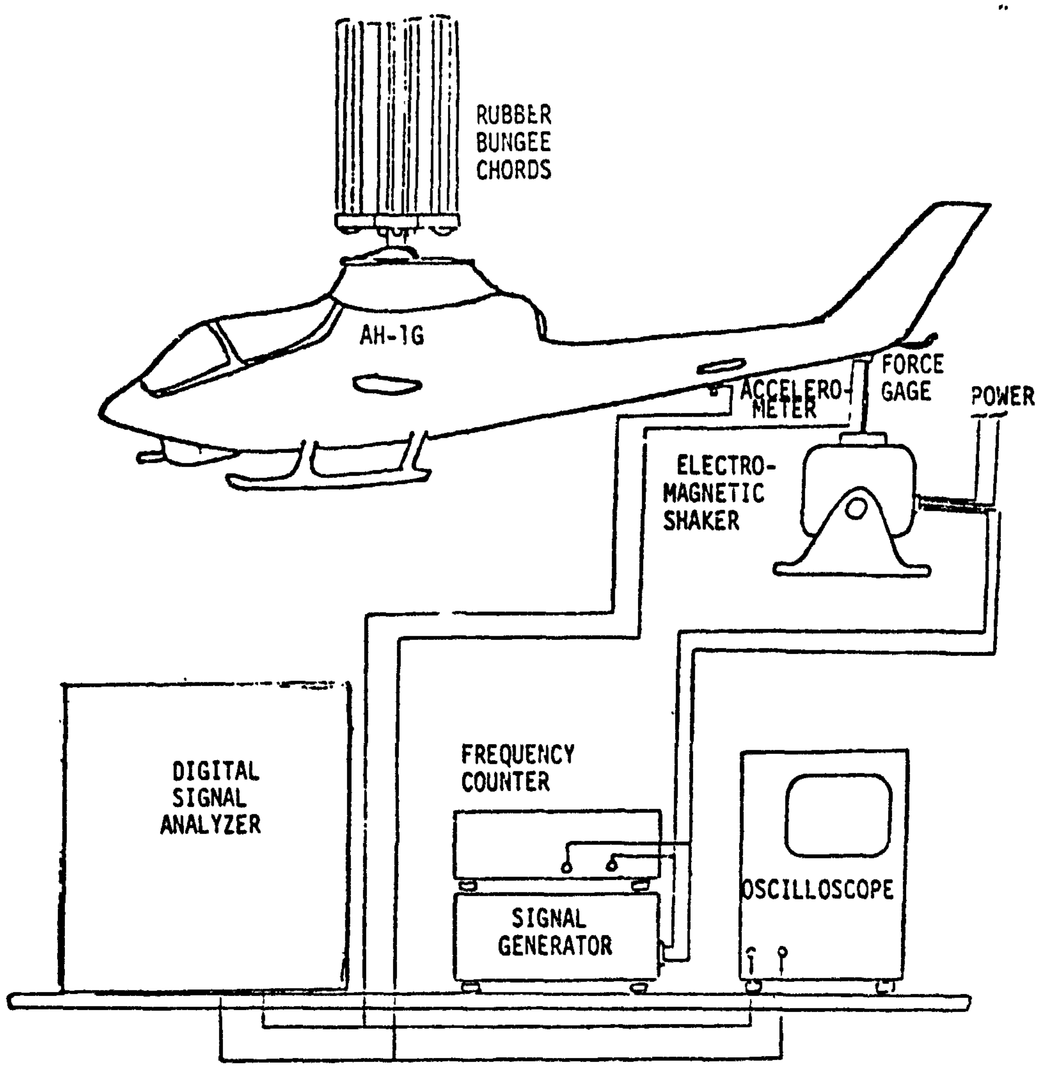

Figure 18. Schematic of setup for global parameter testing.

Fourier transforms of the data. It also computes the least squares estimate of the frequency domain transfer function between the input and output spectra, which is the mobility between the response and forcing coordinates. All the frequency functions computed by the analyzer over the specified frequency interval can be stored on cassette tapes for future restoration and analysis. The oscilloscope allows the monitoring of the time domain signals emanating from the force and response transducers. The frequency counter is used to precisely measure the frequencies of harmonic signals when required.

The accuracy with which the global parameters can be estimated is critically dependent on the quality of the data acquired for this purpose. For each pair of force and response locations, a random shake is done with the frequency bandwidth set to span twice the range of interest (in this case 0-200 Hz, since the modes of interest are between 2-100 Hz). This is done to insure that the modes up to 100 Hz are not coupled to modes occurring beyond 100 Hz, as may be the case when a local mode is present. For each new shaking station, several force levels are tested until the range of applied force is reached where the mobility plots do not depend on the force level anymore. This is one of the linearity requirements on the mobility plots. Having established the required force level and the absence of local coupling modes at higher frequency, another random shake is done, this time with the bandwidth set at 2-100 Hz. The above procedure is repeated for all the accelerometers which have been selected for global parameter testing.

The ratio of modal acceleration coefficient to damping (A_{jkn}/g_n) varies not only from mode to mode but also from mobility to mobility, for a given mode, and the prominence of the various modes of the structure will be different in each of the mobilities recorded. That is to say, a given mode i occurring at Ω_i may appear very prominently on mobility $\ddot{Y}_{jk}(\omega)$, while the same mode may not be so significant in the mobility $\ddot{Y}_{j\ell}$, where ℓ designates a response coordinate different from k. This will especially

be the case if the mode shape associated with mode i has a much larger mode element at coordinate k than coordinate ℓ. The prominence of a mode may also be due to light damping. Thus, by examining the set of broad-band mobilities recorded, it is possible to associate each mode i with the mobility where the mode most prominently appears.

Although it is possible to obtain rough estimates of the natural frequencies and damping of the structural elastic modes from these broad-band mobility plots especially when damping is very light (e.g. peaks of the imaginary mobility plots, and frequency separation of the peaks in the real mobility plots), there are a number of specific reasons why broad-band mobility data is not suitable for global parameter extraction. Among these reasons are:

Measurement Accuracy - The low frequency resolution associated with broad-band mobility measurements tends to introduce errors into the measured mobility values due to the phenomenon of leakage. Leakage has to do with a spreading of the energy contained at each discrete frequency over a relatively narrow band nearby. Although considerable effort is exerted into reducing leakage effects (e.g., by appropriately windowing) by the equipment manufacturers, the phenomenon still has to be reckoned with when the frequency resolution gets below certain limits. For acceptable measurements, bandwidths of about 25% of the center frequency have been recommended.

Parameter Extraction Accuracy - Also associated with low frequency resolution are inaccuracies in the parameter extraction methods due to the frequency spacing between successive data points. The polar plot of mobilities, (see Figure 12) in the vicinity of a mode, describes a circular arc. Most methods for extracting natural frequencies, damping and modal acceleration coefficients are based on fitting a continuous circle through measured data and in some cases computing the rate of change of the arc length with frequency. Since the frequency data is discrete, arcs of the circle are necessarily approximated by segments. The error incurred by approximating

a circular arc by a straight line segment increases as the frequency spacing between successive data points increases. Narrow-band data with bandwidth less than 25% of the natural frequency of a given mode found to yield sufficiently accurate results. Initial estimates of the natural frequencies can be obtained from the broad-band data.

For sufficient frequency resolution and to minimize leakage, the following bandwidths are recommended for use in narrow-band testing using the HP5420A signal analyzer.

TABLE 5. BANDWIDTH RECOMMENDATIONS.

Natural Frequency Ω_i Equal to or greater than	But less than	Bandwidth
2 Hertz	3 Hertz	.5 Hertz
3	4	.781
4	6	1.000
6	8	1.5625
8	12	2.000
12	16	3.125
16	25	4.000
25	32	6.250
32	50	8.000
50	64	12.500
64	100	16.000

In cases of g greater than .25, use a broader bandwidth. In all cases use the natural frequency as the center frequency.

SWEPT SINE TESTING

For all the narrow-band mobility measurements, the excitation was achieved by applying pure sine wave signals to the electromagnetic shaker and varying the frequency of the sine waves over the range spanned by the bandwidth. This so-called swept sine technique was preferred to other excitation techniques over a narrow frequency band. Other reasons for choosing the swept sine technique include:

1. The energy input into each measurement frequency is maximum.
2. By choosing the right sweep speed (see below), the steady state sinusoidal response of the structure is achieved at each measurement frequency. This is one of the assumptions made in the derivation of the generalized linear model.
3. Measurements are more accurate and reproducible.
4. The sampling frequencies and the adequate number of averages are more easily determined.
5. Good linearity and reciprocity checks are obtained.
6. High resolution of close modes can be achieved by selecting the right sweep speed.

Consider an undamped single-degree-of-freedom linear system, described by the following equation of forced vibrations:

$$m\ddot{x} + kx = Fe^{i\omega t} \tag{41}$$

If the forcing frequency coincides with the undamped natural frequency, i.e., $\omega = \sqrt{\frac{k}{m}}$, the response of the system is secular and grows linearly with time.

Schematically:

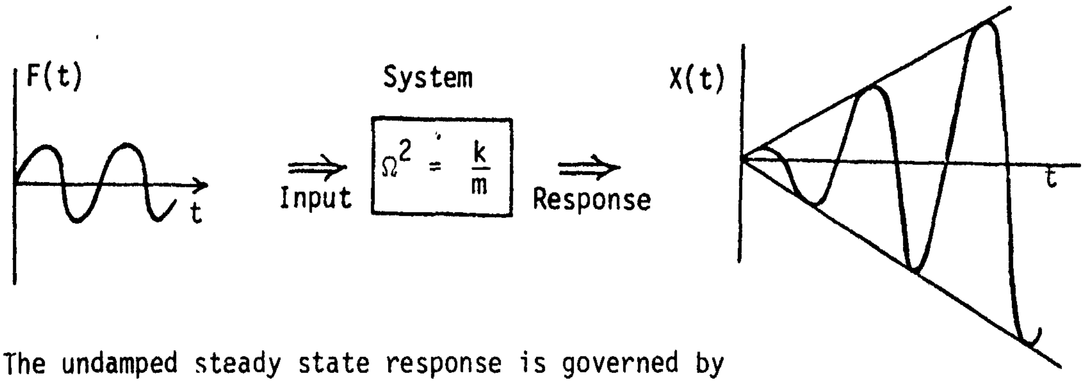

The undamped steady state response is governed by

$$\ddot{x} + \Omega^2 x = \frac{F}{m} e^{i\Omega t} \tag{42}$$

or

$$x(t) = -i \frac{Ft}{2m\Omega} e^{i\Omega t} \tag{43}$$

However, because of the various dissipative mechanisms which constitute damping, the oscillations reach a limiting amplitude after some characteristic time τ.

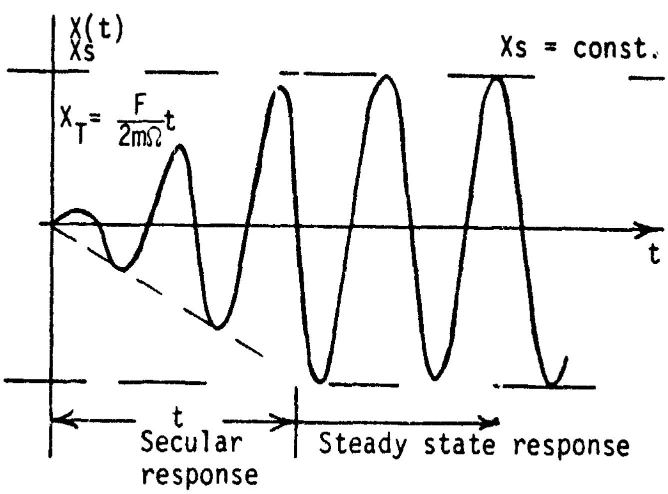

For damped hysteretic damping, g, the steady state response is governed by

$$\ddot{x} + (1 + ig)\Omega^2 x = \frac{F}{m} e^{i\Omega t} \tag{44}$$

or $\quad x(t) = - \frac{F}{mg\Omega^2} e^{i\Omega t}$ (45)

..e steady state amplitude is given by

$$Xs = \frac{F}{mg\Omega^2} \tag{46}$$

and the characteristic time for reaching steady state response can be estimated by equating

$$X_T(\tau) = Xs, \tag{47}$$

which gives $\quad \frac{F}{2m\Omega} \tau = \frac{F}{mg\Omega^2}$ (48)

..hus, $\quad \tau = \frac{2}{g\Omega} = \frac{1}{\pi g f}$ (49)

..ppose there are two neighboring structural modes with the natural frequencies separated by Δf Hz. To resolve these two close modes, the speed ..t which the excitation frequency is changing must be of the order of

$$v = V\Delta_f = \pi g f \, \Delta f \quad \text{Hz/sec} \tag{50}$$

..here $\quad g$ = damping coefficient (lower bound)

f = frequency in Hz

Δ_f = mode resolution in Hz.

estimates of the lower bound of the damping coefficient and the re- ..ired mode resolution are available, the sweep speed required for swept ..ne shake testing is directly proportional to the frequency.

i.e., $\frac{V(\Delta_f)}{f} = \text{const}$ (51)

The relationship between the linear scale and the logarithmic scale on the signal generator is

$$f_{dec} = \log_{10} \frac{f_{Hz}}{f_o} \qquad (52)$$

where f_{Hz} = frequency in Hertz $(f_o \leq f_{yz} \leq 10_{f_o})$

f_{dec} = frequency in decades $(0 \leq f_{dec} \leq 1.0)$

f_o = base frequency on the scale

From equation (52), $f_{Hz} = f_o \times 10^{f_{dec}}$ (53)

Sweep speed $v = \frac{df_{Hz}}{df_{dec}} = \frac{df_{Hz}}{df_{dec}} \times \frac{df_{dec}}{dt}$ Hz/sec (54)

From equation (53), $\frac{df_{Hz}}{df_{dec}} = (f_o \ \ell n\ 10) \times 10^{f_{dec}} = f_{Hz} \ \ell n\ 10$ (55)

$$\text{and} \quad \frac{v}{f_{Hz}} = \frac{df_{dec}}{dt} \ \ell n 10 \qquad (56)$$

Thus, by selecting a constant logarithmic sweep speed (df_{dec}/dt = const. = α), equation (51) is automatically satisfied.

The constant α is determined by substituting the desired value of $\frac{v}{f_{Hz}}$ into equation (56). For example, if at 2 Hz we desire a sweep rate of 0.01 Hz/sec, then

$$\alpha = \frac{0.01(60)}{2\ell n 10} \text{ dec/min} = .13 \text{ dec/min} \qquad (57)$$

ESTIMATION OF GLOBAL PARAMETERS

Various techniques have been developed for estimating the natural frequencies and damping coefficients of the elastic modes of a structure from mobility data. In all cases, certain assumptions have to be made about these modes. The simplest case is when the mode is well separated and lightly damped. For such modes, the natural frequency can be approximated by the peak of the imaginary displacement mobility. The damping coefficient can be estimated as

$$g_n \simeq \frac{1}{2} \frac{\omega_2^2 - \omega_1^2}{\Omega_n^2} \simeq \frac{\omega_2 - \omega_1}{\Omega_n} \tag{58}$$

where ω_2 and ω_1 are the turning point frequencies in the real displacement mobility. The above simple case is almost exclusively reserved for simple structures with uniform distribution of mass, stiffness, and damping. Very few of the modes of the helicopter can be treated this way.

The ds/df^2 method of Kennedy and Pancu - The following is a more general approach which has been found to work well for both classical and complex, close or separated modes. By analogy with equations (32) through (37), the j kth displacement mobility can be expressed as

$$Y_{jk} = \frac{\varepsilon_{jk}}{-\omega^2} + \sum_{n=1}^{N} \left\{ \left(A_{jkn}^R F_n^R - A_{jkn}^I F_n^I \right) + i \left(A_{jkn}^R F_n^I + A_{jkn}^I F_n^R \right) \right\} \tag{59}$$

where $A_{jkn} = A_{jkn}^R + iA_{jkn}^I$ is the j kth modal acceleration coefficient of n-th mode and E_{jk} is the contribution from the rigid body modes.

Recall that

$$F_n(\omega) = F_n^R(\omega) + i\ F_n^I(\omega) = \frac{-1}{\omega^2} \ddot{F}_n(\omega) \tag{60}$$

which gives

$$F_n^{R}(\omega) = \frac{1}{\Omega_n^2} \frac{1 - \omega^2/\Omega_n^2}{\left[1 - \omega^2/\Omega_n^2\right]^2 + g_n^2} \tag{61}$$

and

$$F_n^{I}(\omega) = \frac{1}{\Omega_n^2} \frac{-g_n}{\left[1 - \omega^2/\Omega_n^2\right]^2 + g_n^2} \tag{62}$$

In the immediate vicinity of the nth natural frequency, the displacement mobility can be approximated by

$$\begin{aligned} Y_{jk}\ (\omega \approx \Omega_n) \ \approx & \left[A_{jkn}^{R}\ F_n^{R}\ (\omega) - A_{jkn}^{I}\ F_n^{I}\ (\omega) + C_n^{R}\ \frac{\omega^2}{\Omega_n^2} + d_n^{R}\right] \\ & + i\ \left[A_{jkn}^{R}\ F_n^{I}(\omega) + A_{jkn}^{I}\ F_n^{R}(\omega) + C_n^{I}\ \frac{\omega^2}{\Omega_n^2} + d_n^{I}\right] \end{aligned} \tag{63}$$

In equation (63), the sum of the contributions from all other modes has been reoresented by a complex straight line:

$$\left(C_n^{R} + i\ C_n^{I}\right)\ \frac{\omega^2}{\Omega_n^2} + d_n^{R} + i\ d_n^{I}$$

Dropping the subscripts j, k, n and writing the real and imaginary parts of the displacement mobility separately gives

$$Y^{R}\ (\omega \approx \Omega) \approx\ A^{R}\ F^{R}\ (\omega) - A^{I}\ F^{I}\ (\omega) + C^{R}\ \frac{\omega^2}{\Omega^2} + d^{R} \tag{64}$$

$$Y^{I}\ (\omega \approx \Omega) \approx\ A^{R}\ F^{I}\ (\omega) + A^{I}\ F^{R}\ (\omega) + C^{I}\ \frac{\omega^2}{\Omega^2} + d^{I} \tag{65}$$

If the nth mode is classical and well separated, the imaginary part of the modal acceleration coefficient vanishes and the contributions from other modes are nearly independent of frequency. In other words, A^I, C^R, and C^I vanish. Thus,

$$Y^R\ (\omega \approx \Omega) \simeq A^R\ F^R(\omega) + d^R \tag{66}$$

$$Y^I\ (\omega \approx \Omega) \simeq A^R\ F^I(\omega) + d^I \tag{67}$$

The peak of the imaginary mobility occurs when

$$\frac{dY^I}{d\omega^2} = 0 = A^R\ \frac{d}{d\omega^2}\ F^I(\omega) \tag{68}$$

or

$$\frac{A^R}{2}\ \frac{2/\Omega^2\ g\left(1 - \omega^2/\Omega^2\right)}{\left[\left(1 - \omega^2/\Omega^2\right)^2 + g^2\right]^2} = 0 \tag{69}$$

which is when $\omega^2/\Omega^2 = 1$, as stated previously.

The peaks of the real displacement mobility occur when

$$\frac{dY^R}{d\omega^2} = 0 = A^R\ \frac{d}{d\omega^2}\left(F^R(\omega)\right) \tag{70}$$

or

$$\frac{A^R}{\Omega^4}\ \frac{\left(1 - \omega^2/\Omega^2\right)^2 - g^2}{\left[\left(1 - \omega^2/\Omega^2\right)^2 + g^2\right]^2} = 0 \tag{71}$$

which gives peaks at

$$\frac{\omega_1^2}{\Omega^2} = 1 - g \tag{72}$$

and

$$\frac{\omega_2^2}{\Omega^2} = 1 + g \tag{73}$$

$$\text{or} \quad g = \frac{1}{2}\,\frac{\omega_2^2 - \omega_1^2}{\Omega^2} \qquad \frac{\omega_2 - \omega_1}{\Omega} \tag{74}$$

as stated previously.

When the mode is complex, equations (64) and (65) indicate that both the real and imaginary parts of the displacement mobility contain linear combinations of $F^R(\omega)$, $F^I(\omega)$, ω^2 and constants. The peaks in the mobilities in the general case may not be simply related to the natural frequency and damping coefficients. Naturally, different degrees of approximations are feasible, depending on how complicated the situation really is.

A general technique which has been found applicable to the majority of modes encountered on the AH-1G helicopter is based on the rate of change of the arc length of the modal curve (plotted on the complex plane, i.e., the plot of the Y^I against Y^R with frequency as a parameter).

$$\frac{ds}{d(\omega^2)} = \sqrt{\left[\frac{dY^R}{d(\omega^2)}^{2} + \frac{dY^I}{d(\omega^2)}\right]^2} \tag{75}$$

where s is the arc length.

The rate of change of the arc length with respect to the square of frequency is stationary when

$$\frac{d^2 s}{d(\omega^2)^2} = 0 = \frac{\dfrac{dY^R}{d(\omega^2)}\,\dfrac{d^2Y^R}{d(\omega^2)^2} + \dfrac{dY^I}{d(\omega^2)}\,\dfrac{d^2Y^I}{d(\omega^2)^2}}{\sqrt{\left[\dfrac{dY^R}{d(\omega^2)}\right]^2 + \left[\dfrac{dY^I}{d(\omega^2)}\right]^2}} \tag{76}$$

or

$$\frac{dY^R}{d(\omega^2)}\,\frac{d^2Y^R}{d(\omega^2)^2} + \frac{dY^I}{d(\omega^2)}\,\frac{d^2Y^I}{d(\omega^2)^2} = 0 \tag{77}$$

By substituting equations (64) and (65) into equation (77) and simplifying, the following condition for the peak of the $\frac{ds}{d(\omega)^2}$ plot is obtained:

$$|A|^2 \frac{d}{d(\omega^2)}\left\{\left[\frac{dF^R}{d(\omega^2)}\right]^2 + \left[\frac{dF^I}{d(\omega^2)}\right]^2\right\} + \frac{C^R}{2}\left\{A^R \frac{d^2F^R}{d(\omega^2)^2} - A^I \frac{d^2F^I}{d(\omega^2)^2}\right\}$$

$$+ \frac{C^I}{\Omega^2}\left\{A^R \frac{d^2F^I}{d(\omega^2)^2} + A^I \frac{d^2F^R}{d(\omega^2)^2}\right\} = 0 \qquad (78)$$

where $|A|^2 \equiv (A^R)^2 + (A^I)^2$

For a well separated mode, the constants C^R and C^I will be nearly zero and equation (78) gives

$$\frac{d}{d(\omega^2)}\left\{\left[\frac{dF^R}{d(\omega^2)}\right]^2 + \left[\frac{dF^I}{d(\omega^2)}\right]^2\right\} = 0 \qquad (79)$$

Equation (79) does not involve the modal acceleration coefficients A^R and A^I. Thus, the condition for the peaking of the rate of change of the arc length with respect to frequency squared holds true regardless of how complex the mode is, as long as it is well separated.

Equation (79) can be expanded by making use of equations (61) and (62), and the result is

$$\frac{d}{d(\omega^2)}\left[\frac{\left[\left(1 - \frac{\omega^2}{\Omega^2}\right)^2 - g^2\right]^2 + 4g^2\, 1 - \frac{\omega^2}{\Omega^2}}{\Omega^8\left[\left(1 - \frac{\omega^2}{\Omega^2}\right)^2 + g^2\right]^4}\right] = 0 \qquad (80)$$

Equation (80) can be evaluated to yield

$$\frac{d}{d(\omega^2)}\left[\frac{1}{\Omega^8\left[\left(1-\frac{\omega^2}{\Omega^2}\right)+g^2\right]^2}\right] = \frac{4}{\Omega^{10}}\;\frac{\left(1-\frac{\omega^2}{\Omega^2}\right)}{\left[\left(1-\frac{\omega^2}{\Omega^2}\right)+g^2\right]^3} = 0 \tag{81}$$

Thus, for a well separated mode, the peak of the $\frac{ds}{d(\omega^2)}$ plot will occur at the natural frequency, regardless of whether the mode is complex or classical. Any suitable finite difference scheme can be used to compute $\frac{ds}{d(\omega^2)}$ from measured data using equation (75).

It turns out that even for modes that are not well separated, the peaks of the $\frac{ds}{d(\omega^2)}$ plot still give good approximations to the natural frequencies. To establish why this is so, consider equation (78) term by term. The first term vanishes at the natural frequency, as we have already seen. The remaining terms can be rearranged as

$$\frac{1}{\Omega^2}\;\frac{d^2F^R}{d(\omega^2)^2}\left(C^RA^R + C^IA^I\right) + \frac{1}{\Omega^2}\;\frac{d^2F^I}{d(\omega^2)^2}\left(C^IA^R - C^RA^I\right) \tag{82}$$

At the natural frequency $\frac{d^2F^R}{d(\omega^2)^2} = 0$ (83)

the remaining term becomes

$$-\frac{2}{\Omega^8 g^3}\left(C^IA^R - C^RA^I\right)$$

Lightly damped modes generally tend to be classical and well separated. This is understandable, since in the limit of zero damping a classical undamped mode results. Thus the low damping which will tend to drive $2/\Omega^8 g^3$ up also drives $(C^IA^R - C^RA^I)$ down, effectively neutralizing the expression. This consequently reduces the error incurred by approximating

the natural frequency by the peak of the $ds/d(\omega^2)$ plot. Experience has shown that modes which are too close to be resolved by the $ds/d(\omega^2)$ routine may probably not be resolvable by any other method presently known.

The diameter of the modal circle that fits the curvature of the displacement mobility plot (on the polar plane) in the vicinity of the natural frequency is

$$D = \frac{|A|}{g\Omega^2} \tag{84}$$

At the natural frequency,

$$\left.\frac{dY^R}{d(\omega^2)}\right|_{\omega = \Omega} = \frac{-A^R}{g^2\Omega^4} + \frac{C^R}{\Omega^2} \tag{85}$$

and

$$\left.\frac{dY^I}{d(\omega^2)}\right|_{\omega = \Omega} = \frac{-A^I}{g^2\Omega^4} + \frac{C^I}{\Omega^2} \tag{86}$$

Substituting equation (85) into equation (86) gives

$$\left.\frac{ds}{d(\omega^2)}\right|_{\omega = \Omega} = \frac{|A|}{g^2\Omega^4} + \text{Error of approximation} \tag{87}$$

The plot of arc length s against ω^2 has a characteristic S shape, as shown by the sketch below:

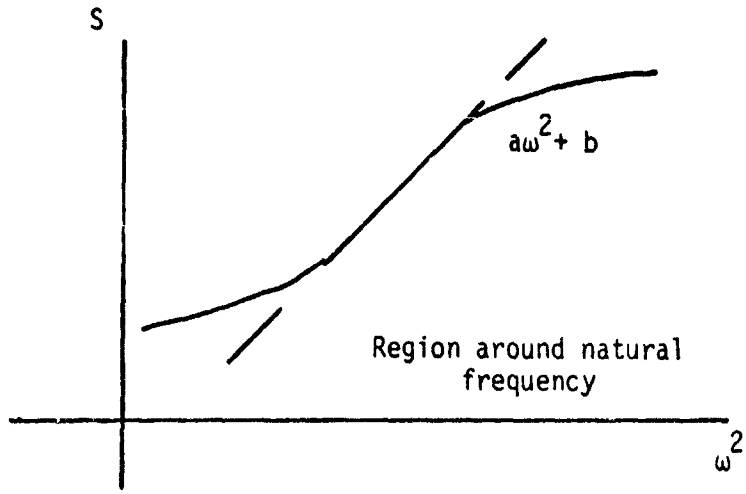

By fitting the best straight line to the inflection region of the S curve, one obtains a, the gradient of this line.

$$a \simeq |A|/g^2\Omega^4 \tag{88}$$

From equations (84) and (88), the damping coefficient is evaluated as

$$g \simeq D/a\Omega^2 \tag{89}$$

where D is the diameter of the circle fit to mobility data, a is the gradient of the line fit to the S plot and Ω is the natural frequency.

TESTING FOR ORTHONORMAL MODES AND MODE SHAPES

The mode shapes of any structure are related to the modal acceleration coefficients as shown in equation (28); i.e.,

$$A_{jkn} = \frac{1}{m_n} \phi_{jn} \phi_{kn} \tag{90}$$

where ϕ_{jn} and ϕ_{kn} are mode-shape elements at the jth and kth coordinates of the nth mode; m_n is the generalized mass of the nth mode. There are two basic types of orthonormal modes which can be distinguished by considering the nature of the response and the excitation. The ordinary vibration orthonormal mode element, ψ, has units of length/force. The products of the jth and kth orthonormal mode elements and the mode frequency function summed over the modes define the jk vibration mobility. On the other hand, the strain orthonormal mode element, $\psi^{(\varepsilon)}$, has units of the square root of the reciprocal of force times length. The products of the jth strain and kth vibration orthonormal mode elements and the mode frequency function summed over the modes define the jk strain mobility. The types of orthonormal modes used in analytical testing and the corresponding types of mobilities are summarized in Table 6.

TABLE 6. SUMMARY OF MOBILITY AND ORTHONORMAL MODE ELEMENTS.

Mobility	Modal Acceleration (Residue)	Units Of Modal Acceleration
$\frac{\partial q_j}{\partial f_k}$	$\psi_j \; \psi_k$	length/force
$\frac{\partial \varepsilon_j}{\partial f_k}$	$\psi_j(\varepsilon) \; \phi_k$	1/force
$\frac{\partial \Delta_{qj}}{\partial \Delta_k}$	$\psi_j(\varepsilon) \quad \psi_k(\varepsilon) \; \delta_k \delta_j$	length/force
$\frac{\partial q_j}{\partial \gamma_k}$	$\psi_j \quad \psi_k(\varepsilon) \; {\delta_k}^2$	$(\text{length})^2$/force

The orthonormal mode elements are defined as

$$\psi_{jn} \equiv \frac{1}{\sqrt{m_n}} \; \phi_{jn} \tag{91}$$

and

$$\psi_{kn} \equiv \frac{1}{\sqrt{m_n}} \; \phi_{kn} \tag{92}$$

Thus,

$$A_{jkn} = \psi_{jn} \quad \psi_{kn} \tag{93}$$

and

$$A_{jjn} = (\psi_{jn})^2 \tag{94}$$

It follows from equations (93) and (94) that

$$\psi_{kn} = \frac{A_{jkn}}{\sqrt{A_{jjn}}} \tag{95}$$

It can also be deduced that

$$\psi_{kn} \; + \; \pm\sqrt{\frac{A_{jkn} \, A_{\ell kn}}{A_{\ell jn}}} \tag{96}$$

The choice of using either equation (95) or (96) to determine ψ_{kn} depends on the accessibility of the modal acceleration coefficients involved. Note that two shaking stations are involved in equation (96), whereas only one shaking station is involved in equation (95). It may turn out that the driving point data that yields A_{jjn} are such that accurate estimations of the A_{jjn} for a number of the modes are not easy. This may in part be due to a strong local mode coupling or a residual effect. In cases where this is so, it may be better to shake at a number of coordinates and then use schemes similar to that in equation (96).

Consistency of the phase angle in equation (96) is achieved in the following manner. For an orthonormal mode element, in the nth mode, of large magnitude, say ψ_{kn}, let

$$\psi_{kn} = \left| \sqrt{\frac{|A_{jkn}| \cdot |A_{\ell kn}|}{|A_{\ell jn}|}} \right| \angle \frac{1}{2} (\phi_{jkn} + \phi_{\ell kn} - \phi_{\ell jn}) \tag{97}$$

where ϕ is phase angle. For any other orthonormal mode element, say p,

$$\psi_{pn} = \left| \sqrt{\frac{|A_{jpn}| \cdot |A_{\ell pn}|}{|A_{\ell jn}|}} \right| \angle (\phi_{pkn} - \phi_{kn}) \tag{98}$$

Mode shapes of the structure normalized with respect to the highest mode element can be obtained directly from the modal acceleration coefficients as

$$\{\phi_n\} = \frac{1}{A_{j,max,n}} \begin{Bmatrix} A_{j1n} \\ A_{j2n} \\ \vdots \\ A_{jNn} \end{Bmatrix} \tag{99}$$

where

$A_{j,max,n}$ is the modal acceleration coefficient with the maximum amplitude in the column corresponding to the nth mode, when shaking at the jth coordinate. The generalized mass corresponding to the mode shape thus normalized is computed from equation (90) as

$$M_n = \phi_{jn} \quad \phi_{kn}/A_{jkn} = A_{jjn}/(A_{j,max,n})^2 \tag{100}$$

In order to obtain the elements of the orthonormal modes and mode shapes, the acceleration coefficients of all the modes for the mobilities relating the response coordinates to the shaking coordinates have to be determined. The computational scheme for determining the modal acceleration coefficients requires mobility data at discrete frequencies. The technique, herein referred to as the matrix difference method, was developed by F. D. Bartlett, Jr. of the Structures Laboratory, USARTL (AVRADCOM). The matrix difference method is well suited to processing large numbers of transducers for modal analysis using multiplexing data acquisition systems common in the helicopter industry. The natural frequencies and modal damping must be determined beforehand.

For two frequencies ω_i^+ and ω_i^- in the region of the natural frequency of the ith modes, equation (34) could be written thus:

$$\Delta_i \ddot{Y}_{jk} = \ddot{Y}_{jk}(\omega_i^+) - \ddot{Y}_{jk}(\omega_i^-) = \sum_{n=1}^{N} A_{jkn} \Delta_i \ddot{F}_n \tag{101}$$

where

$$\Delta_i \ddot{F}_n = \ddot{F}_n(\omega_i^+) - \ddot{F}_n(\omega_i^-)$$

Equation (101) can be written for all the remaining modes, having selected the corresponding pairs of frequencies. The resulting system of equations is the matrix difference equation:

$$\left\{ \begin{matrix} \Delta_1 Y_{jk} \\ \Delta_2 Y_{jk} \\ \vdots \\ \Delta_N Y_{jk} \end{matrix} \right\} = \begin{bmatrix} \Delta_1 F_1 & \Delta_1 F_2 & \cdots & \Delta_1 F_N \\ \Delta_2 F_1 & \Delta_2 F_2 & \cdots & \Delta_2 F_N \\ \cdot & \cdot & & \cdot \\ \Delta_N F & \Delta_N F_2 & & \Delta_N F_N \end{bmatrix} \left\{ \begin{matrix} A_{jk1} \\ A_{jk2} \\ \\ A_{jkN} \end{matrix} \right\} \tag{102}$$

or $$\left\{ \Delta Y_{jk} \right\} = [\Delta F] \left\{ A_{jk} \right\} \tag{103}$$

from which $\{A_{jk}\} = [\Delta F]^{-1} \{\Delta Y_{jk}\}$ (104)

An immediate observation about the matrix difference scheme is that all contributions to the mobilities near a given mode which are weakly varying with frequency, such as the effects of distant modes or rigid body modes, are subtracted out. By proper selection of ω_i^+ and ω_i^- , ${}_iF_n$ can be made such that $\Delta_k F_i$ is large and $\Delta_i F_j$ is small for all $j \neq i$. Experience shows that

$$\omega_i^+ = \Omega_i(1 + g_i/_2) \tag{105}$$

and

$$\omega_i^- = \Omega_i(1 - g_i/_2) \tag{106}$$

are the most effective choices for the upper and lower discrete frequencies. For these discrete frequencies, the matrix $[\Delta F]$ is well conditioned for inversion since the off-diagonal terms are small compared to the diagonal terms.

Test procedure - Figure 19 shows the schematic of the instrumentation setup for the shake test for orthonormal modes and mode shapes. Signals from all the accelerometers and from the force gage are transmitted via telemetry to a computer where the transfer functions between the response coordinates and the force coordinate are computed and printed out. The excitation signals are sinusoidal at the discrete frequencies ω_i^+ and ω_i^- for $i = 1, 2, \ldots N$. The same force levels used for the swept sine global parameter shake test are also used for the modal shake test at the corresponding discrete frequencies.

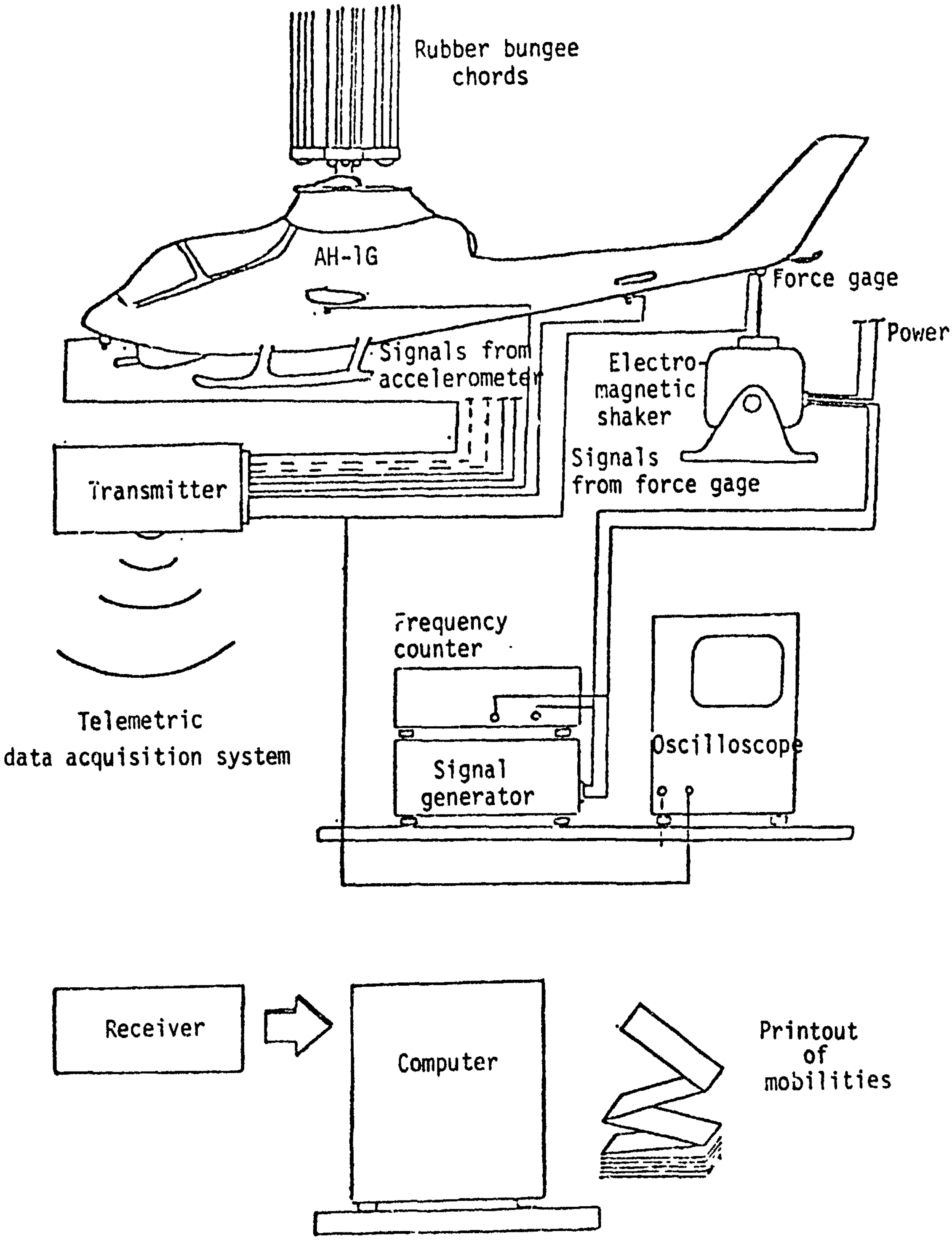

Figure 19. Schematic of setup for matrix difference method of modal testing.

DERIVATION OF MOBILITIES

Underlying any technique of modal analysis is the principle of linear decomposition of structural response mobility into contributions from the natural modes occurring between a chosen frequency interval. The preceding methods estimate not only the natural frequencies and damping coefficients of each mode but also the acceleration coefficients of each modal contribution to the mobility between response and forcing coordinates.

Subsequent to the determination of the modal parameters and modal constants, the next logical step is to reconstruct mobilities both between a pair of forcing and response coordinates over a continuous frequency interval and at a chosen frequency between several pairs of forcing and response coordinates. By comparing the mobility derived over a continuous frequency range with the measured mobility over the same frequency range, some assessment of the accuracy of the global parameter estimations can be made. The comparison of discrete frequency mobilities for a large number of coordinate pairs allows the assessment of the acceptability of the orthonormal mode and mode-shape calculations. The results of these comparisons build the confidence in the mobilities which are derived but not actually measured.

Comparison of measured and simulated mobilities over frequency band - Global parameters Ω_n and g_n of system modes occurring within a specified frequency range can be satisfactorily estimated using methods based on the properties of the mode functions, $F(\omega)$. The matrix difference method can then be used to calculate the modal acceleration coefficients (A^R_{jkn}, A^I_{jkn}) of the relevant elastic modes. Table 7 summarizes the parameters estimated between 0 and 50 Hz from the tail vertical shake/nose vertical acceleration data. Figure 20 shows plots of the mobility measured between 0 and 50 Hz. Using the parameters of Table 7 and equation (31), without including the rigid body coefficients, the plots of Figures 21, 22, and 23 were generated.

The computed and measured mobilities are superimposed in Figures 22 and 23. It is seen that the two plots agree to within a frequency independent complex constant, which is an estimate of the contribution of the rigid body modes.

TABLE 7. ESTIMATED PARAMETERS BETWEEN 0-50 Hz (TAIL VERTICAL SHAKE, NOSE VERTICAL ACCELERATION)

Mode No. n	Natural frequency n (Hz)	Damping coefficient g_n	Nose/tail modal acceleration coefficient	
			Real $A^R_{ZN,\ ZT,\ n}$ (g/lb)	Imaginary $A^I_{ZN,\ ZT,\ n}$ (g/lb)
1	7.33	0.062	7.26×10^{-4}	1.40×10^{-4}
2	8.09	0.12	4.48×10^{-4}	-3.55×10^{-4}
3	13.5	0.13	-1.57×10^{-5}	-4.97×10^{-6}
4	15.97	0.085	2.25×10^{-5}	1.39×10^{-4}
5	16.35	0.05	5.18×10^{-5}	-1.04×10^{-6}
6	17.63	0.08	1.37×10^{-4}	-5.54×10^{-5}
7	22.1	0.15	-7.28×10^{-5}	-4.06×10^{-4}
8	28.4	0.11	-1.06×10^{-4}	1.13×10^{-4}
9	40.7	0.12	7.84×10^{-6}	-2.16×10^{-5}
10	45.3	0.026	4.02×10^{-5}	1.42×10^{-4}

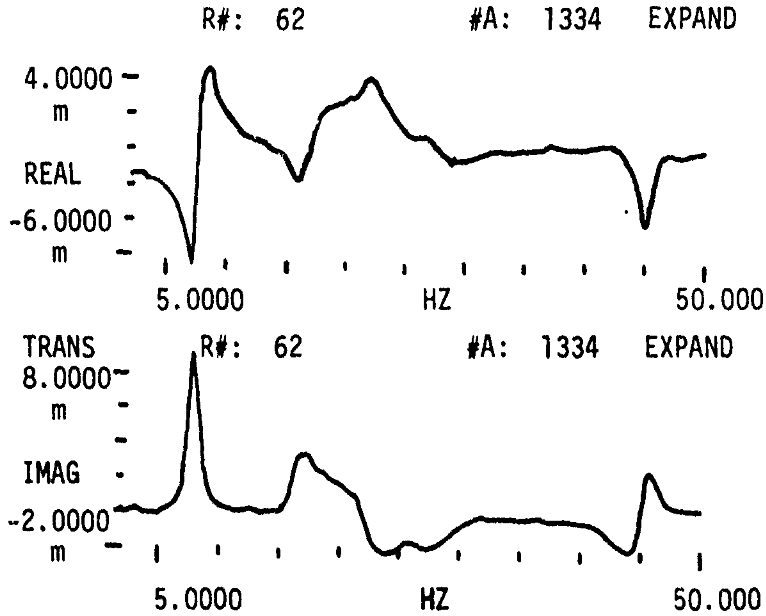

Figure 20. Measured acceleration mobility data between 2 and 50 Hz.

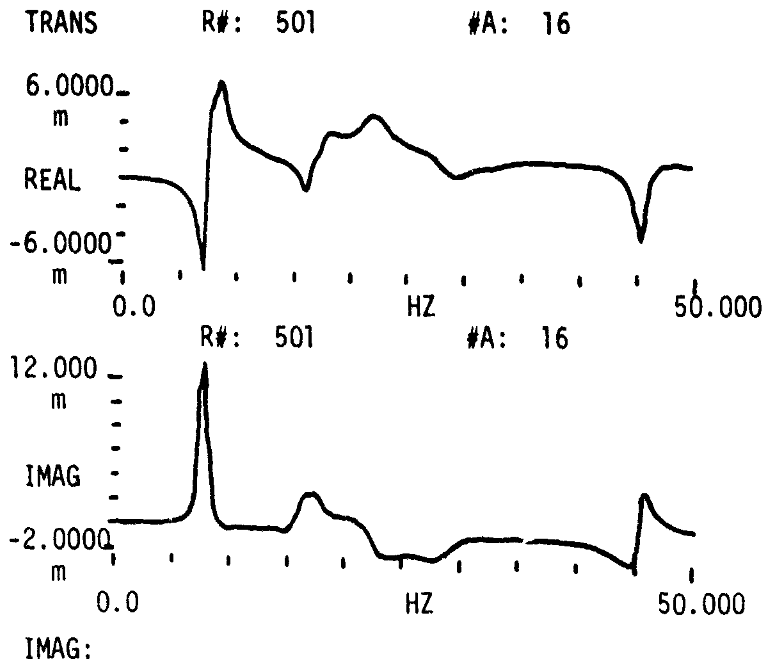

Figure 21. Numerical simulation of the elastic component of the acceleration data.

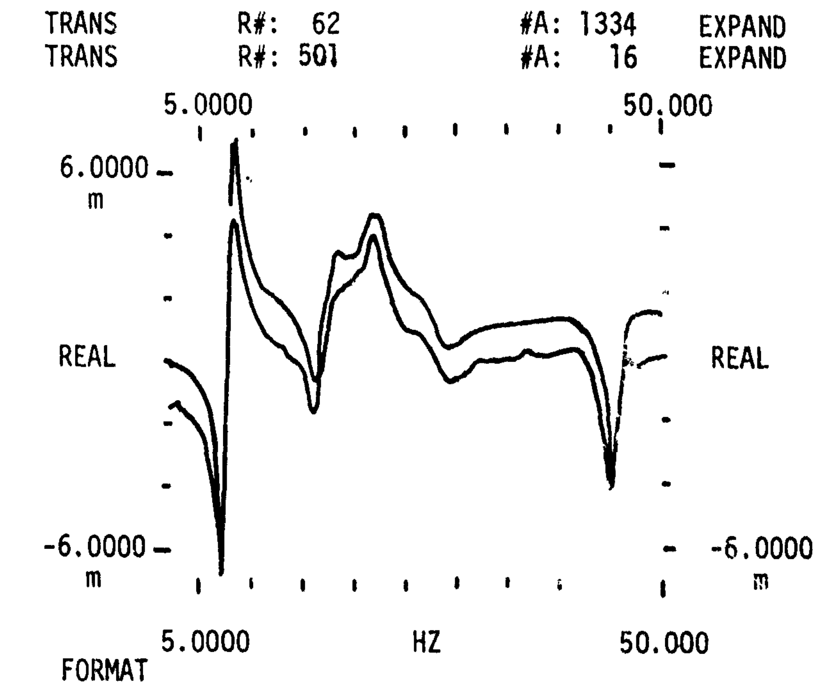

Figure 22. Real parts superimposed.

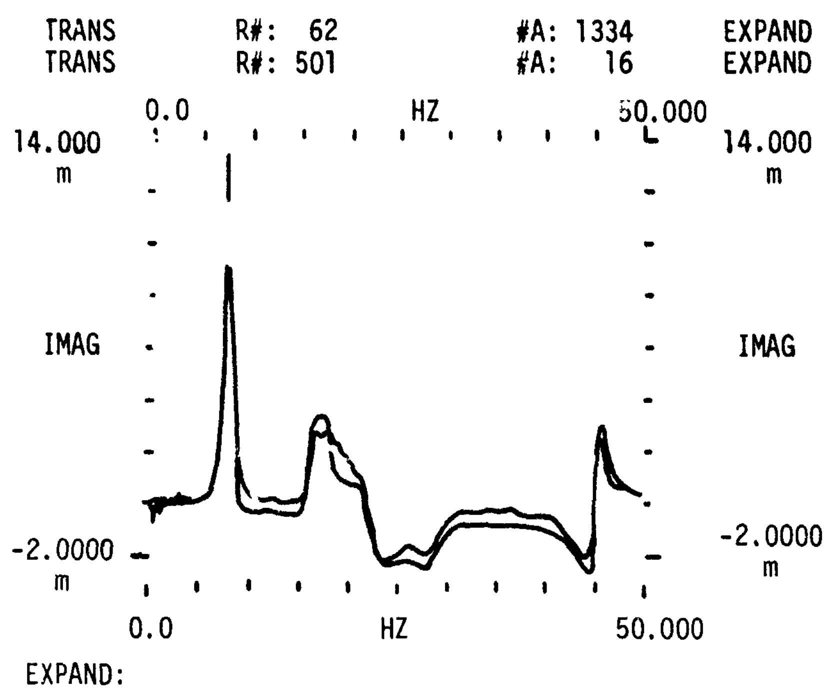

Figure 23. Imaginary parts superimposed.

Modal Series Method - Equation (31) can be rewritten in the following form:

$$\ddot{Y}_{jk} = E_{jk} + R^{L}_{jk}(\omega) + \sum_{n=1}^{N} A_{jkn}\,\ddot{F}_n(\omega) + R^{H}_{jk}(\omega) \tag{107}$$

where

$R^{L}_{jk}(\omega)$ is the low frequency mobility residual; i.e., contributions to the mobility by elastic modes which occur at frequency below the lower test frequency limit.

$R^{H}_{jk}(\omega)$ is the high frequency mobility residual.

The rigid body acceleration coefficient, E_{jk}, is determined from geometry and weights data.

If the lower test frequency limit is near zero, it follows that $R_L = 0$. The higher test frequency limit is usually selected high enough so that R^H can be safely assumed to vanish for all but certain driving point mobilities which may suffer either from local mode effects or from high frequency mode residuals.

When all the global modal parameters (natural frequencies and damping coefficients) and the modal acceleration coefficients have been determined (Table 8), the acceleration mobilities between pairs of motion coordinates which do not include the shaking coordinate can be computed from

$$\ddot{Y}_{\ell,m} = E_{\ell,m} + \sum_{n=1}^{N} \frac{A_{\ell kn}A_{mkn}}{A_{kkn}}\,\ddot{F}_n(\omega) \tag{108}$$

where k is the coordinate of the shaking station for the data which generated $A\ell_k$ and A_{mk}. It is necessary to select the shaking station k such that there is no local mode or high frequency residual effect on the estimated value of A_{kkn}.

If only N_k of the modes are well defined by shaking at k, while the remaining N_p modes are better defined by the shake at p, then

$$\ddot{Y}_{\ell,m} = E_{\ell,m} + \sum_{n=1}^{N_k} \frac{A_{\ell kn}A_{mkn}}{A_{kkn}}\,\ddot{F}_n(\omega) + \sum_{n=1}^{N_p} \frac{A_{\ell pn}A_{mpn}}{A_{ppn}}\,\ddot{F}_n(\omega) \tag{109}$$

TABLE 8. SUMMARY OF ESTIMATED MODAL PARAMETERS, AH-1G HELICOPTER.

High gross wt.		Low gross wt.				Mean gross wt.				High gross wt. aft c.g.			
Vert.shake		Vert.shake		Lat.shake		Vert.shake		Lat.shake		Vert.shake		Lat.shake	
Ω_n	g_n	Ω_n	g_n	Ω_n	g_n	Ω_n	g_n	Ω_n	g_n	Ω_n	g_n	Ω_n	g_n
7.32	.066	7.19	.07	6.29	.16	7.15	.08	6.17	.14	7.28	.07	6.28	.16
8.08	.187	8.01	.17	7.51	.05	8.16	.18	7.38	.08	8.35	.08	7.53	.05
13.23	.138	14.78	.1	8.53	.11	13.67	.08	14.39	.15	13.94	.06	8.55	.11
15.99	.103	16.44	.065	14.66	.17	15.04	.07	16.16	.09	15.52	.08	11.0	.12
17.6	.083	17.71	.09	17.36	.1	15.92	.05	29.05	.114	21.48	.16	14.35	.18
22.06	.148	19.14	.12	25.46	.1	16.98	.11			23.71	.11	16.39	.068
27.91	.17	20.69	.2	27.88	.14	17.88	.07			25.59	.31	18.45	.13
		24.6	.1	29.66	.15	19.83	.13			29.96	.13	21.93	.074
		28.31	.12	32.42	.24	21.63	.16			31.63	.1	24.12	.108
		32.88	.1	33.59	.36	24.12	.08					29.38	.112
		34.99	.06			25.15	.14						
		37.75	.08			28.44	.13						
						32.42	.06						

THE TECHNIQUE OF FORCE DETERMINATION ON THE AH-1G

THEORY

The frequency domain equation relating the vector of N response coordinates to the vector of M forces acting steadily on a linear system is given by

$$\begin{Bmatrix} \ddot{y}_1 (\omega) \\ \ddot{y}_2 (\omega) \\ \vdots \\ \ddot{y}_n (\omega) \end{Bmatrix} = \begin{bmatrix} \ddot{Y}_{11} (\omega) & \ddot{Y}_{12} (\omega) & \ddot{Y}_{1M} (\omega) \\ \ddot{Y}_{21} (\omega) & \ddot{Y}_{22} (\omega) & \ddot{Y}_{2M} (\omega) \\ \vdots & \vdots & \vdots \\ \ddot{Y}_{n1} (\omega) & \ddot{Y}_{N2} (\omega) & \ddot{Y}_{NM} (\omega) \end{bmatrix} \begin{Bmatrix} F_1 (\omega) \\ F_2 (\omega) \\ \vdots \\ F_M (\omega) \end{Bmatrix} \quad (110)$$

or

$$\{\ddot{y}\} = [\ddot{Y}] \{F\} \quad (111)$$

where

$\ddot{y}_i (\omega)$ is the Fourier Transform of the acceleration response of coordinate i at the frequency .

$\ddot{F}_j (\omega)$ is the Fourier Transform of the vibratory load at coordinate j.

$\ddot{Y}_{ij} (\omega)$ is the acceleration mobility between coordinates i and j, otherwise defined as the transfer function between the response coordinate i and the forcing coordinate j, by reciprocity $\ddot{Y}_{ij} = Y_{ji}$.

All the quantities in equation (110) are complex numbers. For N>M, the least squares estimate of the force vector can be obtained as

$$\{\hat{F}\} = \left[\left([\ddot{Y}]^{*T} [\ddot{Y}]\right)^{-1} [\ddot{Y}]^{*T}\right] \{\ddot{y}\} \tag{112}$$

where $[\ddot{Y}]^{*T}$ is the conjugate transpose of $[\ddot{Y}]$. The accuracy of $\{\ddot{F}\}$ can be assessed by reconstructing accelerations using

$$\{\ddot{y}\} = [\ddot{Y}] \{\hat{F}\} \tag{113}$$

A comparison of the reconstructed accelerations $\{\hat{\ddot{y}}\}$ with the measured accelerations $\{\ddot{y}\}$ will usually indicate the acceptability of the derived forces. Of course when N = M, both $\{\hat{\ddot{y}}\}$ and $\{\ddot{y}\}$ will check exactly, regardless of whether the forces are correct or not. However, N is usually much larger than M because of the need to represent the response of the structure at many more coordinates than there are forces. In these instances $\{\hat{\ddot{y}}\}$ and $\{\ddot{y}\}$ will not check acceptably unless the designated forces and the mobilities are correct.

Considerable engineering judgement is required to identify the force coordinates that are responsible for in-flight vibratory excitations. It is not acceptable to simply assume forces acting at arbitrary coordinates. The success of the method depends on both the accuracy of the mobilities and the correctness of the coordinates of the excitation loads.

REQUIRED DATA

The essential data required for determining forces are the in-flight accelerations $\{\ddot{y}\}$ and the elements of the mobility matrix $[\ddot{Y}]$. The in-flight accelerations are measured directly during specified aircraft flight conditions. The mobility matrix $[\ddot{Y}]$ is obtained from shake tests on the ground. Two techniques are available for obtaining mobilities:

1. Direct mobility measurement; i.e., $\ddot{Y}_{ij}$ is measured directly as the transfer function between the acceleration at coordinate i when shaking at coordinate j. This is the direct shake data.

2. Derivation of mobilities using the techniques of modal testing.

SELECTION OF FORCE COORDINATES

The principal vibratory loads acting in the AH-1G helicopter originate from the main rotor. Forces from the main rotor are transmitted to the ship through the main rotor shaft and the control rods. Because the rotor system is teetered, no vibratory pitching and rolling hub moments exist.

Originally it was anticipated that the rotor shaft vibratory forces and moments would be vertical, longitudinal and lateral forces and an inplane vibratory moment (torque). Direct shaking was done at the hub with a moment to determine the mobility. However the mobility obtained with this moment excitation was negligible and the inplane vibratory moment is not a contributor to the vibratory level of the vehicle. This is illustrated in Table 9 in which the lateral response of the tail is shown because it was the highest response due to a moment input.

TABLE 9. LATERAL MOBILITY AT THE TAIL.

Direction of shake	Mag. of shake	Absolute response-g/1000
Lateral at hub	1000 lb	.287
Torque at hub	1000 ft-lb	.020

It is seen from the above table that the response of the vehicle is much greater to a force input than a moment input. Preliminary calculation of forces and moments acting on the AH-1G showed that the moment (torque) excitation was negligible. Therefore, only three shaft forces at the hub (vertical, longitudinal, and lateral) are considered to be the major contributors of main rotor excitation forces.

Another possible source of two-per-rev excitation is the control loads. To attempt to determine the magnitude of the control loads, acceleration transducers were placed to determine acceleration in flight and mobilities in test at the location of the reaction points in the fuselage of the longitudinal, lateral and collective controls. Since the reaction points of the control loads are not conveniently located on the fuselage to do direct shaking to obtain the mobilities, the mobilities were derived using techniques of modal testing.

The locations of these transducers to obtain control forces are given in Table 3 and are designated as Z LONG, Z LATR, AND Z COLL. It is seen from this table that the location and reaction of these control forces are essentially the same on the fuselage. Further, the hub vertical force is at station location of 200 inches. Thus, all four vertical forces are essentially located at the same station on the fuselage. With only accelerometer transducers it was impossible to determine the magnitude of each individual force. However, the resultant of all of the vertical forces was obtained accurately. To distinguish the magnitudes of the separate vertical forces, further instrumentation would be required such as strain gaging the control rods.

Another possible source of two-per-rev excitation is rotor fuselage interface. The possibility of excitations from the horizontal stabilizer and wing was investigated, but these excitations were determined to have an insignificant effect on the fuselage response. However, it was determined that in addition to the expected main rotor forces, a two-per-rev lateral force at the tail rotor was required to duplicate the measured flight accelerations. One possible source of this force is main rotor, vertical stabilizer and/or main rotor, tail rotor interference problems. However, to determine the actual source of this lateral force would required increased instrumentation such as strain gages on the vertical pylon and in the tail rotor gearbox area. This was out of the scope of the existing program which required acceleration transducers only.

For each of the flight conditions selected, a set of forces was calculated:

1. Vertical shaft force
2. Longitudinal shaft force
3. Lateral shaft force
4. Lateral tail rotor gearbox force

Thirty seven response coordinates were used in each of the force calculations. Equation (113) was used to reconstruct the accelerations at all the response coordinates. A convenient way of comparing the rederived accelerations with the measured ones is the plot of difference vectors between these two arrays of complex numbers.

On the polar plane, a complex number can be represented by a vector from the origin to the (Real, Imaginary) coordinates of the number. The difference between two complex numbers can likewise be represented by a vector joining the (Real, Imaginary) coordinates of the two numbers For a large number of complex number pairs, this plot of difference vectors for all the pairs gives an instant picture of how well the two complex arrays compare. If both arrays are identical, the plot will be filled with points. Poor comparison between two arrays will show up as a multitude of sticks whose lengths are comparable to their distances from the origin.

Examples of these difference vector plots are shown in Figure 24; the array of measured accelerations is compared to the array of accelerations derived using forces calculated at the four coordinates (VERT, LONG, LATR and TRGB). It is seen in this figure that there is very little difference in the predicted values and actual values, and that these forces give a reasonable prediction when compared to the actual measured data.

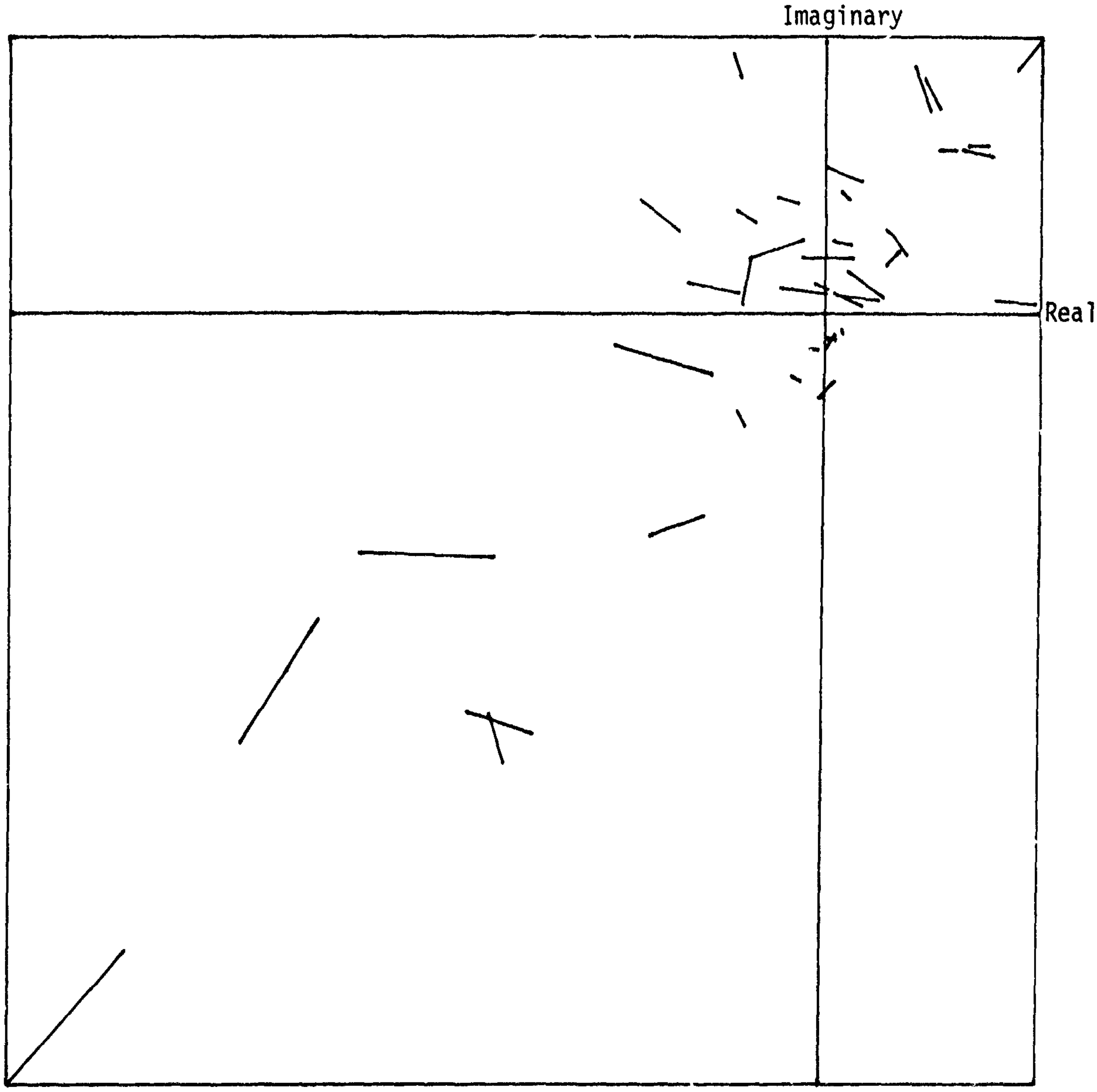

Figure 24. Difference vectors.

Forces

Table 10 gives the calculated forces for three weight configurations for six flight conditions. Although 32 flight conditions were done, six critical conditions were selected to calculate forces and to do ground flying. The selected flight conditions are given in the table. The flight test data obtained in all of the flights were analyzed to select two flight conditions in each of the three flight categories that gave the highest vibration level. The three flight categories are 1) steady state, 2) tow missile mission maneuvers, and 3) gunnery maneuvers. These forces are used in the ground flying phase of the program.

GROUND FLYING

In this program ground flying was done primarily to verify the magnitude and phases of the two-per-rev forces calculated from the flight test response and calibration matrix. However, another purpose of this phase was to determine the feasibility of ground flying so that reliability testing could be done on the complete helicopter using simulated actual flight loads. This would advance the state of the art in fatigue testing on a complete system. Thus, time could be accumulated by flying in the hanger rather than actual flying.

Test Vehicle

The aircraft model for this phase of the program was the Army AH-1G, serial No. 67-15684. This is the same vehicle used in the flight test and calibration phases of the program. For the ground flying phase, the test vehicle was configured identically to the shake test of calibration configuration. Figure 25 shows the vehicle in the test bay.

Test Conditions

The test vehicle weight and c.g. configurations are identical to the shake test configurations. Table 11 shows those configurations that will be used in the ground flying task of this program.

TABLE 10. CALCULATED FORCES

	1 MAG	1 PHASE	2 MAG	2 PHASE	3 MAG	3 PHASE	4 MAG	4 PHASE	5 MAG	5 PHASE	6 MAG	6 PHASE
8465LB G.W. 196.33 C.G. — FLIGHT CONDITION												
VERT @ HUB	1342	65°	909	36°	1090	136°	1153	344°	3540	75°	2639	76°
LONG @ HUB	309	112°	212	99°	150	140°	188	31°	562	108°	757	120°
LATR @ HUB	205	240°	112	228°	35	237°	97	159°	428	236°	515	240°
LATR @ TRGB	146	218°	34	166°	2	42°	10	314°	174	263°	81	257°
9075LB G.W. 196.35 C.G.												
VERT @ HUB	1332	69°	546	6°	1212	132°	1066	336°	3608	76°	2803	71°
LONG @ HUB	360	119°	312	117°	204	139°	143	56°	642	109°	463	107°
LATR @ HUB	254	234°	189	221°	55	226°	80	177°	383	238°	245	242°
LATR @ TRGB	100	214°	42	181°	2	249°	10	274°	155	258°	86	230°
9500LB G.W. 196.20 C.G.												
VERT @ HUB	1158	74°	587	41°	1090	169°	1118	20°	3240	77°	2205	46°
LONG @ HUB	447	169°	504	106°	278	164°	255	77°	1036	108°	1224	130°
LATR @ HUB	335	214°	263	213°	124	304°	174	218°	855	222°	610	230°
LATR @ TRGB	81	206°	52	195°	10	231°	6	199°	99	259°	98	230°

FLIGHT CONDITION.

1. Maximum straight and level flight (V_H)
2. 45 degree right turn at .7 V_H
3. Sideward flight right to 35 K_t reverse sideward flight left to $35K_t$
4. Approach and landing
5. Rolling pullout at V_L - left
6. Rolling pullout right after point target dive to $.9V_L$

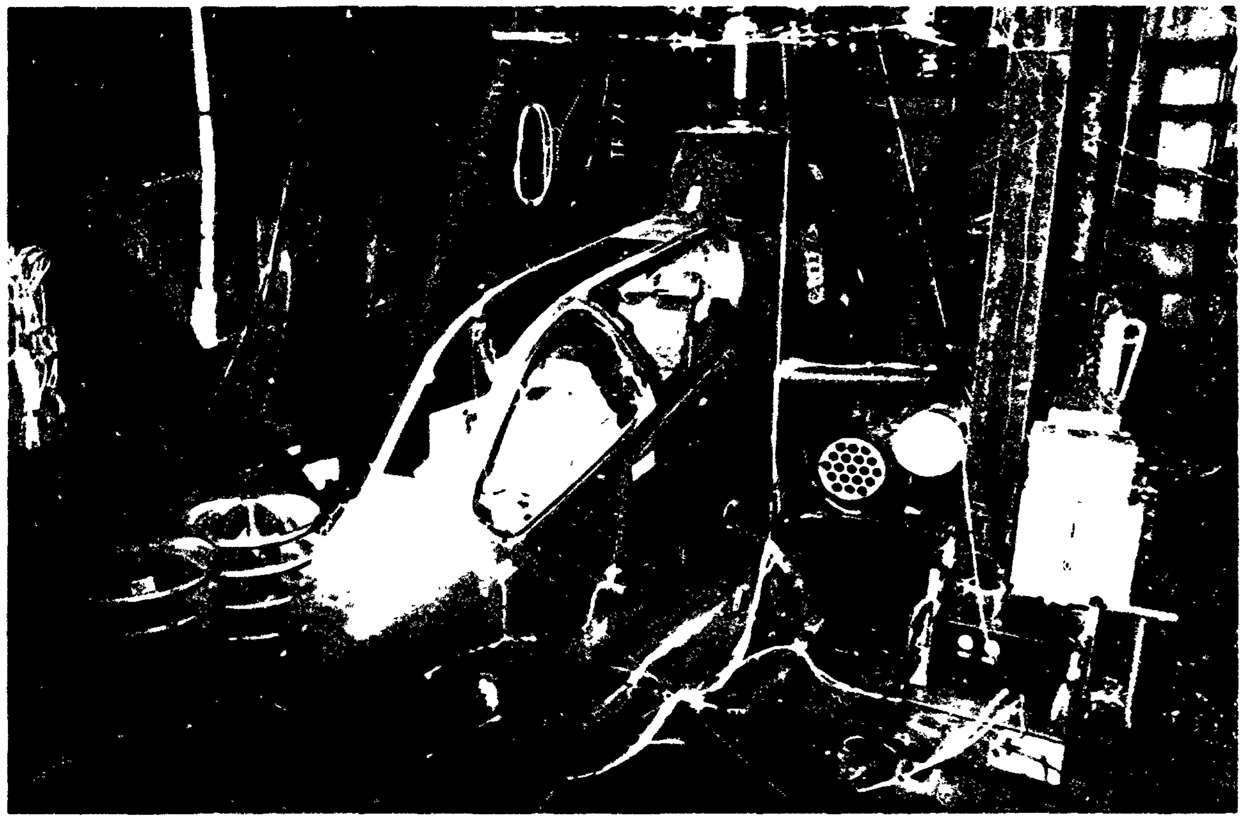

Figure 25. AH-1G test vehicle.

TABLE 11 GROUND FLYING CONFIGURATIONS

Gross weight (lb)	c.g.	Configuration
8465	196.33	Clean
9075	196.35	2 rocket launchers 19 rocket launchers
9500	196.20	4 rocket launchers 19 rocket/launcher

Table 12 shows the two-per-rev harmonic content of the vibration response of the vehicle for the flight conditions selected. These two-per-rev responses were used with the calibration matrix to calculate the forces shown in Table 10 and to determine how the ground flying responses match the flight test results.

Test Procedure

The aircraft was hoisted until it was supported entirely by the bungee system. The aircraft was allowed to remain in this condition for approximately 30 minutes to allow the bungees to stretch to their maximum load length and to provide a null condition for resistance calibrating and nulling all the load cells and accelerometers. Then the servo-hydraulic system was energized and the three main rotor hydraulic cylinders were located at mid-stroke via the set-point controls on the main control console. The helicopter was lifted an additional distance with the electric hoist until the hydraulic cylinders could be bolted to their respective main rotor attachment points. Finally, the electromagnetic shaker was attached to the tail rotor gearbox attachment point. The helicopter was now entirely supported by the bungees at the main rotor hub and the four load cells for vibratory load

TABLE 12. FLIGHT RESPONSE, g'

PICKUP	144K 8465# 196.33 C.G. REAL	IMAG *	136K 9075# 196.35 C.G. REAL	IMAG *	124K 9500# 196.20 C.G. REAL	IMAG *	126K 9500# 199.51 C.G. REAL	IMAG *
	Flight Condition V_H							
Z50	-.210	-.046	-.340	-.078	-.194	- 049	-.216	- 090
Z100T	-.117	-.079	-.124	- 088	-.125	- 061	-.139	- 091
Z210T	-.130	-.011	-.175	- 002	-.181	-.199	-.200	- 048
Z340	.333	-.395	.294	-.341	.237	-.199	.282	-.188
Z400	.248	-.239	.215	-.212	.183	-.102	.001	-.234
Z460	-.001	.053	041	.050	058	087	031	094
Z540	-.508	.577	-.426	.574	-.282	.405	-.477	.400
Z90%	-.008	-.038	-.058	-.049	- 064	- 044	-.097	- 070
Z90L	-.137	-.147	-.102	-.146	- 086	- 083	- 099	-.127
Z140R	.038	- 058	- 001	-.064	- 013	- 054	- 041	- 076
Z140L	-.073	-.167	- 040	-.155	-.035	-.095	- 042	-.119
Z200R	.260	-.018	.060	.140	.171	- 012	.120	- 001
Z200L	-.140	-.371	- 032	-.432	.044	-.280	061	-.329
Z260R	.175	-.231	.120	-.210	084	-.162	089	-.181
Z260L	.147	-.338	.137	.013	.134	-.177	.161	-.175
Z396R	.211	-.232	.146	-.163	.028	-.119	097	-.150
Z396L	.137	-.354	.126	-.326	.239	-.102	.133	.277
ZLONG	.094	-.123	069	-.110	040	-.085	032	- 096
ZLATR	.023	-.174	046	-.159	035	-.101	036	-.111
ZCOLL	.001	-.208	025	-.131	020	-.119	020	-.131
Y50	-.136	.141	-.071	.046	-.015	034	026	039
Y90	-.051	.090	- 047	C33	-.021	-.007	- 013	- 003
Y140	-.022	.050	- 038	015	- 030	- 022	- 026	- 024
Y220B	-.069	-.038	013	- 023	- 013	-.034	-.014	- 091
Y220T	-.266	.322	-.274	.413	-.240	.306	-.289	.306

* Change in sign required for compatibility between test and analysis

TABLE 12. CONTINUED

Flight Condition - V_H

PICKUP	144K 8465# 196.33 C.G.		136K 9075# 196.35 C.G.		124K 9500# 196.20 C.G.		126K 9500# 199.51 C.G.	
	REAL	IMAG*	REAL	IMAG*	REAL	IMAG*	REAL	IMAG*
Y300	.040	-.079	- 053	-.100	-.104	-.178	-.102	-.246
Y380	-.176	.085	-.314	-.014	-.329	-.153	-.356	-.313
Y440	-.503	.347	-.620	.148	-.622	- 087	-.681	-.345
Y490	-.764	.433	-.430	.262	-.445	.163	-.458	.096
Y517	-1.233	1.107	-.937	.670	-.850	.734	-.921	.599
X140	.027	.023	.030	.009	.002	-.027	- 021	022
X180T	-.225	-.118	-.280	-.162	-.212	-.171	-.248	-.245
X540	-.523	.576	-.444	.535	-.304	.324	-.465	.288
X200R	.112	.089	.120	-.083	.095	-.105	.113	-.096
X200L	-.007	.119	- 014	.128	-.039	.107	- 028	.102

* Change in sign required for compatibility between test and analysis

TABLE 12. CONTINUED

	Flight Condition - 45° RT Coordinated Turn at $.7V_H$							
	103K		94K		91K		99K	
	8465#		9075#		9500#		9500#	
	196.33 C.G.		196.35 C.G.		196.20 C.G.		199.51 C.G.	
PICKUP	REAL	IMAG *	REAL	IMAG *	REAL	IMAG *	REAL	IMAG *
Z50	-.115	-.037	-.170	-.073	-.225	- 018	-.242	-.110
Z100T	- 053	-.069	- 072	- 068	-.116	-.032	-.127	-.100
Z210T	-.047	- 080	-.203	-.103	-.184	-.089	-.186	-.131
Z340	.310	-.173	.143	.274	017	-.235	.315	-.123
Z400	- 008	-.237	.217	-.003	.172	.009	-.208	- 091
Z460	-.052	-.005	-.031	.003	- 013	028	- 063	.028
Z540	-.666	.158	-.545	-.076	-.448	029	-.665	.138
Z90R	-.015	.011	- 038	.011	-.088	.006	-.112	.064
Z90L	-.058	-.118	- 080	-.120	-.103	-.061	-.115	-.122
Z140R	-.004	-.029	- 001	.013	-.029	-.004	-.045	-.062
Z140L	-.010	-.126	- 027	-.106	- 048	-.063	-.052	-.113
Z200R	.155	.066	.174	.145	.129	.112	.121	046
Z200L	.018	-.278	.005	-.304	.012	-.195	069	-.262
Z260R	.195	-.105	006	-.158	.103	-.053	.152	-.123
Z260L	.185	-.188	.172	-.101	.133	-.084	.176	-.139
Z396R	.238	- 026	.205	.048	.127	.021	-.008	-.200
Z396L	.177	-.146	081	.196	.182	.029	.074	.204
ZLONG	.085	-.055	073	- 021	.040	-.034	.054	- 075
ZLATR	.063	-.114	049	- 074	039	-.060	050	- 090
ZCOLL	052	-.137	042	- 093	.030	-.070	043	-.109
Y50	- 061	.079	- 020	.036	-.019	.001	- 035	- 018
Y90	- 019	.069	- 011	041	- 020	--	-.008	-.015
Y140	- 004	.048	- 012	020	-.020	- 013	--	-.018
Y220B	.045	.030	002	- 021	-.003	-.046	.011	-.057
Y220T	-.142	.125	-.245	.227	-.235	.229	-.245	.219

* Change in sign required for compatibility between test and analysis

TABLE 12. CONTINUED

Flight Condition - 45°RT Coordinated Turn at $.7V_H$								
	103K 8465# 196.33 C.G.		94K 9075# 196.35 C.G.		91K 9500# 196.20 C.G.		99K 9500# 199.51 C.G.	
PICKUP	REAL	IMAG*	REAL	IMAG*	REAL	IMAG*	REAL	IMAG*
Y300	056	-.045	- 015	-.111	- 059	-.144	-.012	-.184
Y380	- 021	- 018	-.137	-.141	-.218	-.158	- 097	-.257
Y440	-.116	.020	-.310	-.161	-.449	-.151	-.260	-.331
Y490	-.232	-.019	-.347	-.114	-.480	- 054	-.324	-.212
Y517	-.400	-.065	-.358	.063	-.523	.283	-.409	.092
X140	.028	.020	032	022	.029	.005	.026	.003
X180T	-.118	-.123	-.288	-.227	-.270	-.195	-.238	-.259
X540	-.619	.173	-.499	-.063	-.417	-.027	-.593	.106
X200R	.083	-.037	.087	- 064	092	-.109	.095	-.085
X200L	.011	.067	.016	.118	.011	.084	--	.101
X190R	.025	- 064	- 022	-.104	--	-.105	.024	-.126
X220L	.012	.020	021	.027	.023	.016	.013	.018

* Change in sign required for compatibility between test and analysis

TABLE 12. CONTINUED

Flight Condition - Sideward Flt Rt. to 35K reverse Sideward Flt Lft. to 35K

PICKUP	8465# 196.33 C.G. REAL	IMAG*	9075# 196.35 C.G. REAL	IMAG*	9500# 196.20 C.G. REAL	IMAG*	9500# 199.51 C.G. REAL	IMAG*
Z50	-.093	-.050	-.106	-.059	-.124	092	-.215	- 058
Z100T	-.104	-.080	-.104	- 081	-.110	031	-.153	- 081
Z210T	-.111	- 030	-.147	-.052	-.101	081	-.149	054
Z340	-.282	-.277	-.221	-.267	-.245	-.105	- 038	-.268
Z400	-.165	-.186	-.134	-.191	-.145	-.072	- 026	-.174
Z460	-.005	-.006	- 010	-.002	- 001	- 003	- 005	013
Z540	.326	.432	.245	.426	.261	.138	- 017	.391
Z90R	-.086	-.033	-.097	-.041	- 094	042	-.133	- 050
Z90L	-.093	-.064	-.088	-.078	-.108	.032	-.138	- 079
Z140R	-.095	-.043	-.097	-.046	-.092	.016	-.101	- 060
Z140L	-.103	-.075	- 091	- 081	-.111	.009	-.106	- 087
Z200R	-.123	-.038	-.164	- 060	-.093	-.061	- 036	- 087
Z200L	-.179	-.139	-.159	-.192	-.218	-.085	- 095	-.225
Z260R	-.218	-.142	-.189	-.150	-.195	- 034	- 078	-.160
Z260L	-.234	-.179	-.180	-.192	-.206	-.078	- 080	-.209
Z396R	-.186	-.175	-.119	-.139	-.147	- 036	- 049	-.121
Z396L	-.167	-.228	-.136	-.197	-.115	- 088	- 024	-.224
ZLONG	-.121	-.073	-.106	- 075	-.111	- 015	- 064	- 089
ZLATR	-.129	-.085	-.111	-.093	-.115	- 026	- 064	-.101
ZCOLL	-.133	- 094	-.117	-.096	-.137	- 019	- 086	-.112
Y50	-.015	.035	-.015	022	- 099	- 031	.001	- 033
Y90	-.011	.022	- 010	015	- 059	--	-.009	-.012
Y140	-.011	.013	- 009	007	- 047	.004	-.010	-.004
Y220B	-.005	-.005	- 007	- 015	- 028	- 003	- 013	- 013
Y220T	-.030	-.002	- 064	058	087	.115	-.017	.122

* Change in sign required for compatibility between test and analysis

TABLE 12. CONTINUED

Flight Condition - Sideward Flt Rt to 35K Reverse
Sideward Flt Lft to 35K

PICKUP	8465# 196.33 C.G.		9075# 196.35 C.G.		9500# 196.20 C.G.		9500# 199.51 C.G.	
	REAL	IMAG*	REAL	IMAG*	REAL	IMAG*	REAL	IMAG*
Y300	- 002	- 032	- 001	- 038	- 056	005	- 038	- 028
Y380	.022	- 023	011	- 014	- 067	042	- 058	020
Y440	.055	.051	010	075	- 058	.122	- 084	054
Y490	.018	025	- 010	040	- 071	040	- 035	051
Y517	.012	.012	- 009	- 007	028	- 054	046	-.009
X140	.015	- 010	.014	- 009	005	029	.011	- 017
X180T	-.049	.025	-.133	- 028	-.155	.111	-.134	- 055
X540	.345	.464	.271	.440	.268	.130	013	.395
X200R	.011	- 054	027	- 064	- 016	- 062	019	- 078
X200L	.016	021	.022	.049	.034	004	027	044
X190R	- 030	- 056	- 036	- 073	- 092	- 039	- 054	- 086
X220L	020	.001	017	001	006	-.025	008	- 007

* Change in sign required for compatibility between test and analysis

TABLE 12. CONTINUED

	Flight Condition - Approach and Landing							
	8465# 196.33 C.G.		9075# 196.35 C.G.		9500# 196.20 C.G.		9500# 199.51 C.G.	
PICKUP	REAL	IMAG*	REAL	IMAG*	REAL	IMAG*	REAL	IMAG*
Z50	034	-.089	- 005	- 051	- 045	- 072	028	- 088
Z100T	.089	- 038	062	- 026	018	-.065	045	-.035
Z210T	.066	- 091	002	- 075	- 053	- 057	- 026	- 084
Z340	.345	.148	.299	.158	.269	- 066	.263	.241
Z400	.248	.110	.217	.118	.185	- 029	.177	.192
Z460	N.G.	N.G.	-.005	-.039	- 022	008	- 026	- 018
Z540	-.684	-.315	-.546	-.368	-.499	069	-.467	-.497
Z90R	036	- 007	027	.009	.007	- 020	041	- 005
Z90L	086	-.051	060	- 027	008	- 074	050	- 033
Z140R	.054	010	038	018	029	- 020	053	011
Z140L	.107	-.022	.076	-.003	036	-.063	062	- 001
Z200R	057	.004	.052	.093	079	078	068	.127
Z200L	.220	-.030	.204	-.002	.137	-.139	.141	017
Z260R	.232	.080	.178	.096	.156	- 044	.187	.134
Z260L	.284	.066	.228	094	.182	- 079	.205	.135
Z396R	.166	.178	.157	.123	.172	018	.172	.170
Z396L	.346	.155	.257	084	.221	053	.199	.174
ZLONG	.114	039	090	043	078	- 029	094	063
ZLATR	.139	016	.100	028	075	- 058	092	046
ZCOLL	.153	014	.119	.029	084	- 063	096	042
Y50	- 008	062	.015	042	058	- 002	086	002
Y90	-.016	.042	003	030	026	001	.047	009
Y140	-.012	026	003	014	012	- 004	028	002
Y220B	-.018	003	- 002	-.015	-.001	-.024	020	- 019
Y220T	-.112	.041	-.145	-.013	-.173	.152	-.241	.044

* Change in sign required for compatibility between test and analysis

TABLE 12. CONTINUED

Flight Condition - Approach and Landing

PICKUP	8465# 196.33 C.G. REAL	8465# 196.33 C.G. IMAG*	9075# 195.35 C.G. REAL	9075# 195.35 C.G. IMAG*	9500# 196.20 C.G. REAL	9500# 196.20 C.G. IMAG*	9500# 199.51 C.G. REAL	9500# 199.51 C.G. IMAG*
Z50	034	-.089	- 005	- 051	- 045	- 072	028	- 088
Z100T	.089	- 038	062	- 026	018	-.065	045	-.035
Z210T	.066	- 091	002	- 075	- 053	- 057	- 026	- 084
Z340	.345	.148	.299	.158	.269	- 066	.263	.241
Z400	.248	.110	.217	.118	.185	- 029	.177	.192
Z460	N.G.	N.G.	-.005	-.039	- 022	008	- 026	- 018
Z540	-.684	-.315	-.546	-.368	-.499	069	-.467	-.497
Z90R	036	- 007	027	.009	.007	- 020	041	- 005
Z90L	086	-.051	060	- 027	008	- 074	050	- 033
Z140R	.054	010	038	018	029	- 020	053	011
Z140L	.107	-.022	.076	-.003	036	-.063	062	- 001
Z200R	057	.004	.052	.093	079	078	068	.127
Z200L	.220	-.030	.204	-.002	.137	-.139	.141	017
Z260R	.232	.080	.178	.096	.156	- 044	.187	.134
Z260L	.284	.066	.228	094	.182	- 079	.205	.135
Z396R	.166	.178	.157	.123	.172	018	.172	.170
Z396L	.346	.155	.257	084	.221	053	.199	.174
ZLONG	.114	039	090	043	078	- 029	094	063
ZLATR	.139	016	.100	028	075	- 058	092	046
ZCOLL	.153	014	.119	.029	084	- 063	096	042
Y50	- 008	062	.015	042	058	- 002	086	002
Y90	-.016	.042	003	030	026	001	.047	009
Y140	0.012	026	003	014	012	- 004	028	002
Y220B	-.018	003	- 002	-.015	-.001	-.024	020	- 019
Y220T	-.112	.041	-.145	-.013	-.173	.152	-.241	.044

* Change in sign required for compatibility between test and analysis

TABLE 12. CONTINUED

Flignt Condition - Approach and Landing

PICKUP	8465# 196.33 C.G.		9075# 196.35 C.G.		9500# 196.20 C.G.		9500# 199.51 C.G.	
	REAL	IMAG *	REAL	IMAG *	REAL	IMAG *	REAL	IMAG *
Y300	- 010	- 047	014	- 059	-.032	- 072	038	- 083
Y380	- 061	- 084	- 027	- 071	- 080	- 090	028	-.135
Y440	-.141	-.118	- 080	.132	-.174	- 056	029	-.221
Y490	-.110	-.102	- 011	- 001	-.101	- 098	018	-.128
Y517	.182	.154	- 046	016	053	- 052	- 003	- 048
X140	.001	.011	003	015	019	.002	016	018
X180T	.041	-.165	- 027	-.161	-.113	-.136	-.014	-.220
X540	-.660	-.307	-.546	-.340	-.482	036	-.438	-.481
X200R	.003	-.004	.041	-.019	065	-.069	060	- 010
X200L	.005	.059	023	062	010	056	-.007	.069
X190R	041	- 022	045	- 043	037	- 066	047	- 045
X220L	- 008	.014	.001	.016	016	012	007	014

* Change in sign required for compatibility between test and analysis

TABLE 12. CONTINUED

	Flight Condition - Rolling Pullout LFT @ V_L							
	187K		186		180		180	
	8465#		9075#		9500#		9500#	
	196.33 C.G.		196.35 C.G.		196.20 C.G.		199.51 C.G.	
PICKUP	REAL	IMAG*	REAL	IMAG*	REAL	IMAG*	REAL	IMAG*
Z50	-.368	-.214	-.359	-.310	-.461	-.432	-.416	-.392
Z100T	-.194	-.362	-.183	-.363	-.246	-.429	-.222	-.419
Z210T	-.156	- 073	-.242	-.107	-.452	- 086	-.318	-.069
Z340	.468	-1.264	.461	-1.044	.500	-.800	.587	-.750
Z400	.351	-.870	.327	-.719	.412	-.549	.440	-.470
Z460	- 061	- 068	001	- 094	.079	- 061	057	- 015
Z540	-.942	1.755	-.863	1.367	-.784	1.036	-1.000	1.058
Z90R	-.121	-.169	-.150	-.238	-.219	-.234	-.186	-.286
Z90L	-.217	-.410	-.186	-.380	-.229	-.422	-.222	-.415
Z140R	- 043	.217	-.065	-.255	-.103	-.196	- 070	-.265
Z140L	-.122	-.459	- 099	-.388	-.117	-.391	-.111	-.392
Z200R	.211	0.145	.159	-.269	.161	0.128	.253	-.188
Z200L	-.115	-.910	-.039	-.893	.048	-.894	070	-.803
Z260R	.136	-.679	.086	-.636	072	-.510	.137	-.537
Z260L	.144	-1.020	.197	-.792	.239	-.649	.315	-.628
Z396R	.155	-.498	.127	-.524	.125	-.432	.195	-.312
Z396L	.328	-.775	.372	-.614	.623	-.466	.593	-.328
ZLONG	.073	-.401	046	-.341	036	-.266	.077	-.309
ZLATR	- 001	-.520	014	-.398	031	-.334	.048	-.351
ZCOLL	- 038	-.590	- 024	-.494	- 019	-.413	026	-.396
Y50	- 014	.252	.087	.146	.260	.333	.277	.264
Y90	-.012	.191	.011	.088	076	.194	.111	.149
Y140	-.013	.122	- 021	.056	- 001	.110	030	.081
Y220B	.015	036	- 046	- 037	-.102	- 026	- 058	- 065
Y220T	-.311	.565	-.375	.511	-.577	.701	-.447	.622

* Change in sign required for compatibility between test and analysis

TABLE 12. CONTINUED

Flight Condition - Rolling Pullout LFT @ V_L								
	187K 8465# 196.33 C.G.		186 9075# 196.35 C.G.		180 9500# 196.20 C.G.		180 9500# 199.51 C.G.	
PICKUP	REAL	IMAG*	REAL	IMAG*	REAL	IMAG*	REAL	IMAG*
Y300	- 073	- 022	-.183	- 082	-.326	-.160	-.280	-.213
Y380	-.292	.402	-.475	.205	-.754	- 209	-.695	-.116
Y440	-.541	1.162	-.803	.656	-1.293	.347	-1.210	.155
Y490	-.563	1.134	-.483	.797	.884	.479	-.877	.706
Y517	- 039	1.815	-.059	1.593	-.173	1.715	-.263	1.719
X140	.063	.007	050	--	045	-.077	038	- 067
X180T	-.310	- 025	-.371	-.164	-.669	-.335	-.470	-.240
X540	-.996	1.817	-.880	1.443	-.890	.963	-1.091	.982
X200P	.141	-.211	.140	-.181	.153	-.219	.161	-.227
X200L	061	.167	030	.230	015	096	-.007	.119
X190R	062	-.190	053	-.204	- 011	-.310	054	-.231
X220L	050	048	044	042	062	- 033	045	- 027

* Change in sign required for compatibility between test and analysis

TABLE 12. CONTINUED

Flight Condition - Rolling Pullout RT								
	164 $8465^{\#}$ 196.33 C.G.		162 $9075^{\#}$ 196.35 C.G.		162 $9500^{\#}$ 196.20 C.G.		162 $9500^{\#}$ 199.51 C.G.	
PICKUP	REAL	IMAG*	REAL	IMAG*	REAL	IMAG*	REAL	IMAG*
Z50	-.488	-.214	-.225	-.199	-.595	-.265	-.576	-.499
Z100T	-.281	-.301	- 099	-.251	-.319	-.303	-.309	-.465
Z210T	-.409	- 033	-.160	-.104	- 514	.051	-.576	- 015
Z340	.511	-.982	.372	-.828	.669	-.554	.819	-.309
Z400	.399	-.714	.318	-.546	.527	-.334	.620	-.146
Z460	.021	-.170	046	- 064	092	055	055	.138
Z540	-.963	1.090	-.719	1.061	-1.102	.871	-1.409	.616
Z90R	-.142	- 073	-.070	-.160	-.222	-.089	-.238	-.205
Z90L	- 309	-.386	-.137	-.273	-.287	-.333	-.313	-.479
Z140R	- 041	-.106	-.015	-.182	-.052	-.081	-.076	-.119
Z140L	-.183	-.394	- 077	-.296	-.129	-.307	-.150	-.391
Z200R	.294	086	.189	-.217	.284	.116	.264	.254
Z200L	-.216	-.808	-.092	-.691	072	-.815	.108	-.876
Z260R	.168	-.429	.107	-.510	.183	-.376	.262	-.292
Z260L	.190	-.796	.162	-.619	.375	-.520	.459	-.365
Z396R	.188	-.270	.152	-.446	.217	-.253	.352	-.205
Z396L	.398	-.864	.319	-.500	.604	-.311	.556	-.109
ZLONG	.087	-.241	047	-.271	.126	-.185	.140	-.130
ZLATR	- 016	-.379	011	-.318	083	-.269	078	-.225
ZCOLL	- 058	-.416	- 027	-.360	.049	-.319	075	-.293
Y50	037	.106	003	095	.384	.242	.426	.411
Y90	017	.146	- 023	.063	.156	.152	.219	.248
Y140	002	.118	- 036	045	.051	.078	.118	.136
Y220B	017	.123	-.016	-.015	-.070	- 031	.015	-.039
Y220T	-.416	.704	-.205	.299	-.478	.916	-.618	.861

*Change in sign required for compatibility between test and analysis

TABLE 12. CONCLUDED

Flight Condition - Rolling Pullout RT

PICKUP	164 8465# 196.33 C.G.		162 9075# 196.35 C.G.		9500# 196.20 C.G.		9500# 199.51 C.G.	
	REAL	IMAG *	REAL	IMAG *	REAL	IMAG *	REAL	IMAG *
Y300	- 060	035	-.112	- 093	-.270	-.244	-.146	-.396
Y380	-.238	.401	-.351	.020	-.691	-.213	-.567	-.616
Y440	-.399	.881	-.736	.293	-1.239	- 047	-1.125	-.702
Y490	-.367	.608	-.383	.280	-.776	.216	-.945	- 055
Y517	-.232	.819	-.461	.716	-.176	.992	-.685	1.093
X140	069	039	037	-.011	044	-.058	055	- 060
X180T	-.637	-.132	-.243	- 098	-.866	-.273	-.796	-.469
X540	-.975	1.336	-.795	1.091	-1.194	.759	-1.438	.383
X200R	.146	-.125	.102	-.133	.168	-.190	.242	-.186
X200L	088	.159	023	.144	.004	.083	.005	.102
X190R	- 022	-.192	045	-.140	- 071	-.273	- 011	-.279
X220L	.056	.052	034	022	063	-.016	.052	-.006

* Change in sign required for compatibility between test and analysis

application registered zero load. During the ground flying conditions the set-point controls remained locked and only the command controls were manipulated, thus insuring that only vibratory loads (no steady loads) were applied to the helicopter.

The magnitude and phase of the four vibratory loads applied to the helicopter were controlled by the four command controls and the four phase controls located on the servo-hydraulic main control panel. These command and phase settings were manually adjusted by using the Hewlett-Packard 5420A Digital Signal Analyzer as a load monitor.

The 5420A Analyzer was used as a load monitor by placing the device in its Transfer Function Setup State. The vertical load at the main rotor hub was used as the reference for the phasing of the remaining three vibratory loads, and the signal from its load cell was fed into channel #2 of the analyzer for this purpose. Channel #1 of the analyzer received the signal from the main rotor lateral, main rotor longitudinal, or tail rotor gearbox lateral load cell, depending on which of the three vibratory loads was being measured. With the cursor set at 10.8 Hertz (the excitation frequency used for ground flying), the values of magnitude and phase displayed on the screen of the analyzer were the ratio of the channel #1 load to the channel #2 load and the phase angle of channel #1 with respect to channel #2, respectively.

The usual procedure for setting up a particular ground flying condition consisted of:

1. Adjusting the main rotor vertical load to its proper magnitude with the command control. (The phase control knob remained locked at 0 phase.)
2. Adjusting the tail rotor lateral load to the proper load ratio and phase relationship with the tail command and phase controls.
3. Adjusting the main rotor lateral load to the proper load ratio and phase relationship using the lateral command and phase controls.

4. Adjusting the main rotor longitudinal load to the proper load ratio and phase relationship using the longitudinal command and phase controls.

5. Recording all the accelerometer outputs and load cell outputs via the telemetry link.

Ground Flying Results

Table 13 and Figures 26 through 43 show the results of the ground flying. It is seen from the figures that the magnitude of the two-per-rev response was duplicated in all flight conditions and weight configurations. It is further seen in the table that the phasings of the responses were also in very good agreement. In most cases the large phasing discrepancies occur in very low vibration levels.

It is also seen from Table 13 that the applied forces in the ground flying were a very good representation of the force determination calculated forces in both magnitude and phase. However, they were not precise. It was not necessary to apply the forces exactly, since results obtained are well within the scatter band of any measured flight test data.

Because of these excellent results, it is seen that forces acting on the fuselage can be determined from accelerations obtained in flight and the calibration matrix obtained in a shake test. Force determination can become a useful tool in the development of a new vehicle in that forces can be determined when rotor changes are made and structural changes can be made and shake testing done to determine a new flight response.

Further, since these forces can be applied to duplicate the response of the vehicle in flight, ground flying is feasible. With ground flying, a flight spectrum can be duplicated in the hangar; thus, valuable test time can be accumulated without the cost of many hours of flight time.

TABLE 13. GROUND FLYING RESULTS

Flight Condition - Level flight		Vehicle Gross Weight - 8465 lb.		
Force Direction	Force Determination		Applied	
	Mag.-lb.	Phase deg.	Mag.-lb.	Phase deg.
Vertical at Hub	1342.	65	1291.	65
Longitudinal at Hub	309.	112	337.	118
Lateral at Hub	205.	240	185.	250
Lateral at Tail Rotor Gearbox	146.	218	147.	211

Pickup Location	Flight		Results (g's)			
			Force Determination		Ground Flying	
	Mag.	Phase	Mag.	Phase	Mag.	Phase
Z50	0.121	168	0.136	168	0.236	136
Z100T	0.141	146	0.111	108	0.173	110
Z210T	0.130	175	0.139	147	0.176	126
Z340	0.517	50	0.457	50	0.428	42
Z400	0.344	44	0.322	48	0.318	39
Z460	0.053	269	0.038	290	0.031	1
Z540	0.769	229	0.803	233	0.709	220
Z90R	0.039	102	0.055	10	0.068	97
Z90L	0.201	133	0.170	130	0.218	121
Z140R	0.069	57	0.091	14	0.059	61
Z140L	0.182	114	0.162	105	0.104	109
Z200R	0.261	4	0.323	2	0.207	345
Z200L	0.397	111	0.363	111	0.318	104
Z260R	0.290	53	0.307	49	0.273	45
Z260L	0.369	66	0.341	59	0.283	55
Z396R	0.314	48	0.340	41	0.383	35
Z396L	0.300	69	0.333	61	0.271	48
ZLONG	0 155	53	0.149	34	0.119	40
ZLATR	0.176	82	0.166	77	0.151	77
ZCOLL	0.208	90	0.195	73	0.168	74
Y50	0.196	226	0.202	232	0.262	221
Y30	0.103	240	0.105	249	0.126	236
Y140	0.055	246	0.055	260	0.048	255
Y220B	0.079	151	0.083	12	0.113	21
Y220T	0.418	230	0.341	238	0.144	276
Y300	0.089	63	0.090	117	0.143	80
Y300	0.195	206	0.325	188	0.265	162
Y440	0.611	215	0.700	206	0.657	187
Y490	0.878	210	1.075	215	1.050	202
Y517	1.657	222	1.393	221	1.450	208
X140	0.035	320	0.038	315	0.046	311
X100T	0.254	152	0.327	150	0.371	130
X540	0.778	228	0.745	234	0.020	220
X200R	0.143	28	0.114	36	0.129	28
X200L	0.119	267	0.097	280	0.121	267
X190R	0.107	68	0.104	86	0.101	92
X220L	0.038	275	0.035	291	0.054	271

TABLE 13. CONTINUED

Flight Condition - Rt. Bank Turn	Vehicle Gross Weight - 8465 lb.			
Force Direction	Force Determination		Applied	
	Mag.-lb.	Phase deg.	Mag.-lb.	Phase deg.
Vertical at Hub	909.	36	948.	36
Longitudinal at Hub	212.	99	220.	99
Lateral at Hub	112.	228	114.	226
Lateral at Tail Rotor Gearbox	34.	166	34.	169

Pickup Location	Flight		Results (g's)			
			Force Determination		Ground Flying	
	Mag.	Phase	Mag.	Phase	Mag.	Phase
Z50	0.121	162	0.114	154	0.146	124
Z100T	0.087	128	0.061	96	0.093	91
Z210T	0.093	120	0.088	119	0.129	102
Z340	0.355	29	0.339	23	0.345	17
Z400	0.237	92	0.232	22	0.270	18
Z460	0.052	175	0.042	210	0.021	43
Z540	0.684	193	0.632	203	0.561	195
Z90R	0.019	216	0.016	5	0.062	96
Z90L	0.131	116	0.092	108	0.102	97
Z140R	0.029	98	0.052	357	0.055	67
Z140L	0.126	95	0.089	73	0.087	75
Z200R	0.168	337	0.196	346	0.094	1
Z200L	0.279	86	0.202	74	0.152	54
Z260R	0.221	28	0.234	21	0.220	21
Z260L	0.264	45	0.250	30	0.234	24
Z396R	0.239	6	0.223	13	0.275	14
Z396L	0.229	40	0.260	34	0.270	23
ZLONG	0.101	33	0.111	11	0.094	24
ZLATR	0.130	61	0.114	41	0.104	35
ZCOLL	0.147	69	0.136	39	0.121	33
Y50	0.100	232	0.041	160	0.064	168
Y30	0.072	255	0.017	209	0.029	185
Y140	0.048	265	0.018	244	0.008	237
Y220B	0.054	326	0.044	302	0.034	325
Y220T	0.189	221	0.207	233	0.112	254
Y300	0.072	39	0.011	143	0 021	28
Y300	0.028	139	0.096	164	0.063	152
Y440	0.118	190	0.226	178	0.190	170
Y490	0.233	175	0.273	174	0.276	171
Y517	0.405	171	0.337	170	0.354	173
X140	0.034	324	0.027	302	0.031	304
X100T	0.170	134	0.236	133	0.242	111
X540	0.643	196	0.569	205	0.509	199
X200R	0 091	24	0.055	344	0. 8	335
X200L	0.068	69	0.039	307	0.035	283
X190R	0.069	301	0.062	75	0.062	78
X220L	0.023		0.018	298	0.029	262

TABLE 13. CONTINUED

Flight Condition - Sideward	Vehicle Gross Weight - 8465 lb.			
Force Direction	Force Determination		Applied	
	Mag.-lb.	Phase deg.	Mag.-lb.	Phase deg.
Vertical at Hub	1090.	136	1149.	136
Longitudinal at Hub	150.	140	157.	142
Lateral at Hub	35.	237	36.	282
Lateral at Tail Rotor Gearbox	2.	42	0.	107

Pickup Location	Flight		Results (g's)			
			Force Determination		Ground Flying	
	Mag.	Phase	Mag.	Phase	Mag.	Phase
Z50	0.106	152	0.032	196	0.127	188
Z100T	0.131	142	0.079	146	0.122	165
Z210T	0.115	165	0.133	157	0.143	155
Z340	0.395	136	0.341	129	0.351	125
Z400	0.249	132	0.235	130	0.268	124
Z460	0.008	130	0.036	330	0.005	27
Z540	0.541	307	0.615	313	0.597	304
Z90R	0.092	159	0.061	152	0.109	171
Z90L	0.113	145	0.070	152	0.105	169
Z140R	0.104	156	0.074	141	0.105	160
Z140L	0.127	144	0.092	138	0.103	156
Z200R	0.129	163	0.139	138	0.124	145
Z200L	0.227	142	0.172	137	0.143	138
Z260R	0.260	147	0.249	137	0.246	134
Z260L	0.295	143	0.249	131	0.249	129
Z396R	0.255	137	0.234	131	0.270	125
Z396L	0.283	126	0.270	129	0.281	125
ZLONG	0.141	149	0.107	137	0.117	143
ZLATR	0.154	147	0.121	136	0.120	141
ZCOLL	0.163	145	0.144	135	0.138	138
Y50	0.038	247	0.014	7	0.008	309
Y30	0.025	243	0.002	350	0.004	313
Y140	0.017	230	0.008	44	0.002	76
Y220B	0.007	135	0.004	128	0.004	121
Y220T	0.030	176	0.063	229	0.029	301
Y300	0.032	94	0.009	219	0.006	177
Y300	0.032	46	0.016	250	0.022	259
Y440	0.075	317	0.053	296	0.061	281
Y490	0.031	306	0.042	321	0.041	294
Y517	0.017	315	0.011	289	0.074	314
X140	0.018	34	0.019	356	0.026	338
X100T	0.055	207	0.113	157	0.124	143
X540	0.578	307	0.586	313	0.569	305
X200R	0.055	78	0.016	37	0.020	26
X200L	0.026	307	0.016	30	0.027	7
X190R	0.064	118	0.051	131	0.045	117
X220L	0.020	357	0.016	346	0.027	327

TABLE 13. CONTINUED

Flight Condition - Approach & Landing	Vehicle Gross Weight - 8465 lb.			
Force Direction	Force Determination		Applied	
	Mag.-lb.	Phase deg.	Mag.-lb.	Phase deg.
Vertical at Hub	1153.	344	1223.	344
Longitudinal at Hub	188.	31	194.	33
Lateral at Hub	97.	159	96.	164
Lateral at Tail Rotor Gearbox	10.	314	10.	303

Pickup Location	Flight		Results (g's)			
			Force Determination		Ground Flying	
	Mag.	Phase	Mag.	Phase	Mag.	Phase
Z50	0.095	69	0.090	97	0.160	61
Z100T	0.097	23	0.071	24	0.127	29
Z210T	0.112	54	0.101	45	0.141	35
Z340	0.375	337	0.406	334	0.419	328
Z400	0.271	336	0.278	335	0.324	328
Z460	0.001	315	0.049	154	0.010	330
Z540	0.753	155	0.745	155	0.701	147
Z90R	0.037	11	0.031	359	0.094	35
Z90L	0.100	31	0.086	35	0.117	31
Z140R	0.055	350	0.060	329	0.089	15
Z140L	0.109	12	0.104	4	0.111	11
Z200R	0.110	301	0.171	312	0.104	334
Z200L	0.222	8	0.224	4	0.184	350
Z260R	0.245	341	0.276	336	0.273	336
Z260L	0.292	347	0.304	339	0 292	334
Z396R	0.243	313	0 245	331	0.312	327
Z396L	0.379	336	0.337	339	0.344	331
ZLONG	0.120	341	0.122	331	0.126	342
ZLATR	0.140	353	0.142	346	0.136	344
ZCOLL	0.154	355	0.168	345	0.154	344
Y50	0.063	263	0.034	318	0.009	304
Y30	0.045	259	0.014	292	0.006	272
Y140	0.029	256	0.013	234	0.004	226
Y220B	0.018	189	0.029	198	0.011	184
Y220T	0.119	200	0.189	161	0.085	180
Y300	0.048	102	0.030	136	0.002	59
Y300	0.104	125	0.044	143	0 021	172
Y440	0.184	140	0.100	178	0.063	174
Y490	0.150	137	0.047	219	0.050	231
Y517	0.238	320	0.075	327	0.078	218
X140	0.011	275	0.024	235	0.029	230
X100T	0.170	76	0.188	72	0.198	49
X540	0.728	155	0.687	157	0.655	150
X200R	0.033	7	0.027	272	0.038	263
X200L	0.059	275	0.047	275	0.048	256
X190R	0.047	28	0.058	14	0.054	10
X220L	0.016	240	0.019	245	0.031	203

TABLE 13. CONTINUED

Flight Condition - Left Pullout	Vehicle Gross Weight - 8465 lb.			
Force Direction	Force Determination		Applied	
	Mag.-lb.	Phase deg.	Mag.-lb.	Phase deg.
Vertical at Hub	3540.	75	3435.	75
Longitudinal at Hub	562.	108	573.	101
Lateral at Hub	428.	236	487.	237
Lateral at Tail Rotor Gearbox	174.	263	181.	255

Pickup Location	Flight		Results (g's)			
			Force Determination		Ground Flying	
	Mag.	Phase	Mag.	Phase	Mag.	Phase
Z50	0.426	150	0.205	172	0.554	105
Z100T	0.411	118	0.265	105	0.476	97
Z210T	0.172	115	0.301	143	0.342	126
Z340	1.348	70	1.176	65	1.069	60
Z400	0.938	63	0.825	64	0.787	59
Z460	0.091	132	0.074	281	0.142	58
Z540	1.992	242	2.041	247	1.545	238
Z90R	0.208	126	0.125	53	0.367	87
Z90L	0.464	118	0.320	123	0.453	112
Z140R	0.221	259	0.200	47	0.321	81
Z140L	0.475	105	0.355	100	0.404	104
Z200R	0.256	34	0.554	29	0.397	43
Z200L	0.917	97	0.766	105	0.529	109
Z260R	0.692	79	0.774	67	0.632	69
Z260L	1.030	82	0.889	70	0.727	69
Z396R	0.522	73	0.767	64	0.803	59
Z396L	0.342	67	0.960	67	0.823	61
ZLONG	0.408	30	0.347	59	0.315	73
ZLATR	0.520	90	0.430	82	0.352	89
ZCOLL	0.591	94	0.503	80	0.395	86
Y50	0.252	267	0.277	294	0.284	267
Y30	0.191	266	0.162	297	0.145	277
Y140	0.123	264	0.092	295	0.069	280
Y220B	0.029	293	0.035	65	0.079	60
Y220T	0.645	241	0.802	229	0.616	240
Y300	0.076	163	0.193	163	0.123	145
Y300	0.497	234	0.489	217	0.471	221
Y440	1.282	245	1.159	239	1.180	232
Y490	1.266	244	1.425	255	1.507	244
Y517	1.815	269	1.667	265	1.778	249
X140	0.062	354	0.068	310	0.066	287
X100T	0.311	175	0.520	155	0.471	127
X540	2.072	241	1.937	247	1.619	240
X200R	0.265	56	0.128	70	0.086	53
X200L	0.178	290	0.191	314	0.197	282
X190R	0.200	72	0.201	91	0.166	89
X220L	0.069	316	0.072	309	0.112	269

TABLE 13. CONTINUED

Flight Condition - Rt. Pullout	Vehicle Gross Weight - 8465 lb.			
Force Direction	Force Determination		Applied	
	Mag.-lb.	Phase deg.	Mag.-lb.	Phase deg.
Vertical at Hub	2639.	76	2596.	76
Longitudinal at Hub	757.	120	751.	119
Lateral at Hub	515.	240	531.	239
Lateral at Tail Rotor Gearbox	81.	257	91.	251

Pickup Location	Flight		Results (g's)			
			Force Determination		Ground Flying	
	Mag.	Phase	Mag.	Phase	Mag.	Phase
Z50	0.533	156	0.356	169	0.559	123
Z100T	0.412	133	0.265	127	0.406	114
Z210T	0.410	175	0.384	161	0.420	142
Z340	1.107	63	0.926	58	0.862	51
Z400	0.818	61	0.641	58	0.632	50
Z460	0.171	83	0.063	225	0.107	73
Z540	1 454	229	1.619	237	1.293	224
Z90R	0.160	153	0.019	34	0.254	106
Z90L	0.494	129	0.361	132	0.431	122
Z140R	0.114	111	0.102	24	0.198	91
Z140L	0.434	115	0.342	107	0.349	113
Z200R	0.306	344	0.435	1	0.295	15
Z200L	0.836	105	0.751	107	0.501	109
Z260R	0.461	69	0.561	57	0.473	59
Z260L	0.818	77	0.725	65	0.592	62
Z396R	0.329	55	0.517	53	0.598	49
Z396L	0.951	65	0.817	66	0.703	56
ZLONG	0.256	70	0.257	41	0.215	61
ZLATR	0.379	92	0.344	31	0.273	86
ZCOLL	0.420	98	0.404	78	0.308	84
Y50	0.112	289	0.116	325	0.112	231
Y30	0.147	277	0.100	306	0.083	294
Y140	0.118	271	0.069	287	0.047	237
Y220B	0.124	278	0.079	273	0.023	343
Y220T	0.818	239	1.003	238	0.630	247
Y300	0.069	210	0.153	182	0.108	167
Y300	0.466	239	0.336	212	0.360	213
Y440	0.967	246	0.832	283	0.302	225
Y490	0.710	239	0.825	248	0.379	237
Y517	0.351	254	0.805	257	0.938	248
X140	0.079	331	0.092	323	0.089	309
X100T	0.651	168	0.824	154	0.790	137
X540	1.654	234	1.510	240	1.323	231
X200R	0.192	41	0.106	29	0.089	0
X200L	0.182	299	0.197	327	0.134	304
X190R	0.193	97	0.226	103	0.206	107
X220L	0.076	317	0.081	326	0.107	290

TABLE 13. CONTINUED

Flight Condition - Level	Vehicle Gross Weight - 9075 lb.			
Force Direction	Force Determination		Applied	
	Mag.-lb.	Phase deg.	Mag.-lb.	Phase deg.
Vertical at Hub	1332.	69	1302.	69
Longitudinal at Hub	360.	119	347.	119
Lateral at Hub	254.	234	263.	234
Lateral at Tail Rotor Gearbox	100.	214	99.	216

Pickup Location	Flight		Results (g's)			
			Force Determination		Ground Flying	
	Mag.	Phase	Mag.	Phase	Mag.	Phase
Z50	0.243	161	0.157	154	0.227	131
Z100T	0.152	145	0.114	114	0.160	108
Z210T	0.175	179	0.184	165	0.185	147
Z340	0.450	49	0.401	49	0.392	44
Z400	0.302	45	0.269	48	0.300	43
Z460	0.065	309	0.050	283	0.030	41
Z540	0.715	233	0.699	235	0.632	221
Z90R	0.076	140	0.037	117	0.091	122
Z90L	0.178	125	0.151	117	0.179	113
Z140R	0.064	91	0.037	74	0.066	99
Z140L	0.160	104	0.130	82	0.141	98
Z200R	0.152	293	0.169	343	0.108	350
Z200L	0.433	94	0.386	90	0.328	81
Z260R	0.242	60	0.231	60	0.237	52
Z260L	0.138	355	0.320	57	0.270	51
Z396R	0.219	48	0.238	55	0.322	45
Z396L	0.350	69	0.288	43	0.294	45
ZLONG	0.130	58	0.104	43	0.092	49
ZLATR	0.166	74	0.159	68	0.134	66
ZCOLL	0.183	82	0.171	68	0.151	65
Y50	0.085	213	0.104	234	0.121	211
Y30	0.057	215	0.052	215	0.055	211
Y140	0.041	202	0.036	193	0.020	197
Y220B	0.026	61	0.047	93	0.061	54
Y220T	0.496	236	0.497	236	0.277	249
Y300	0.113	118	0.133	118	0.113	92
Y300	0.314	177	0.309	167	0.210	162
Y440	0.637	193	0.663	188	0.500	187
Y490	0.504	211	0.795	206	0.738	205
Y517	1.152	216	0.880	220	1.002	215
X140	0.031	343	0.032	323	0.041	332
X100T	0.323	150	0.406	150	0.390	136
X540	0.695	230	0.595	235	0.613	224
X200R	0.146	35	0.101	44	0.123	23
X200L	0.129	264	0.107	278	0.124	265
X190R	0.122	75	0.109	95	0.107	101
X220L	0.028	305	0.052	289	0.047	290

TABLE 13. CONTINUED

Flight Condition - Rt. Bank Turn	Vehicle Gross Weight - 9075 lb			
Force Direction	Force Determination		Applied	
	Mag.-lb.	Phase deg.	Mag.-lb.	Phase deg.
Vertical at Hub	546.	6	565.	6
Longitudinal at Hub	312.	117	325.	121
Lateral at Hub	189.	221	192.	220
Lateral at Tail Rotor Gearbox	42.	181	44.	184

Pickup Location	Flight		Results (g's)			
			Force Determination		Ground Flying	
	Mag.	Phase	Mag.	Phase	Mag.	Phase
Z50	0.185	157	0.169	152	0.196	144
Z100T	0.099	137	0.064	136	0.073	129
Z210T	0.228	153	0.164	164	0.171	141
Z340	0.309	298	0.262	349	0.292	344
Z400	0.217	1	0.174	349	0.226	342
Z460	0.031	186	0.046	190	0.013	228
Z540	0.550	172	0.500	174	0.536	165
Z90R	0.040	196	0.041	191	0.064	159
Z90L	0.144	124	0.080	118	0.085	125
Z140R	0.013	266	0.025	275	0.007	180
Z140L	0.109	104	0.042	57	0.039	90
Z200R	0.226	320	0.201	303	0.136	308
Z200L	0.304	89	0.186	55	0.140	35
Z260R	0.158	88	0.151	349	0.179	346
Z260L	0.199	30	0.194	2	0.189	351
Z396R	0.211	347	0.143	346	0.213	340
Z396L	0.212	292	0.188	349	0.208	347
ZLONG	0.076	16	0.088	336	0.081	337
ZLATR	0.089	56	0.088	8	0.084	355
ZCOLL	0.102	66	0.090	9	0.086	358
Y50	0.041	241	0.041	152	0.073	151
Y30	0.042	255	0.028	149	0.036	155
Y140	0.023	239	0.027	143	0.016	154
Y220B	0.021	85	0.019	102	0.027	349
Y220T	0.334	223	0.383	226	0.251	246
Y300	0.112	98	0.080	105	0.037	54
Y300	0.197	134	0.172	135	0.099	145
Y440	0.349	153	0.351	153	0.245	165
Y490	0.365	162	0.373	171	0.351	175
Y517	0.364	190	0.375	187	0.433	180
X140	0.039	325	0.030	323	0.045	317
X100T	0.367	142	0.405	138	0.435	128
X540	0.503	173	0.388	175	0.451	167
X200R	0.108	36	0.075	8	0.106	343
X200L	0.119	278	0.067	286	0.056	274
X190R	0.106	102	0.079	103	0.093	102
X220L	0.034	208	0.031	295	0.033	304

TABLE 13. CONTINUED

Flight Condition - Sideward	Vehicle Gross Weight - 9075 lb.			
Force Direction	Force Determination		Applied	
	Mag.-lb.	Phase deg.	Mag.-lb.	Phase deg.
Vertical at Hub	1212.	132	1170.	132
Longitudinal at Hub	204.	139	200.	138
Lateral at Hub	55.	226	57.	225
Lateral at Tail Rotor Gearbox	2.	249	5.	242

Pickup Location	Flight		Results (g's)			
			Force Determination		Ground Flying	
	Mag.	Phase	Mag.	Phase	Mag.	Phase
Z50	0.121	151	0.080	165	0.163	161
Z100T	0.132	142	0.096	145	0.139	150
Z210T	0.156	161	0.160	154	0.157	156
Z340	0.347	130	0.312	122	0.297	119
Z400	0.233	125	0.210	125	0.227	117
Z460	0.010	169	0.039	318	0.016	111
Z540	0.491	300	0.570	306	0.481	297
Z90R	0.105	157	0.084	151	0.121	159
Z90L	0.118	138	0.092	148	0.118	153
Z140R	0.107	155	0.081	149	0.107	154
Z140L	0.122	138	0.100	136	0.101	148
Z200R	0.175	160	0.144	144	0.155	147
Z200L	0.249	130	0 206	130	0.178	129
Z260R	0.241	142	0.221	133	0.202	129
Z260L	0.263	133	0.235	126	0.213	123
Z396R	0.183	131	0.230	129	0.235	118
Z396L	0.239	125	0.224	121	0.234	117
ZLONG	0.130	145	0.095	135	0.098	140
ZLATR	0.145	140	0.118	131	0.100	134
ZCOLL	0.151	141	0.133	131	0.116	132
Y50	0.027	236	0.041	351	0.005	89
Y30	0.018	236	0.008	343	0.005	118
Y140	0.011	218	0.006	325	0.011	90
Y220B	0.017	115	0.008	143	0.008	75
Y220T	0.086	222	0.106	229	0.065	248
Y300	0.038	92	0.025	95	0.010	91
Y300	0.018	52	0.018	150	0.012	250
Y440	0.076	278	0.030	260	0.053	270
Y490	0.041	256	0.033	286	0.059	269
Y517	0.011	142	0.025	266	0.090	275
X140	0.017	33	0.022	345	0.025	339
X100T	0.136	168	0.186	155	0.175	142
X540	0.517	302	0.494	307	0.492	299
X200R	0.069	67	0.020	359	0.042	357
X200L	0.054	294	0.024	340	0.046	326
X190R	0.081	116	0.070	122	0.050	121
X220L	0.017	357	0.033	326	0.036	328

TABLE 13. CONTINUED

Flight Condition - Approach & Landing   Vehicle Gross Weight - 9075 lb.

Force Direction	Force Determination Mag.-lb.	Force Determination Phase deg.	Applied Mag.-lb.	Applied Phase deg.
Vertical at Hub	1066.	336	1051.	336
Longitudinal at Hub	143.	56	141.	55
Lateral at Hub	80.	177	78.	175
Lateral at Tail Rotor Gearbox	10.	274	10.	279

Pickup Location	Flight		Results (g's)			
			Force Determination		Ground Flying	
	Mag.	Phase	Mag.	Phase	Mag.	Phase
Z50	0.051	96	0.072	108	0.096	69
Z100T	0.067	23	0.039	22	0.076	21
Z210T	0.075	88	0.050	68	0.080	54
Z340	0.338	332	0.346	326	0.357	323
Z400	0.247	331	0.228	329	0.265	322
Z460	0.039	97	0.062	156	0.014	139
Z540	0.658	146	0.664	150	0.640	142
Z90R	0.028	342	0.025	359	0.054	25
Z90L	0.066	24	0.052	26	0.068	30
Z140R	0.042	335	0.050	336	0.057	355
Z140L	0.076	2	0.078	352	0.073	1
Z200R	0.107	299	0.160	316	0.142	323
Z200L	0.204	1	0.202	352	0.186	345
Z260R	0.202	332	0.227	333	0.230	328
Z260L	0.247	338	0.260	333	0.243	328
Z396R	0.199	322	0.226	329	0.260	320
Z396L	0.270	243	0.253	328	0.277	325
ZLONG	0.100	334	0.108	329	0.101	331
ZLATR	0.104	344	0.125	337	0.111	336
ZCOLL	0.122	346	0.136	337	0.128	334
Y50	0.045	290	0.012	244	0.012	13
Y30	0.030	276	0.003	47	0.006	346
Y140	0.014	282	0.010	117	0.005	34
Y220B	0.015	98	0.017	109	0.001	256
Y220T	0.146	185	0.170	181	0.098	201
Y300	0.061	77	0.036	89	0.011	16
Y30C	0.076	111	0.023	109	0.011	251
Y440	0.154	239	0.062	159	0.042	201
Y490	0.011	175	0.064	218	0.055	236
Y517	0.049	199	0.078	268	0.071	215
X140	0.015	281	0.015	258	0.020	260
X100T	0.063	100	0.183	94	0.169	81
X540	0.635	148	0.543	151	0.592	144
X200R	0.045	25	0.016	345	0.032	284
X200L	0.066	290	0.043	271	0.038	255
X190R	0.062	44	0.036	88	0.039	43
X220L	0.016	274	0.019	218	0.017	244

TABLE 13. CONTINUED

Flight Condition - Lft. Pullout	Vehicle Gross Weight - 9075 lb.			
Force Direction	Force Determination		Applied	
	Mag.-lb.	Phase deg.	Mag.-lb.	Phase deg.
Vertical at Hub	3608.	76	3550.	76
Longitudinal at Hub	672.	109	666.	106
Lateral at Hub	383.	238	389.	243
Lateral at Tail Rotor Gearbox	155.	258	154.	258

Pickup Location	Flight		Results (g's)			
			Force Determination		Ground Flying	
	Mag.	Phase	Mag.	Phase	Mag.	Phase
Z50	0.474	139	0.273	141	0.475	102
Z100T	0.407	117	0.281	105	0.419	91
Z210T	0.265	156	0.314	136	0.365	125
Z340	1.141	66	1.009	61	0.978	58
Z400	0.790	66	0.691	63	0.714	56
Z460	0.094	89	0.079	274	0.101	45
Z540	1.617	238	1.753	245	1.461	236
Z90R	0.281	122	0.181	94	0.321	88
Z90L	0.423	116	0.314	112	0.397	105
Z140R	0.263	104	0.181	84	0.288	81
Z140L	0.400	104	0.339	85	0.358	97
Z200R	0.312	59	0.379	41	0.408	46
Z200L	0.894	93	0.762	92	0.640	93
Z260R	0.642	82	0.633	72	0.609	70
Z260L	0.816	76	0.791	67	0.652	65
Z396R	0.539	76	0.669	67	0.738	62
Z396L	0.718	59	0.759	56	0.729	52
ZLONG	0.344	82	0.285	65	0.280	70
ZLATR	0.398	88	0.384	76	0.320	81
ZCOLL	0.495	93	0.422	76	0.364	80
Y50	0.170	301	0.245	286	0.219	280
Y30	0.089	277	0.086	271	0.105	282
Y140	0.060	249	0.050	234	0.027	266
Y220B	0.059	141	0.105	123	0.101	96
Y220T	0.634	234	0.774	237	0.425	248
Y300	0.201	156	0.180	136	0.197	140
Y300	0.517	203	0.394	201	0.428	200
Y440	1.037	219	0.979	226	0.976	218
Y490	0.932	239	1.233	247	1.223	240
Y517	1.594	268	1.368	262	1.576	254
X140	0.050	0	0.065	308	0.057	316
X100T	0.406	145	0.629	141	0.630	127
X540	1.690	239	1.534	245	1.421	238
X200R	0.229	52	0.113	78	0.089	47
X200L	0.232	277	0.225	298	0.240	278
X190R	0.211	76	0.231	87	0.206	99
X220L	0.061	316	0.117	287	0.095	286

TABLE 13. CONTINUED

Flight Condition - Rt. Pullout	Vehicle Gross Weight - 9075 lb.			
Force Direction	Force Determination		Applied	
	Mag.-lb.	Phase deg.	Mag.-lb.	Phase deg.
Vertical at Hub	2803.	71	2751.	71
Longitudinal at Hub	463.	107	476.	111
Lateral at Hub	245.	242	242.	242
Lateral at Tail Rotor Gearbox	86.	230	85.	226

Pickup Location	Flight		Results (g's)			
			Force Determination		Ground Flying	
	Mag.	Phase	Mag.	Phase	Mag.	Phase
Z50	0.300	139	0.178	142	0.371	114
Z100T	0.270	112	0.194	98	0.209	97
Z210T	0.191	147	0.208	125	0.278	128
Z340	0.908	66	0.796	58	0.812	54
Z400	0.632	60	0.536	59	0.596	54
Z460	0.079	54	0.096	271	0.043	52
Z540	1.282	236	1.427	243	1.232	231
Z90R	0.175	114	0.127	86	0.236	99
Z90L	0.305	117	0.225	108	0.296	107
Z140R	0.183	95	0.142	77	0.206	90
Z140L	0.306	105	0.241	82	0.268	93
Z200R	0.288	49	0.316	40	0.291	56
Z200L	0.697	98	0.580	88	0.495	83
Z260R	0.521	78	0.513	68	0.513	63
Z260L	0.640	75	0.613	65	0.541	60
Z396R	0.471	71	0.530	63	0.622	54
Z396L	0.593	57	0.577	55	0.589	53
ZLONG	0.275	80	0.232	62	0.224	69
ZLATR	0.318	88	0.302	72	0.263	74
ZCOLL	0.361	94	0.332	72	0.291	72
Y50	0.095	272	0.131	259	0.110	231
Y30	0.067	250	0.054	234	0.057	235
Y140	0.058	231	0.042	215	0.019	227
Y220B	0.022	137	0.045	110	0.057	58
Y220T	0.363	236	0.491	245	0.253	259
Y300	0.146	140	0.111	125	0.095	98
Y300	0.352	183	0.277	179	0.189	175
Y440	0.792	202	0.627	204	0.496	200
Y490	0.474	216	0.729	223	0.686	216
Y517	0.852	237	0.772	235	0.924	224
X140	0.039	17	0.046	308	0.036	321
X100T	0.262	158	0.420	140	0.449	135
X540	1.350	234	1.223	243	1.163	232
X200R	0.168	52	0.070	54	0.098	18
X200L	0.146	279	0.120	294	0.136	269
X190R	0.147	72	0.156	82	0.138	103
X220L	0.040	327	0.079	281	0.056	272

TABLE 13. CONTINUED

Flight Condition - Level	Vehicle Gross Weight -9500 lb.			
Force Direction	Force Determination		Applied	
	Mag.-lb.	Phase deg.	Mag.-lb.	Phase deg.
Vertical at Hub	1158.	74	1245.	74
Longitudinal at Hub	447.	109	494.	110
Lateral at Hub	335.	214	361.	217
Lateral at Tail Rotor Gearbox	81.	206	89.	209

Pickup Location	Flight		Results (g's)			
			Force Determination		Ground Flying	
	Mag.	Phase	Mag.	Phase	Mag.	Phase
Z50	0.200	166	0.201	146	0.389	137
Z100T	0.139	154	0.063	155	0.229	125
Z210T	0.191	161	0.237	193	0.297	147
Z340	0.309	40	0.230	44	0.352	31
Z400	0.210	29	0.131	28	0.271	26
Z460	0.105	304	0.075	297	0.060	324
Z540	0.494	235	0.504	239	0.585	215
Z90R	0.078	145	0.073	33	0.202	141
Z90L	0.120	136	0.086	53	0.219	125
Z140R	0.056	104	0.031	131	0.137	138
Z140L	0.101	110	0.047	74	0.142	115
Z200R	0.171	4	0.141	36	0.042	322
Z200L	0.283	81	0.330	70	0.277	68
Z260R	0.182	63	0.161	66	0.206	60
Z260L	0.222	53	0.158	46	0.240	36
Z396R	0.122	77	0.128	60	0.268	52
Z396L	0.260	23	0.169	13	0.330	6
ZLONG	0.094	65	0.055	63	0.065	80
ZLATR	0.107	71	0.074	53	0.096	61
ZCOLL	0.121	80	0.092	43	0.113	61
Y50	0.037	246	0.021	316	0.056	238
Y30	0.022	162	0.036	112	0.046	168
Y140	0.037	144	0.048	114	0.059	136
Y220B	0.036	111	0.104	98	0.119	116
Y220T	0.389	232	0.377	222	0.432	222
Y300	0.206	120	0.211	131	0.279	123
Y300	0.363	155	0.396	153	0.531	143
Y440	0.628	172	0.710	168	0.900	156
Y490	0.474	200	0.720	189	0.810	181
Y517	1.123	221	0.771	227	0.939	244
X140	0.027	86	0.023	4	0.028	353
X100T	0.272	141	0.345	168	0.611	122
X540	0.444	227	0.419	232	0.503	211
X200R	0.142	48	0.091	36	0.118	24
X200L	0.114	250	0.126	246	0.091	279
X190R	0.115	70	0.104	123	0.175	90
X220L	0.027	333	0.023	356	0.040	302

TABLE 13. CONTINUED

Flight Condition - Rt. Bank Turn	Vehicle Gross Weight - 9500 lb.			
Force Direction	Force Determination		Applied	
	Mag.-lb.	Phase deg.	Mag.-lb.	Phase deg.
Vertical at Hub	587.	41	664.	41
Longitudinal at Hub	504.	106	594.	113
Lateral at Hub	263.	213	288.	219
Lateral at Tail Rotor Gearbox	52.	195	56.	200

Pickup Location	Flight		Results (g's) Force Determination		Ground Flying	
	Mag.	Phase	Mag.	Phase	Mag.	Phase
Z50	0.226	175	0.196	151	0.416	143
Z100T	0.120	165	0.081	163	0.199	139
Z210T	0.204	154	0.219	187	0.342	138
Z340	0.236	85	0.191	4	0.368	352
Z400	0.172	357	0.118	351	0.289	349
Z460	0.031	234	0.045	261	0.037	269
Z540	0.449	184	0.402	198	0.660	176
Z90R	0.088	184	0.077	31	0.194	149
Z90L	0.120	149	0.086	47	0.182	136
Z140R	0.029	172	0.017	180	0.099	159
Z140L	0.079	127	0.012	96	0.084	129
Z200R	0.171	319	0.117	336	0.127	297
Z200L	0.195	86	0.185	48	0.155	29
Z260R	0.116	27	0.108	19	0.182	4
Z260L	0.157	32	0.130	5	0.229	355
Z396R	0.129	351	0.086	19	0.232	3
Z396L	0.184	351	0.138	344	0.343	341
ZLONG	0.052	40	0.043	5	0.057	339
ZLATR	0.072	57	0.054	12	0.075	351
ZCOLL	0.076	67	0.068	7	0.085	1
Y50	0.019	183	0.010	307	0.036	191
Y30	0.020	180	0.026	102	0.036	154
Y140	0.024	147	0.036	105	0.041	134
Y220B	0.046	94	0.066	86	0.075	110
Y220T	0.328	224	0.295	226	0.385	231
Y300	0.156	112	0.162	117	0.173	112
Y300	0.269	144	0.287	139	0.336	132
Y440	0.474	161	0.495	153	0.580	145
Y490	0.483	174	0.480	174	0.520	170
Y517	0.595	208	0.519	216	0.590	235
X140	0.029	350	0.021	332	0.048	325
X100T	0.333	144	0.382	145	0.816	119
X540	0.418	176	0.334	191	0.550	175
X200R	0.143	50	0.085	14	0.117	353
X200L	0.095	277	0.073	246	0.072	294
X190R	0.105	90	0.114	120	0.213	97
X220L	0.028	325	0.028	333	0.046	300

TABLE 13. CONTINUED

Flight Condition - Sideward   Vehicle Gross Weight - 9500 lb.

Force Direction	Force Determination		Applied	
	Mag.-lb.	Phase deg.	Mag.-lb.	Phase deg.
Vertical at Hub	1098.	169	1062.	169
Longitudinal at Hub	278.	164	271.	161
Lateral at Hub	124.	304	134.	306
Lateral at Tail Rotor Gearbox	10.	231	11.	227

Pickup Location	Flight		Results (g's) Force Determination		Results (g's) Ground Flying	
	Mag.	Phase	Mag.	Phase	Mag.	Phase
Z50	0.154	217	0.146	207	0.215	200
Z100T	0.114	196	0.051	206	0.163	194
Z210T	0.129	219	0.106	250	0.139	189
Z340	0.267	157	0.170	150	0.222	147
Z400	0.162	154	0.091	149	0.169	144
Z460	0.003	108	0.025	337	0.022	126
Z540	0.295	332	0.363	332	0.345	325
Z90R	0.103	204	0.044	102	0.124	208
Z90L	0.113	197	0.048	120	0.148	195
Z140R	0.093	190	0.050	204	0.099	211
Z140L	0.111	185	0.053	162	0.115	192
Z200R	0.111	147	0.169	154	0.096	197
Z200L	0.234	159	0.244	159	0.194	167
Z260R	0.198	170	0.127	159	0.144	162
Z260L	0.220	159	0.126	157	0.167	157
Z396R	0.151	166	0.071	144	0.161	144
Z396L	0.145	143	0.126	151	0.199	146
ZLONG	0.112	172	0.048	173	0.066	189
ZLATR	0.118	167	0.057	160	0.083	178
ZCOLL	0.138	172	0.069	150	0.100	172
Y50	0.101	168	0.078	171	0.030	328
Y30	0.059	180	0.052	184	0.027	326
Y140	0.047	185	0.029	193	0.023	349
Y220B	0.028	174	0.023	189	0.032	0
Y220T	0.144	307	0.171	316	0.197	307
Y300	0.056	185	0.031	277	0.015	344
Y300	0.079	212	0.039	305	0.042	285
Y440	0.135	245	0.092	287	0.088	277
Y490	0.081	209	0.095	267	0.088	262
Y517	0.061	63	0.094	250	0.066	217
X140	0.029	280	0.014	94	0.007	45
X100T	0.191	216	0.142	212	0.292	159
X540	0.298	334	0.326	332	0.325	326
X200R	0.064	104	0.012	213	0.046	28
X200L	0.034	353	0.072	343	0.011	15
X190R	0.100	157	0.065	189	0.102	142
X220L	0.026	77	0.012	142	0.016	323

TABLE 13. CONTINUED

Flight Condition - Approach & Landing	Vehicle Gross Weight - 9500 lb.			
Force Direction	Force Determination		Applied	
	Mag.-lb.	Phase deg.	Mag.-lb.	Phase deg.
Vertical at Hub	1118.	20.	1123.	20
Longitudinal at Hub	225.	77	264.	73
Lateral at Hub	174.	218	178.	221
Lateral at Tail Rotor Gearbox	6.	99	0.	294

Pickup Location	Flight		Results (g's)			
			Force Determination		Ground Flying	
	Mag.	Phase	Mag.	Phase	Mag.	Phase
Z50	0.085	122	0.101	104	0.190	99
Z100T	0.067	75	0.033	132	0.120	73
Z210T	0.078	133	0.095	172	0.103	90
Z340	0.277	14	0.237	4	0.341	-2
Z400	0.187	9	0.131	0	0.247	-3
Z460	0.023	200	0.039	205	0.013	204
Z540	0.504	168	0.513	188	0.598	179
Z90R	0.021	71	0.045	0	0.093	91
Z90L	0.074	84	0.050	23	0.115	72
Z140R	0.035	35	0.030	47	0.065	65
Z140L	0.073	60	0.038	10	0.090	51
Z200R	0.111	315	0.216	352	0.114	-16
Z200L	0.195	45	0.250	21	0.221	22
Z260R	0.162	16	0.164	8	0.210	7
Z260L	0.198	23	0.169	9	0.238	3
Z396R	0.173	354	0.100	356	0.222	0
Z396L	0.227	347	0.164	4	0.290	-3
ZLONG	0.083	20	0.065	13	0.081	9
ZLATR	0.095	38	0.072	13	0.106	14
ZCOLL	0.105	37	0.089	5	0.123	15
Y50	0.058	2	0.085	39	0.035	122
Y30	0.026	358	0.054	52	0.033	137
Y140	0.013	18	0.034	71	0.033	142
Y220B	0.024	92	0.024	69	0.039	155
Y220T	0.230	221	0.223	228	0.247	227
Y300	0.079	114	0.070	135	0.072	131
Y300	0.120	132	0.085	154	0.127	131
Y440	0.183	162	0.147	155	0.189	141
Y490	0.141	136	0.112	146	0.101	149
Y517	0.074	44	0.029	155	0.005	-10
X140	0.019	354	0.021	321	0.025	315
X100T	0.177	130	0.184	133	0.286	80
X540	0.483	184	0.441	187	0.511	181
X200R	0.088	52	0.041	47	0.027	316
X200L	0.057	280	0.058	219	0.049	295
X190R	0.076	61	0.068	95	0.092	56
X220L	0.020	323	0.024	354	0.016	292

TABLE 13. CONTINUED

Flight Condition - Left Pullout   Vehicle Gross Weight - 9500 lb.

Force Direction	Force Determination		Applied	
	Mag.-lb.	Phase deg.	Mag.-lb.	Phase deg.
Vertical at Hub	3240.	77	2854.	77
Longitudinal at Hub	1036.	108	840.	104
Lateral at Hub	855.	222	755.	226
Lateral at Tail Rotor Gearbox	99.	259	89.	264

Pickup Location	Flight		Results (g's)			
			Force Determination		Ground Flying	
	Mag.	Phase	Mag.	Phase	Mag.	Phase
Z50	0.632	137	0.483	148	0.739	105
Z100T	0.495	120	0.174	154	0.507	100
Z210T	0.460	169	0.557	197	0.463	144
Z340	0.943	58	0.642	50	0.570	43
Z400	0.686	53	0.371	45	0.409	41
Z460	0.100	38	0.060	289	0.074	342
Z540	0.299	233	0.289	236	0.839	230
Z90R	0.320	133	0.156	42	0.379	109
Z90L	0.480	118	0.206	57	0.474	99
Z140R	0.221	118	0.109	129	0.259	106
Z140L	0.408	107	0.137	74	0.361	94
Z200R	0.206	38	0.429	47	0.119	45
Z200L	0.895	87	0.853	69	0.634	77
Z260R	0.515	82	0.395	64	0.383	73
Z260L	0.692	70	0.465	55	0.430	54
Z396R	0.450	74	0.236	61	0.404	71
Z396L	0.778	37	0.550	42	0.482	20
ZLONG	0.268	82	0.146	69	0.164	84
ZLATR	0.335	85	0.210	59	0.237	74
ZCOLL	0.413	93	0.261	51	0.266	73
Y50	0.422	308	0.256	40	0.228	324
Y30	0.208	291	0.136	81	0.049	329
Y140	0.110	269	0.099	110	0.040	141
Y220B	0.105	166	0.169	130	0.190	136
Y220T	0.908	231	0.055	229	0.826	231
Y300	0.363	154	0.342	175	0.417	135
Y300	0.755	178	0.613	206	0.645	150
Y440	0.339	195	0.144	215	0.981	163
Y490	0.005	332	0.040	233	0.646	208
Y517	0.724	264	0.979	273	0.433	289
X140	0.089	60	0.060	3	0.084	20
X100T	0.748	153	0.776	164	0.915	118
X540	0.311	227	0.163	234	0.824	236
X200R	0.267	55	0.181	71	0.146	27
X200L	0.097	279	0.302	264	0.163	303
X190R	0.310	92	0.259	126	0.304	88
X220L	0.070	28	0.069	25	0.095	343

TABLE 13. CONCLUDED

Flight Condition - Rt. Pullout	Vehicle Gross Weight -9500 lb.			
Force Direction	Force Determination		Applied	
	Mag.-lb.	Phase deg.	Mag.-lb.	Phase deg.
Vertical at Hub	2205.	46	2321.	46
Longitudinal at Hub	1224.	130	1266.	131
Lateral at Hub	610.	230	650.	229
Lateral at Tail Rotor Gearbox	98.	230	99.	228

Pickup Location	Flight		Results (g's)			
			Force Determination		Ground Flying	
	Mag.	Phase	Mag.	Phase	Mag.	Phase
Z50	0.651	156	0.452	172	0.783	138
Z100T	0.440	136	0.196	188	0.393	119
Z210T	0.517	186	0.528	206	0.728	154
Z340	0.869	40	0.653	24	0.967	7
Z400	0.624	32	0.390	17	0.705	3
Z460	0.107	329	0.100	263	0.126	277
Z540	0.405	218	0.360	213	0.664	191
Z90R	0.239	158	0.189	58	0.317	133
Z90L	0.440	131	0.214	68	0.370	119
Z140R	0.096	123	0.016	156	0.152	112
Z140L	0.333	113	0.036	27	0.227	94
Z200R	0.307	338	0.454	4	0.307	337
Z200L	0.818	85	0.566	49	0.533	51
Z260R	0.418	64	0.392	32	0.538	29
Z260L	0.641	54	0.455	27	0.608	13
Z396R	0.333	49	0.264	30	0.662	21
Z396L	0.679	27	0.501	13	0.805	346
ZLONG	0.224	56	0.161	28	0.212	21
ZLATR	0.282	73	0.191	29	0.257	26
ZCOLL	0.323	81	0.235	24	0.287	29
Y50	0.454	328	0.107	18	0.176	239
Y30	0.218	316	0.074	87	0.068	184
Y140	0.093	303	0.082	117	0.087	128
Y220B	0.077	156	0.141	111	0.227	100
Y220T	0.033	242	0.682	241	0.584	242
Y300	0.364	138	0.371	151	0.523	103
Y300	0.723	163	0.635	175	0.842	119
Y440	0.240	178	0.110	187	0.312	130
Y490	0.806	196	0.010	205	0.847	167
Y517	0.007	260	0.003	249	0.645	259
X140	0.073	53	0.065	349	0.115	15
X100T	0.908	163	0.992	169	0.709	141
X540	0.415	212	0.160	209	0.458	193
X200R	0.254	49	0.224	45	0.253	25
X200L	0.083	273	0.171	260	0.165	319
X190R	0.282	105	0.286	143	0.445	120
X220L	0.065	14	0.088	6	0.094	337

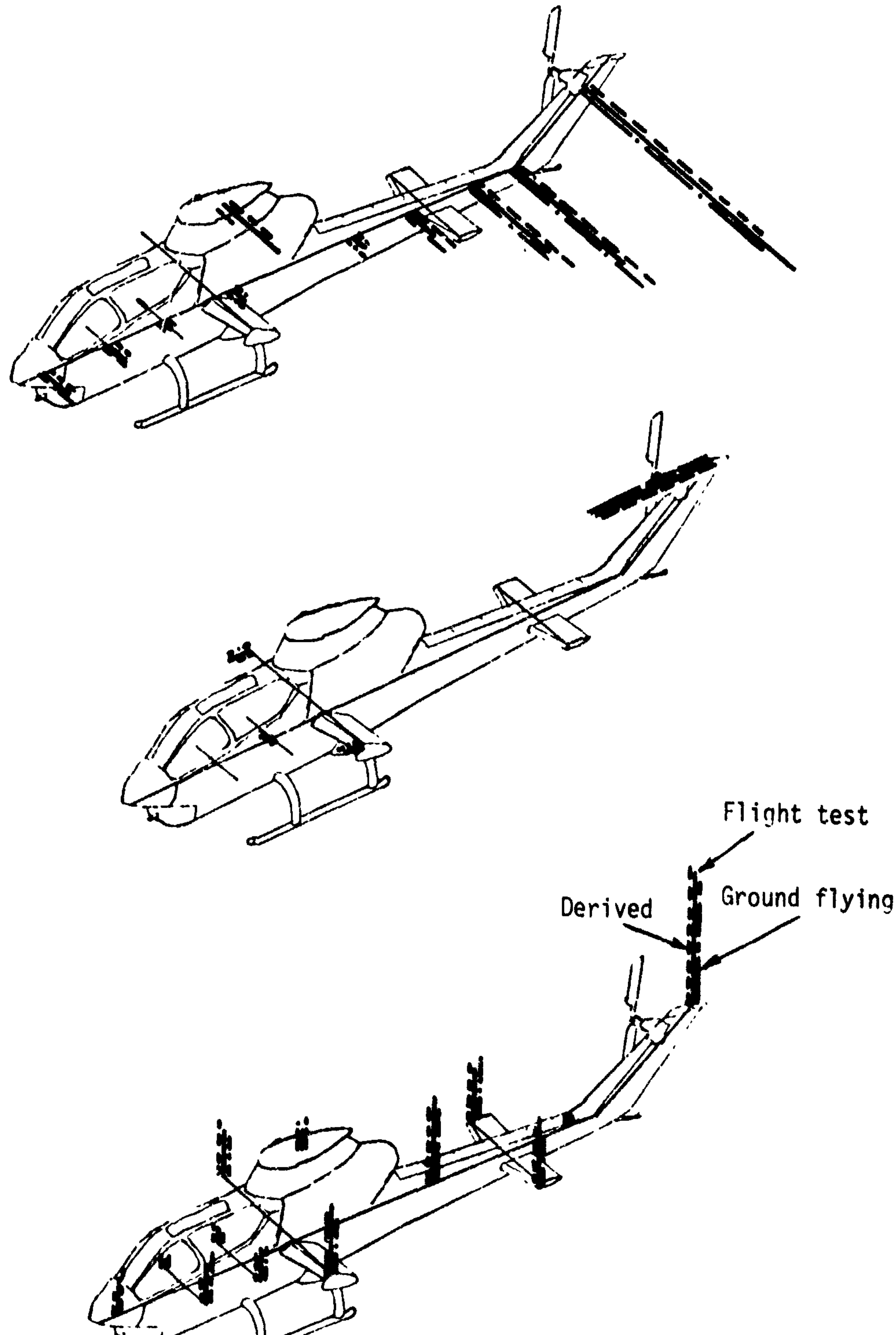

Figure 26. Level flight at a gross weight of 8465 pounds.

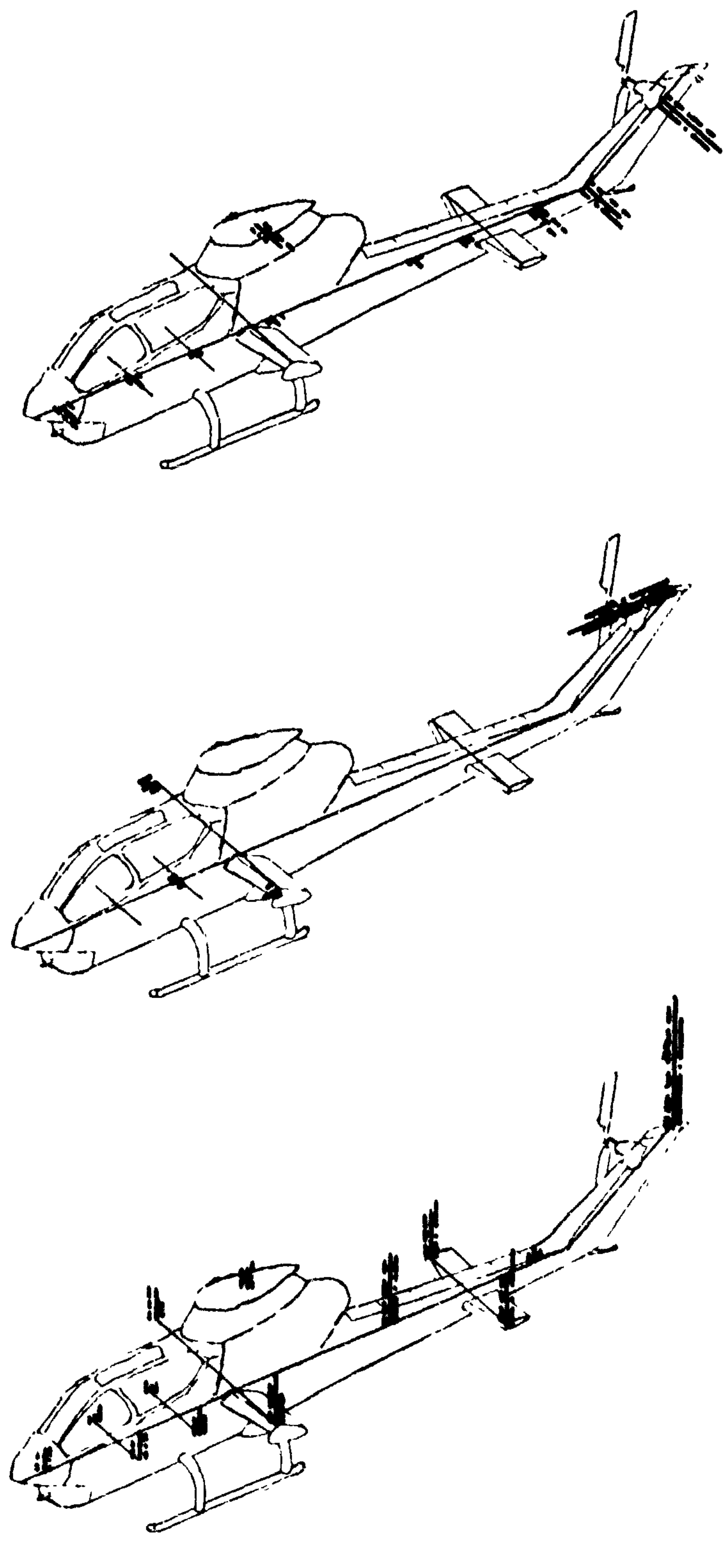

Figure 27. Right bank turn at a gross weight of 8465 pounds.

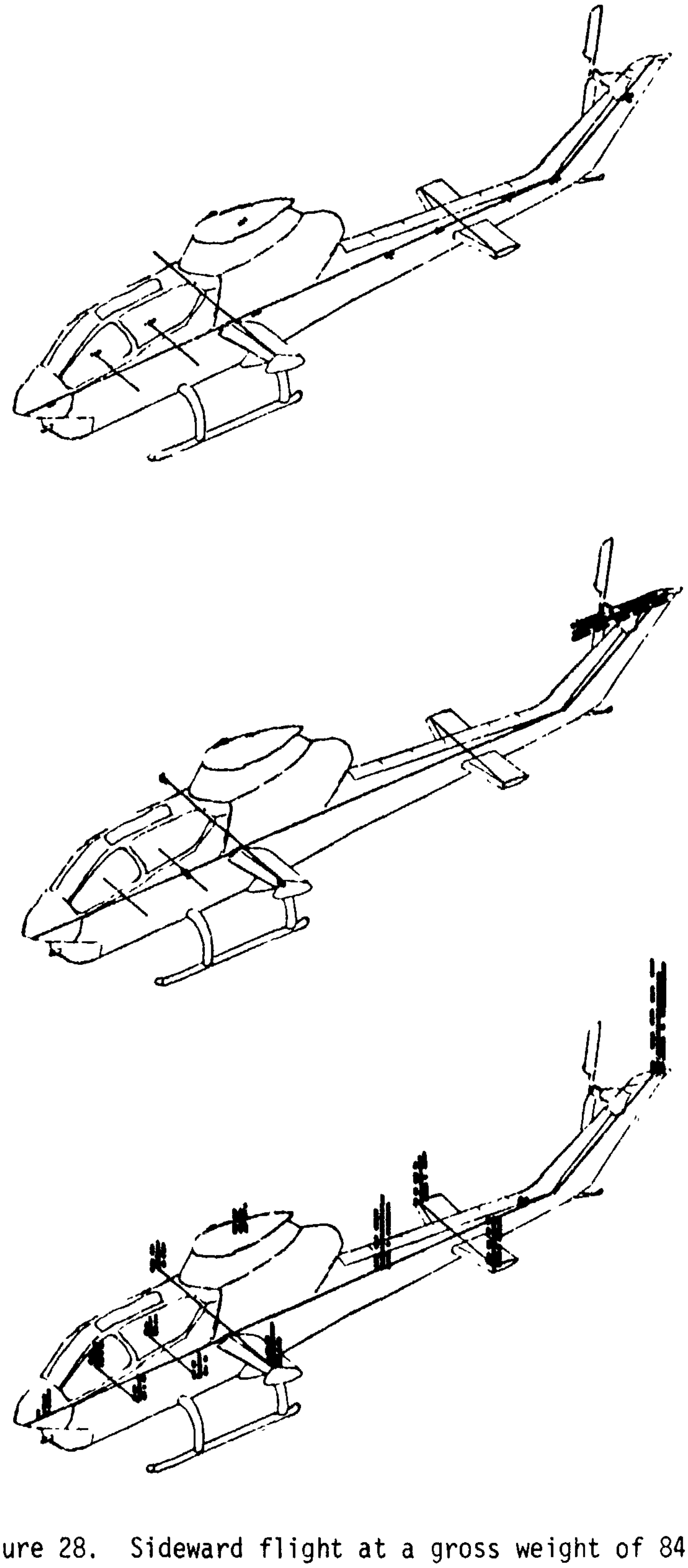

Figure 28. Sideward flight at a gross weight of 8465 pounds.

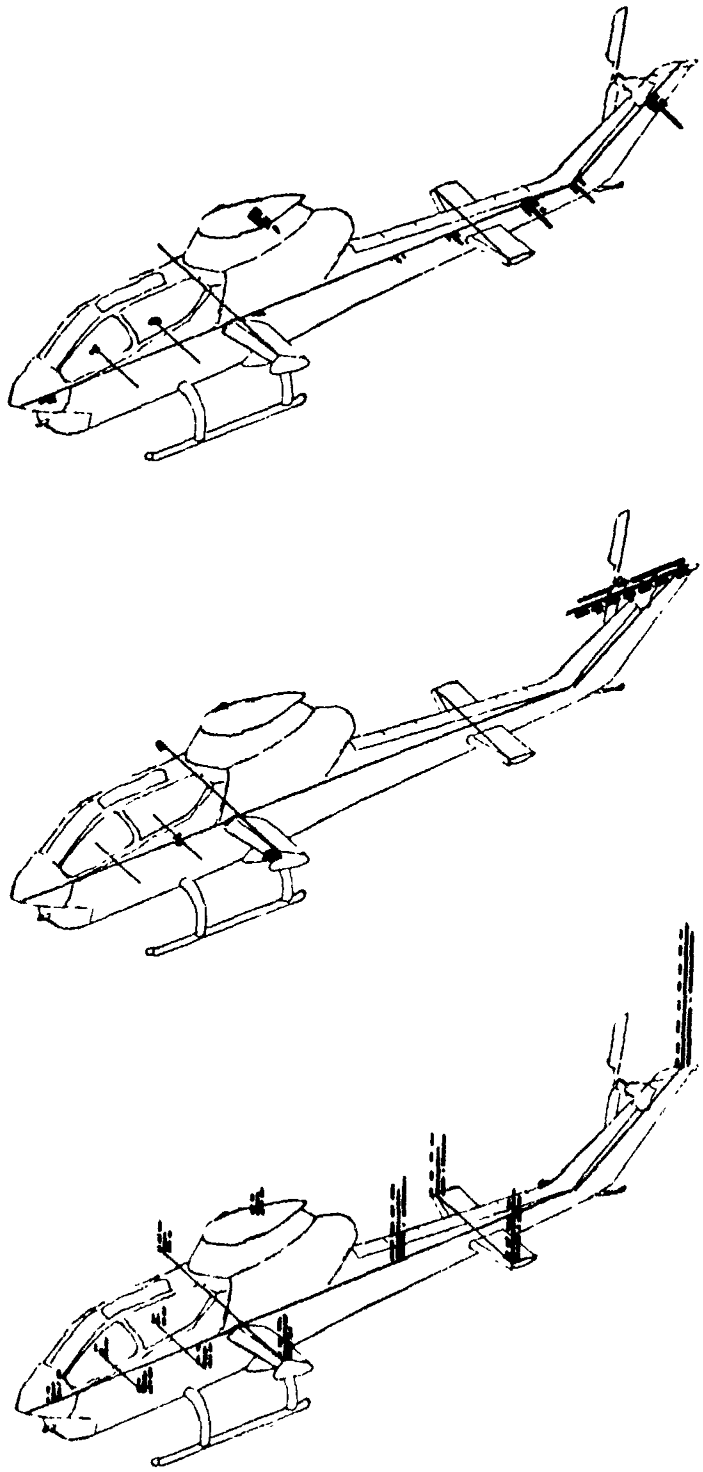

Figure 29. Approach and landing at a gross weight of 8465 pounds.

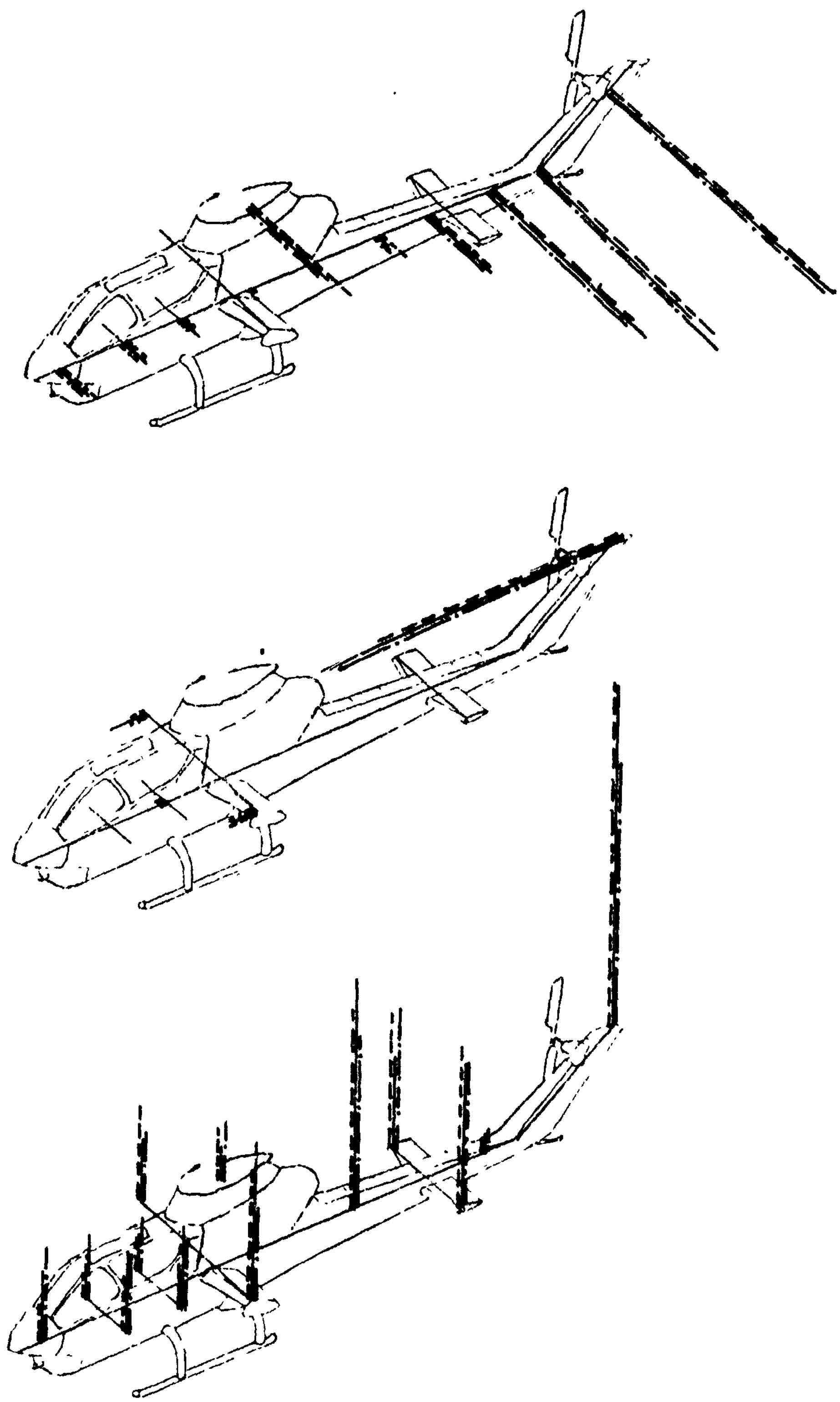

Figure 30. Left rolling pullout at a gross weight of 3465 pounds.

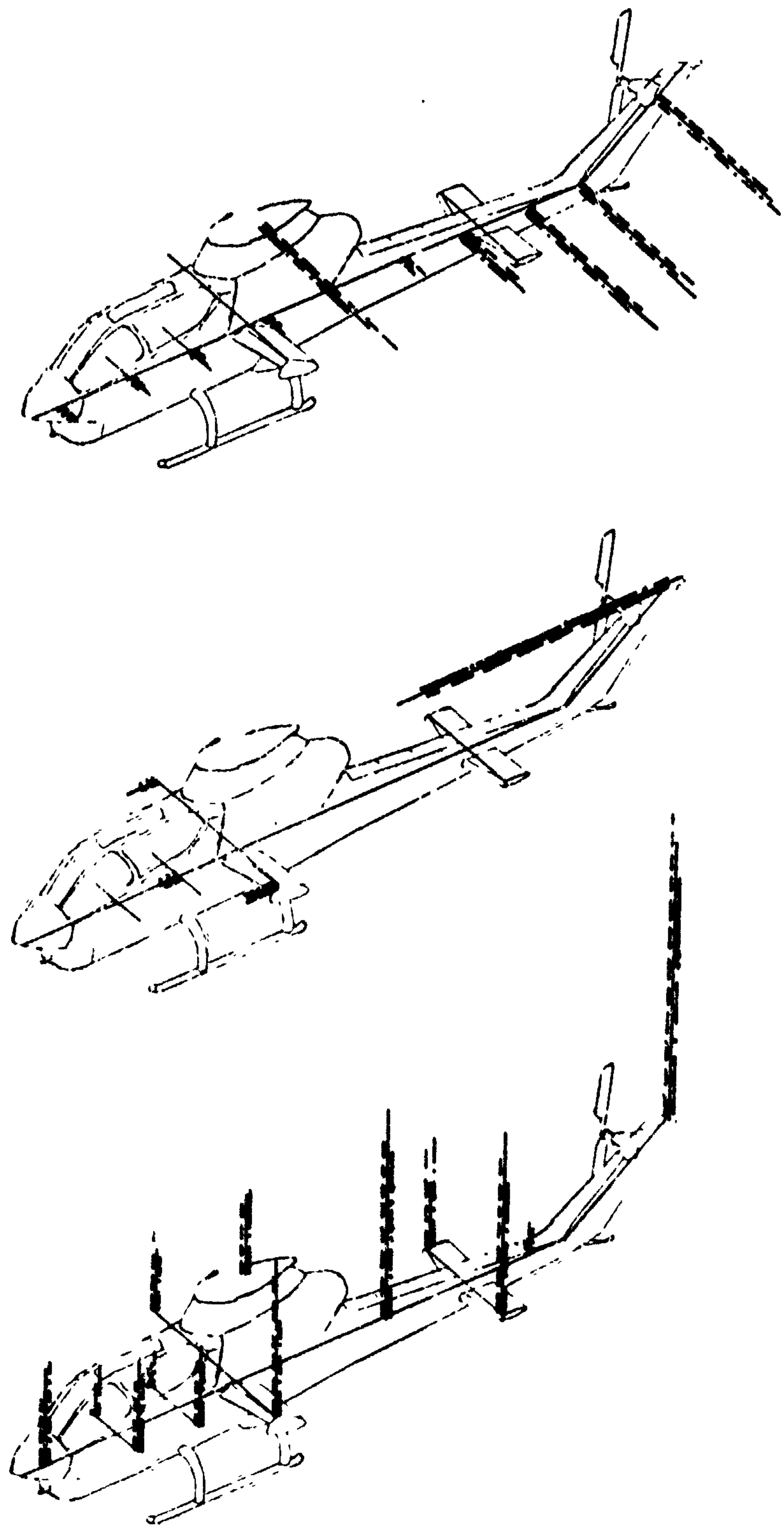

Figure 31. Right rolling pullout at a gross weight of 8465 pounds.

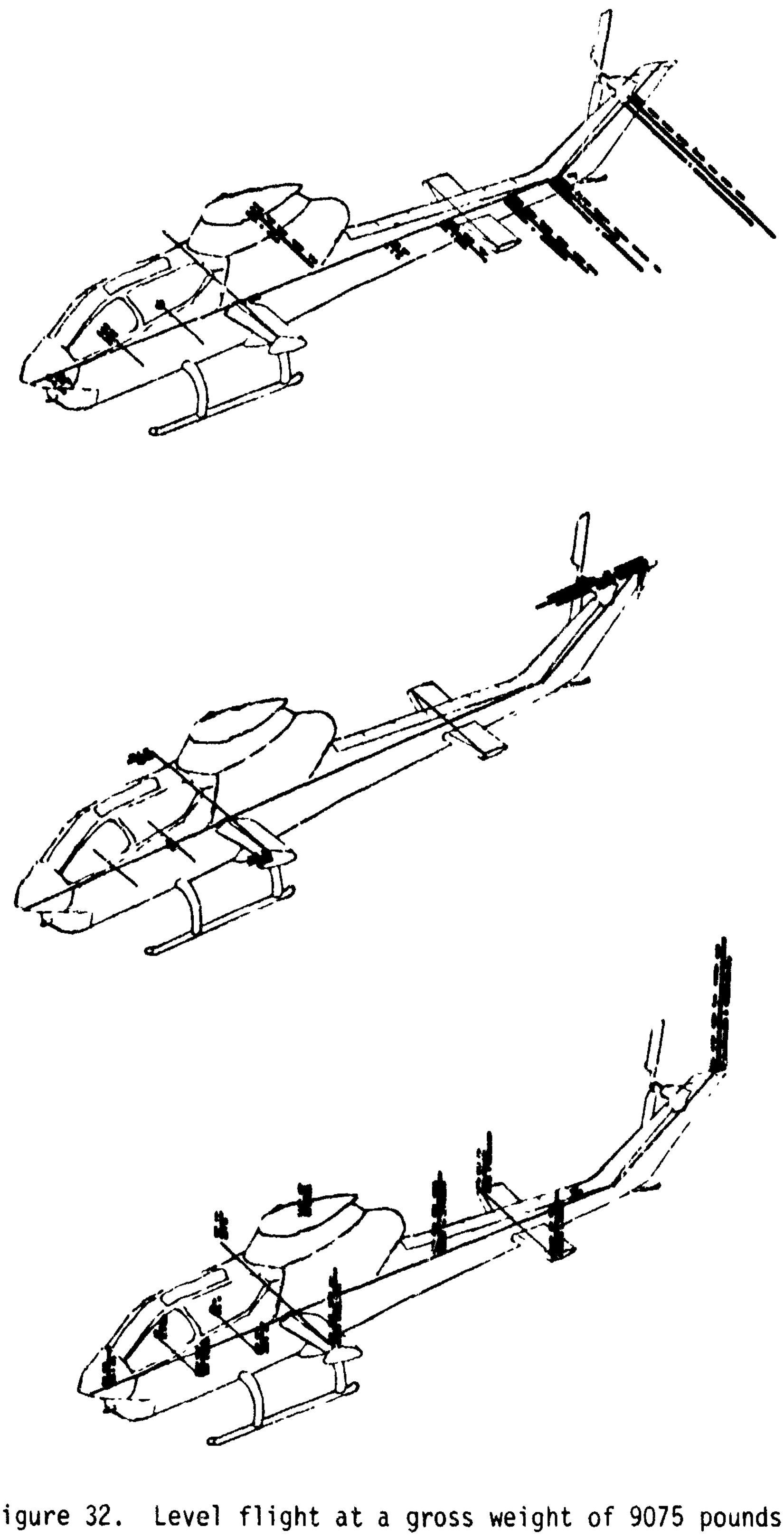

Figure 32. Level flight at a gross weight of 9075 pounds.

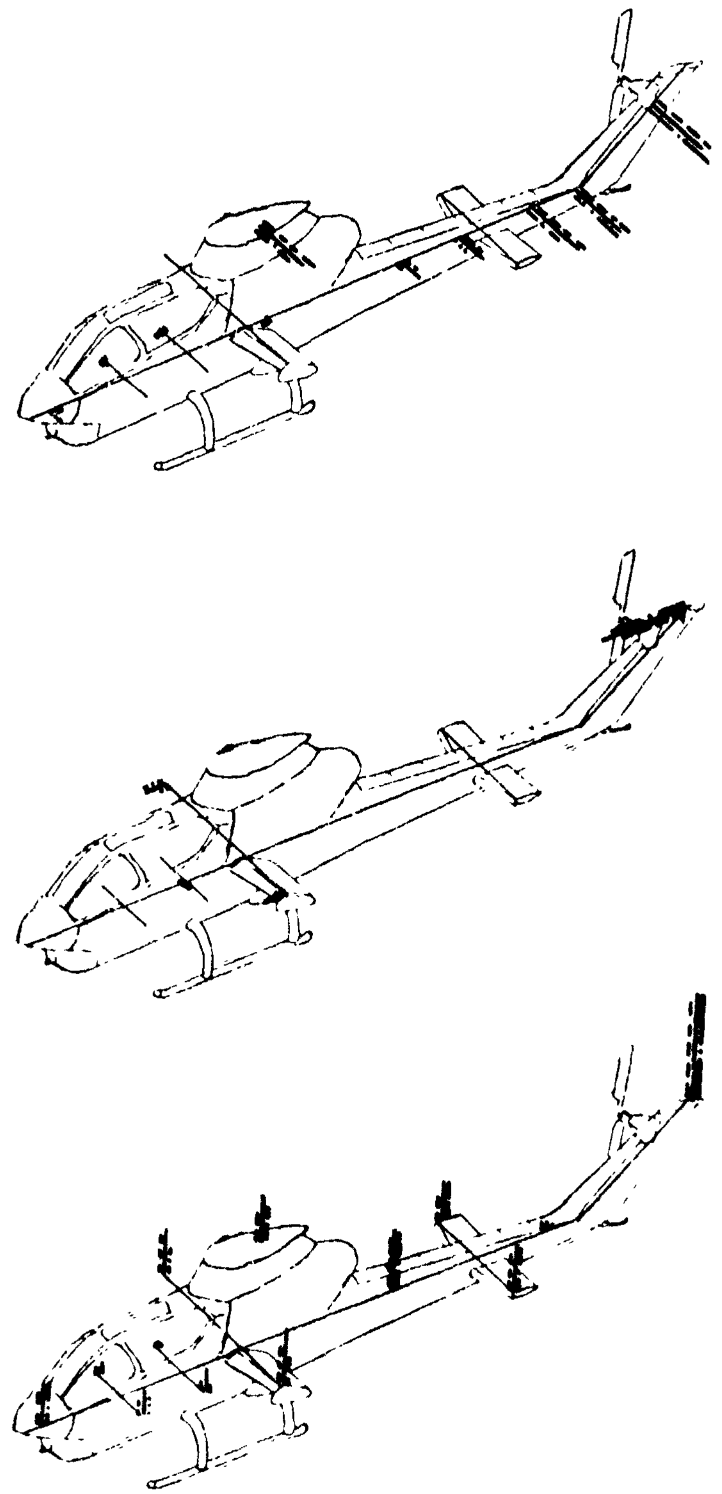

Figure 33. Right bank turn at a gross weight of 9075 pounds.

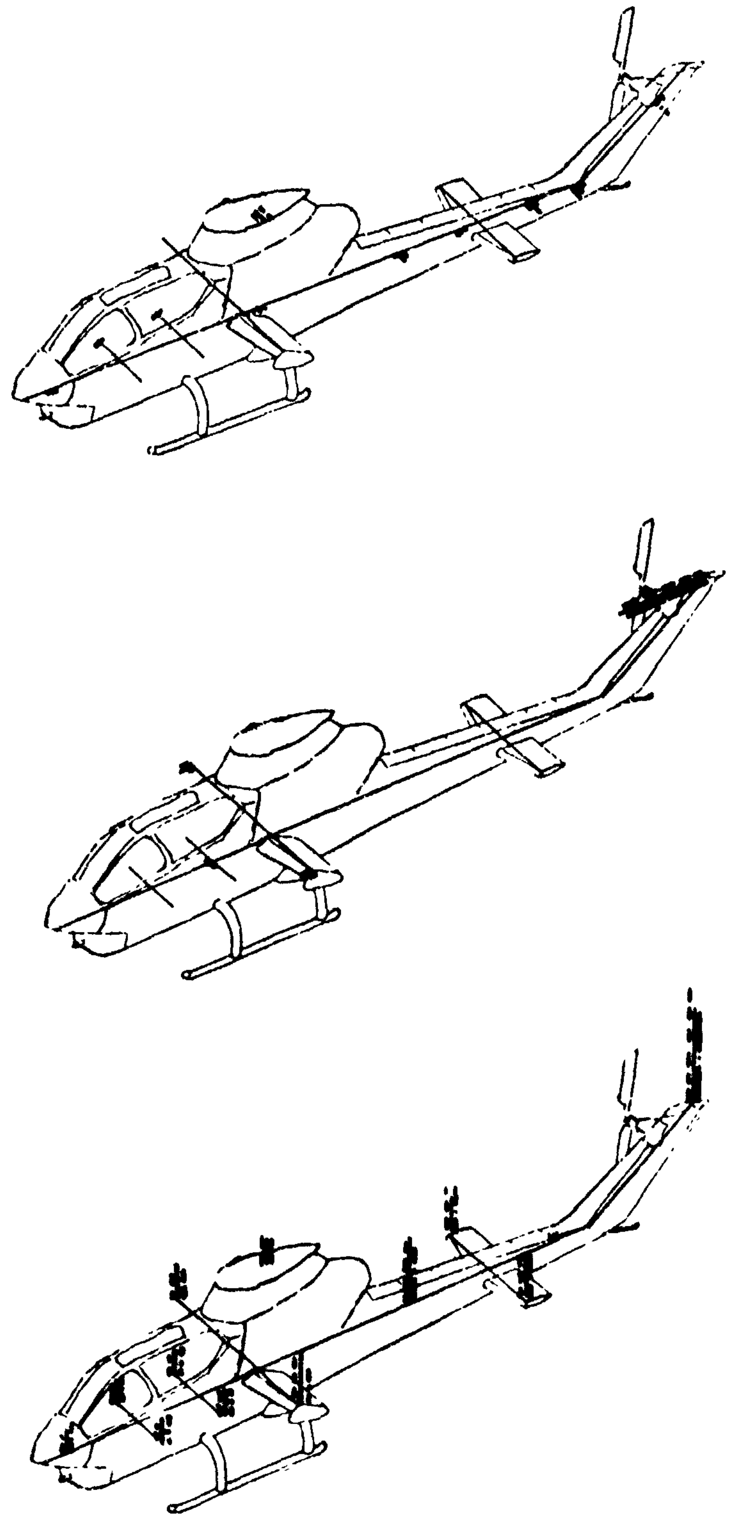

Figure 34. Sideward flight at a gross weight of 9075 pounds.

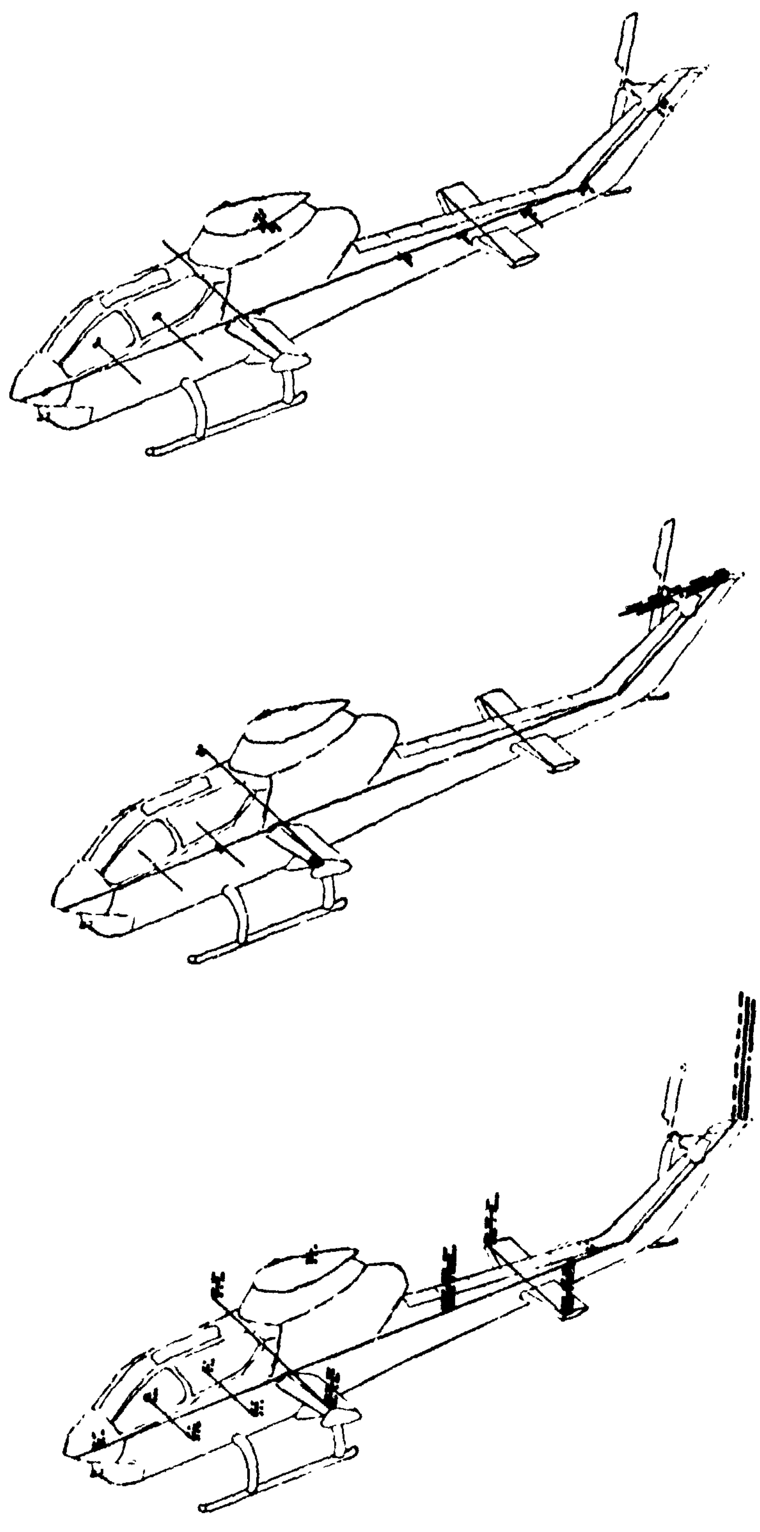

Figure 35. Approach and landing at a gross weight of 9075 pounds.

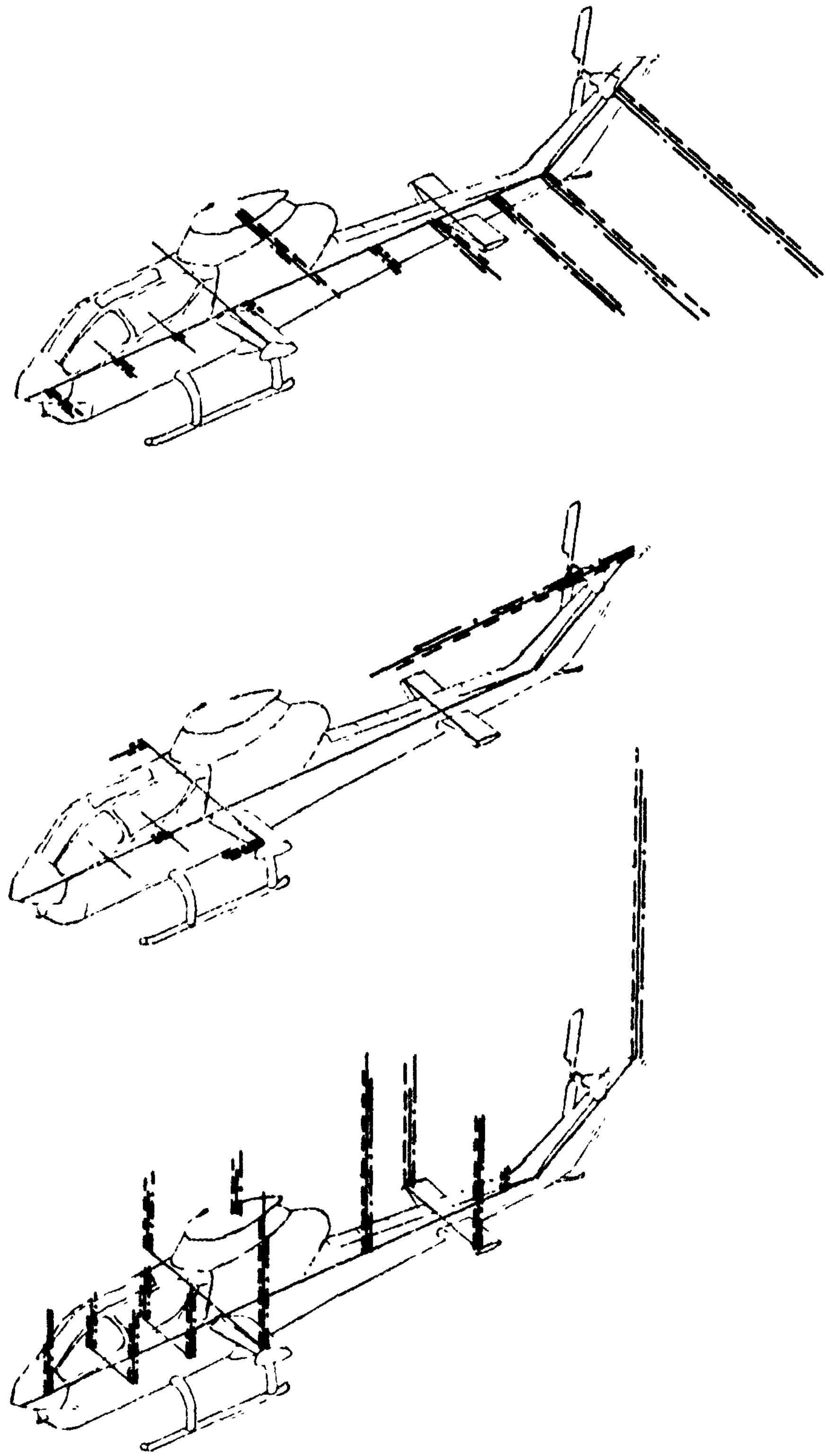

Figure 36. Left rolling pullout at a gross weight of 9075 pounds.

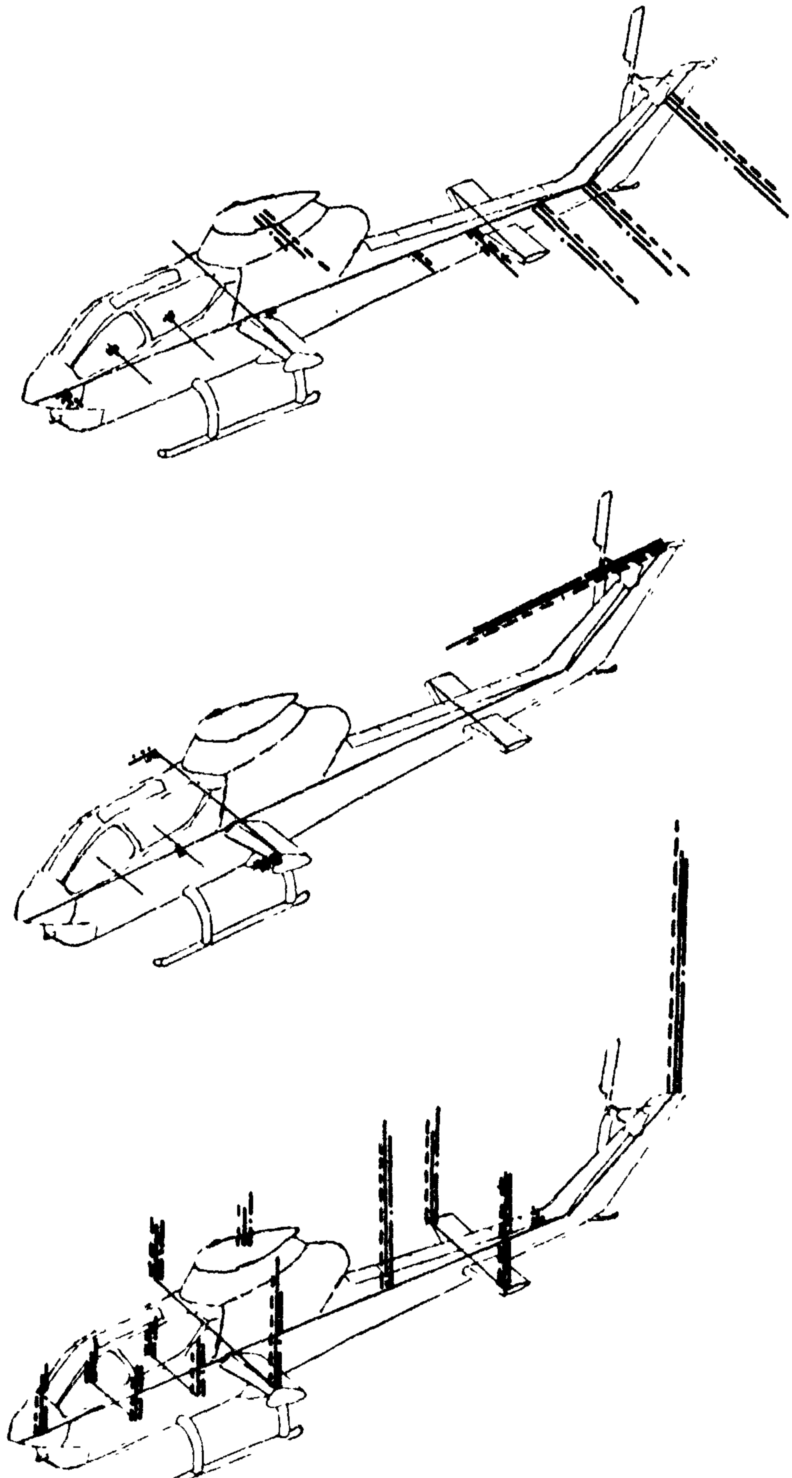

Figure 37. Right rolling pullout at a gross weight of 9075 pounds.

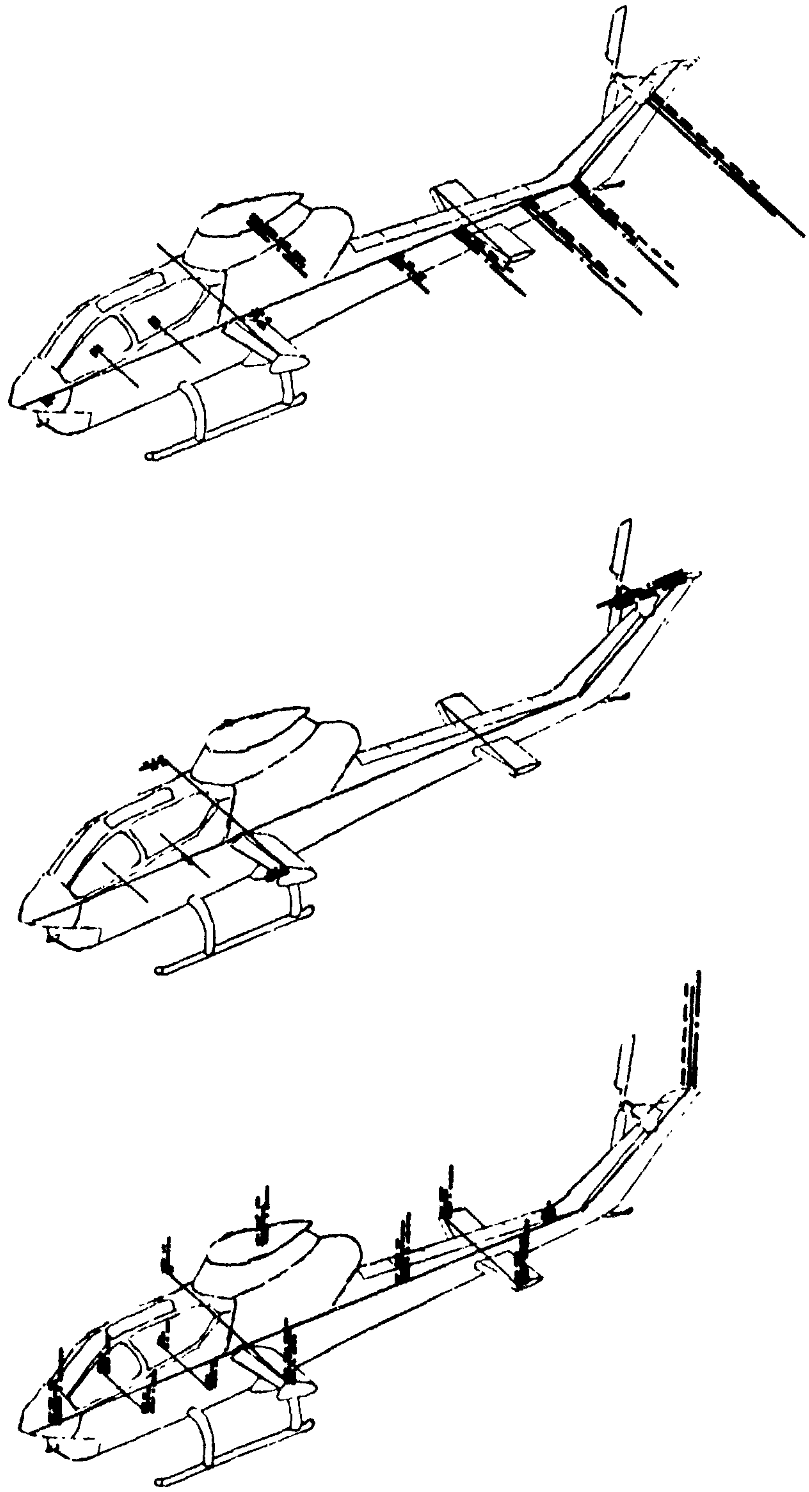

Figure 38. Level flight at a gross weight of 9500 pounds.

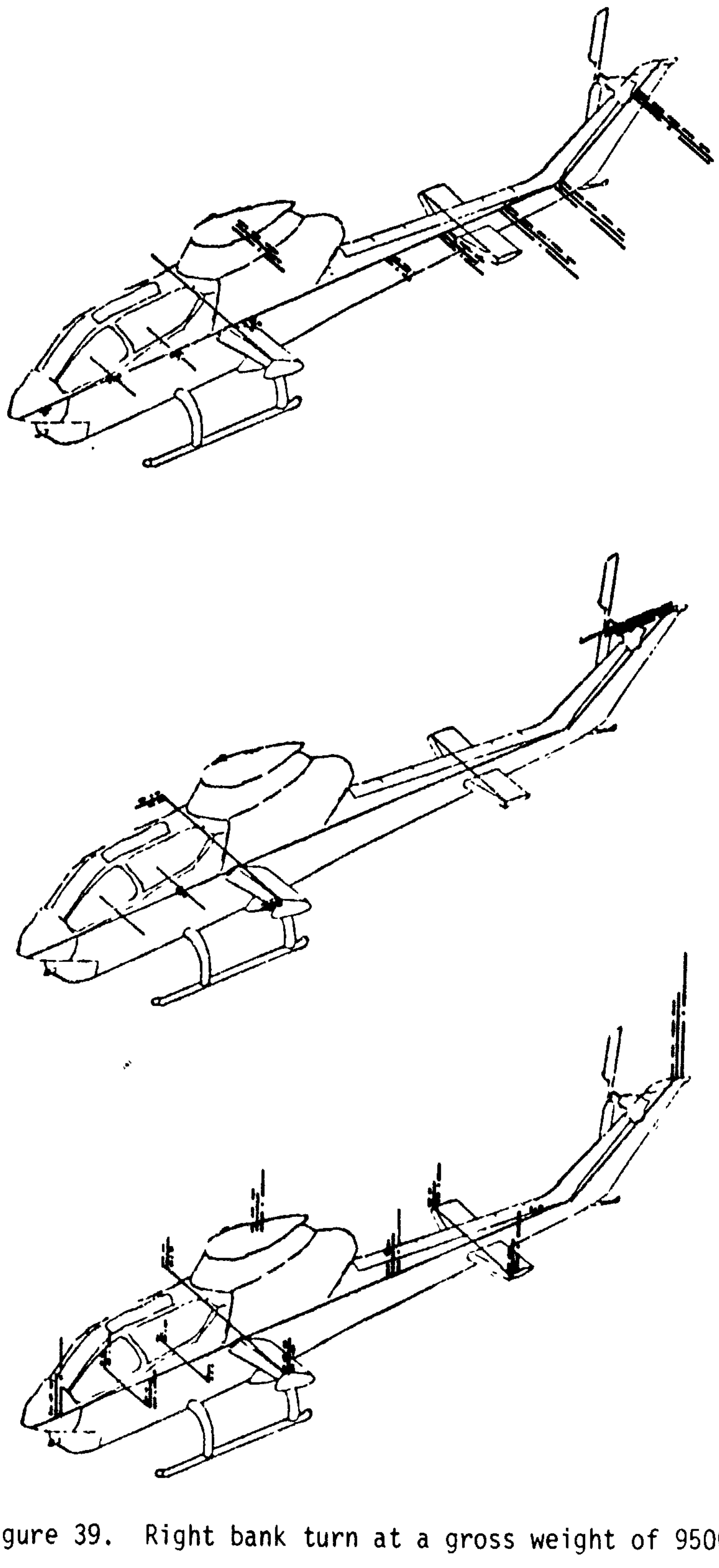

Figure 39. Right bank turn at a gross weight of 9500 pounds.

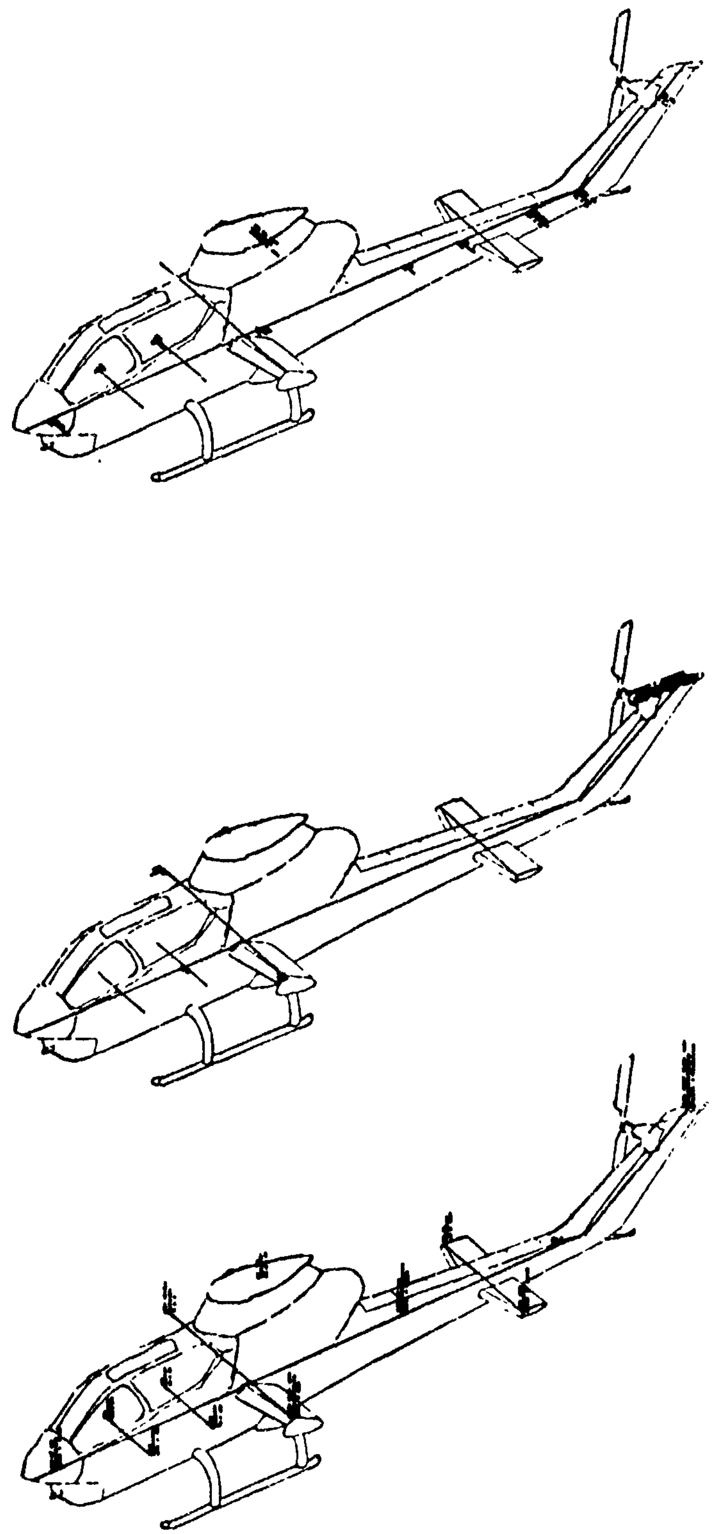

Figure 40. Sideward flight at a gross weight of 9500 pounds.

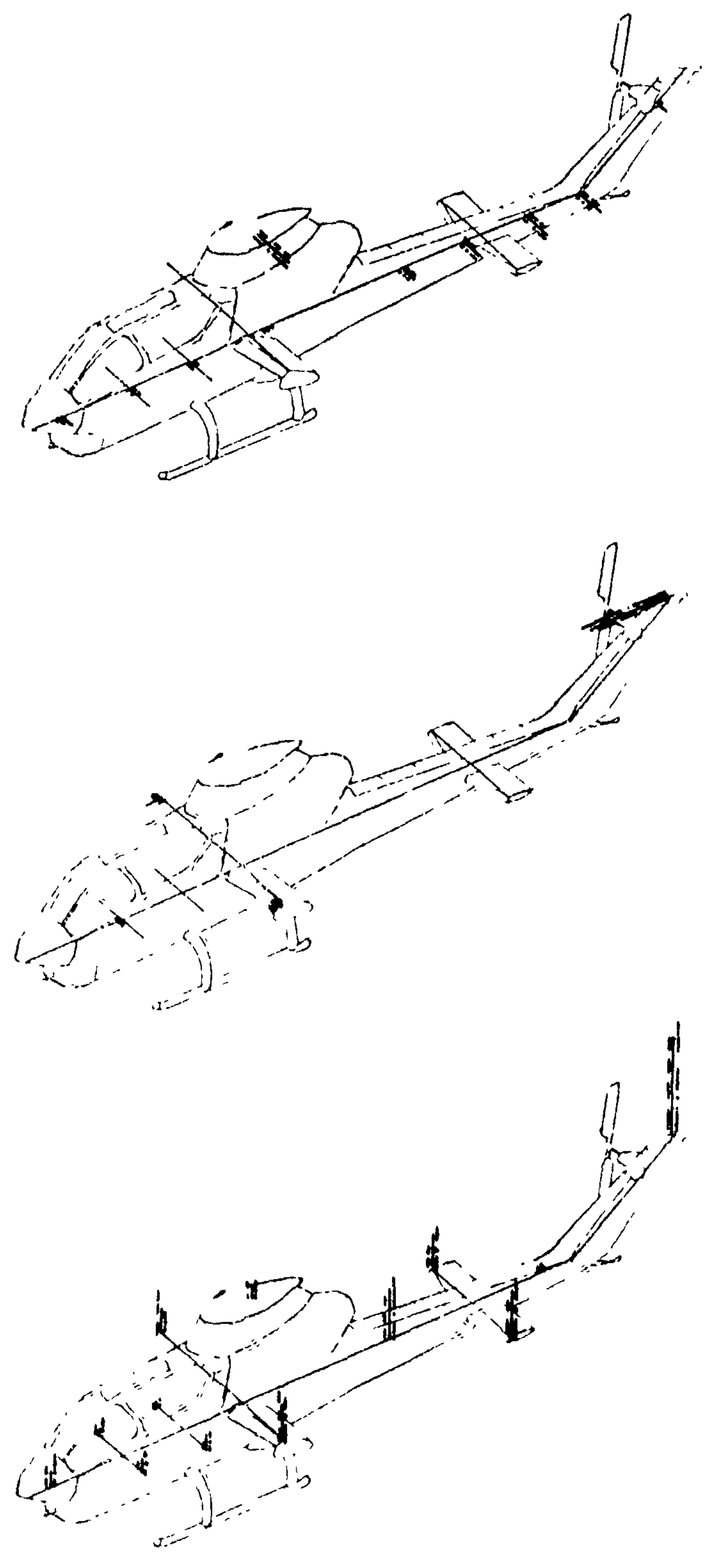

Figure 41. Approach and landing at a gross weight of 9500 pounds

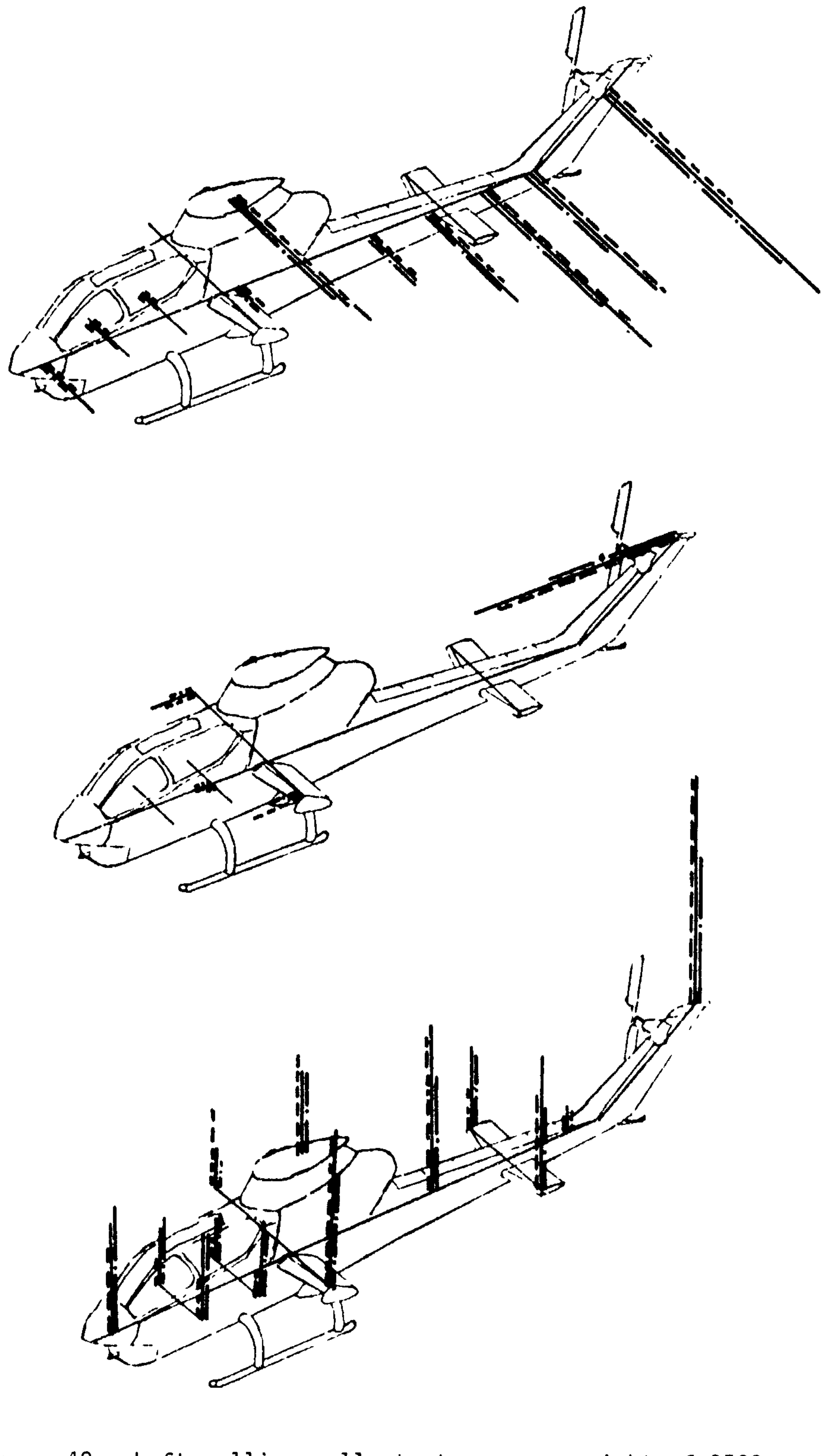

Figure 42. Left rolling pullout at a gross weight of 9500 pounds.

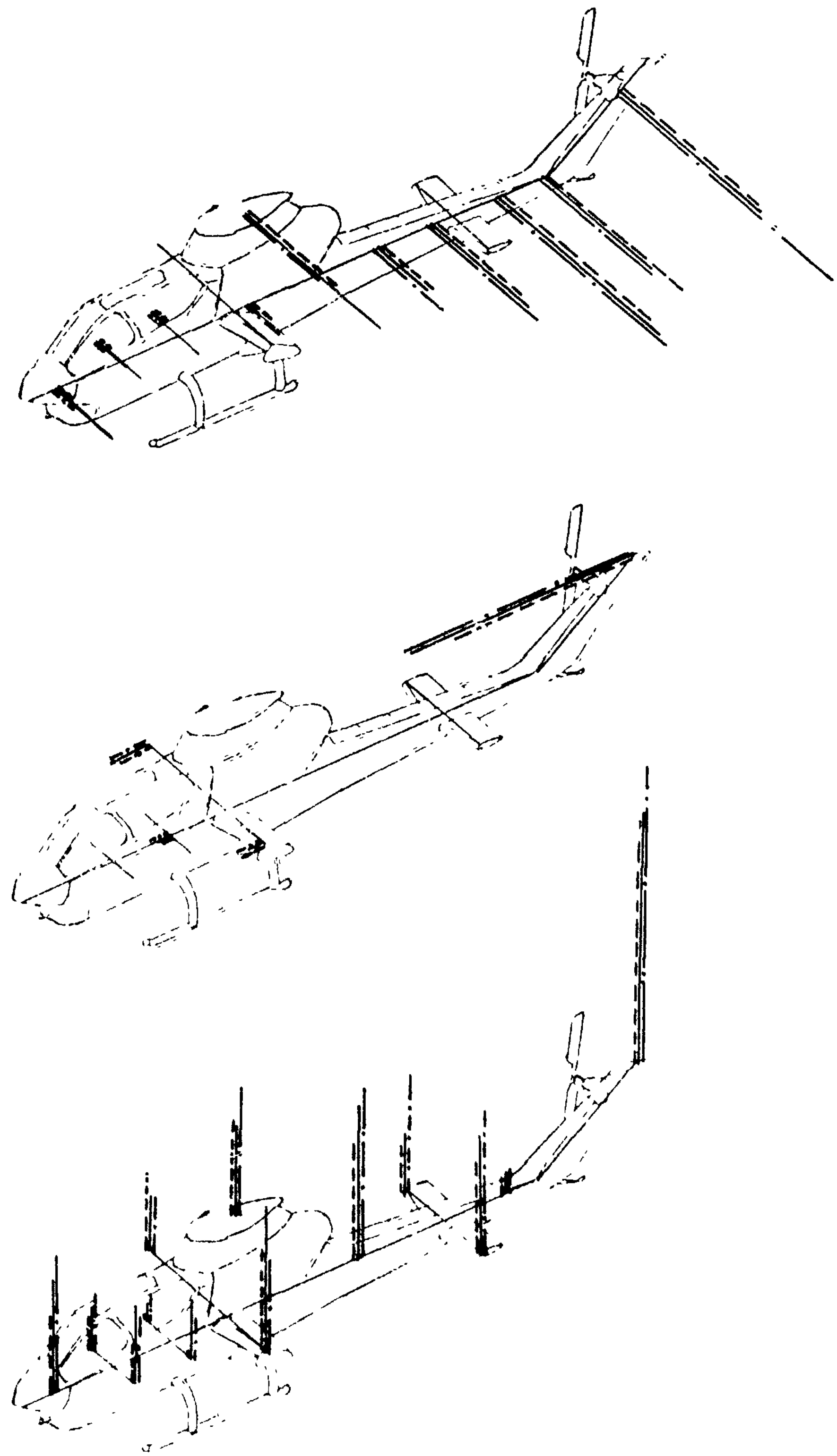

Figure 43. Right rolling pullout at a gross weight of 9500 pounds.

CONCLUSIONS

Force determination is feasible and can be used to

1. Correlate with aeroelastic rotor models

2. Develop and evaluate new rotor systems

3. Evaluate vibration mitigation devices and structural changes of the fuselage

4. Determine fuselage/rotor interference problems

5. Ground fly the vehicle in the hangar to accumulate flight time.

2573-81